University of South-Eastern Norway

FMH606 Master's Thesis 2018

Process Technology

Reduction in Sulphur Emissions from the Norcem Cement Plant in Kjøpsvik

Umesh Pandey

Faculty of Technology, Natural sciences and Maritime Sciences

Campus Porsgrunn

Course: FMH606 Master's Thesis, 2018

Title: Reduction in Sulphur Emissions from the Norcem Cement Plant in Kjøpsvik

Number of pages: 129

Keywords: SO_2 emissions, sulphur emissions, cement plants, Norcem cement plant, reduction in sulphur emissions

Student:	Umesh Pandey
Supervisor:	Lars A. Tokheim
External partner:	**Norcem Kjøpsvik (Annika Steien, Manager of Process and Environment)**
Availability:	Open

Approved for archiving: _____

(supervisor signature)

Summary:

SO$_2$ emissions in the stack gas from the Norcem cement plant in Kjøpsvik was significantly higher than the permitted emission limit in 2017. The plant aims to reduce the emissions by installing a seawater flue gas desulphurization (SWFGD) technology, but an understanding of sulphur behaviour in the kiln process, identification of critical factors, determination of their impact and describing underlying principle behind their effects in the emissions are beneficial for future plant and SWFGD operation. This report presents an analysis of the SO$_2$ emission characteristics in the kiln based on sulphur material balance, and regression model formulation using historical emission data and kiln tests.

Analysis of the historical data shows that SO$_3$ content in the kiln feed and rawmill operation mode are the most significant parameters which vary sulphur emission in the stack gas. In the analysis, it was discovered that bypass water supply, tyre feeding, RDF feeding, coal feeding and energy input per unit ton of clinker from rotary kiln fuels influence the emissions from the plant. Kiln tests varying these parameters were performed to determine the impact of these parameters on the emissions. The results from the kiln tests show that tyre and RDF feeding have the most significant positive impact while rawmill feed had a negligible impact on the SO$_2$ emissions. During the kiln tests, CO level in the kiln inlet was significantly higher with both tyre and RDF feeding and subsequently caused higher emissions. Moreover, the sulphur flow in the hotmeal and rotary kiln gases were considerably higher with both tyre and RDF feeding resulting in higher sulphur flow in the stack gas and lower sulphur flow in the clinker.

Coal feeding in the kiln inlet shows a positive impact on the SO$_2$ emissions indicating that the decrease in coal feeding (increase in waste oil feeding) reduces SO$_2$ emissions from the plant. The positive effects of coal feeding in the kiln inlet could be related to relatively slow and inefficient combustion of coal in comparison to the waste oil thereby causing reducing environment in the kiln. Based on the coefficient value in the model, kiln feed shows a negligible negative impact on the emissions, however, individual investigations show increased emissions with higher kiln feed due to reduced O$_2$ level in the kiln inlet. A similar type of discrepancy between regression model coefficients and individual test assessment was seen in the case of energy input rate from the rotary kiln fuels. Although regression model showed a negligible negative impact, higher emission was observed in the test with energy input rate from rotary kiln fuels at high-levels. Sulphur flow in the bypass gas was significantly higher in the test with energy input rate from rotary kiln fuels indicating that sulphur flow in the bypass gas primarily controls the SO$_2$ emissions in the tests with higher thermal load in the kiln.

Other parameters, bypass water supply and rawmill feed, showed a negligible impact on the emissions variations. Most of the experimental observations and subsequent analysis are affected by the faulty hotdisc operation, lack of perfect orthogonality in the experimental matrix, and fewer numbers of the test run, hence further kiln tests along with spot analysis of different gas streams are recommended to determine exact impacts of these parameters on the emissions variations.

Preface

This report is prepared in partial fulfilment of MS in Process Technology in the University of South-Eastern Norway (USN). The thesis work is performed entirely in Norcem Kjøpsvik under the supervision of Lars Andre Tokheim (Professor, USN, Porsgrunn) and Annika Steien (Manager of Process and Environment, Norcem Kjøpsvik).

During the thesis period, Jan to May 2018, I spent entire time in Kjøpsvik plant reviewing kiln processes and sulphur behaviour in the kiln, planning and performing experimental tests, and analysing process and quality data. This report summarises the work performed during the thesis period. In the experimental design, I had planned to conduct 32 tests in two different phases: the first test set with low sulphur content and another test set with high sulphur content in the kiln feed. Later, I discovered that planning tests and conducting tests in a real industry are entirely different. Even if few tests could be performed according to the experimental design, it is impossible to maintain identical experimental condition for the entire test period. My thesis work was not an exception, and hence the results of this study are strongly influenced by faulty hotdisc operations and constant coal feeding changes in the kiln. Despite this, I believe that this report can provide an overview of sulphur behaviour in the kiln process, a typical sulphur flow in different flow streams and distinguish the most significant kiln factors behind variation in sulphur emissions. Moreover, I believe this report can provide essential background for future research on sulphur emissions from the Kjøpsvik plant and also other cement plants around the globe.

I would also like to express my deepest gratitude to my supervisors, Lars and Annika, for their continuous intellectual support, advice and recommendations during the thesis period. Under their supervision, I was able to learn a systematic approach to tackle a research problem and apply in this thesis work. I would also like to appreciate Annika's effort in helping me integrate with the Norcem work environment as well as new city.

I would like to express my gratitude to the management team of Norcem Kjøpsvik, (Plant manager-Klaus Hvassing, Production manager-Tom Nordal, HR Manager-Kjell-Hugo Solheim, Electrical Department- Jan Erik Nilsen, Quarry Manager-Lisbeth Storhaug), for their technical and logistic support during the thesis period. A special thanks to Anne S. Solheim (Laboratory Manager) and entire laboratory department for analysing dust samples and providing technical support regarding quality data and analysis. I would like to mention Tom Erik Mortensen (Process Technician), and Hans Petter Skjellnes (Production Engineer) for their technical assistance during the thesis work. I would also like to acknowledge all the shift leader, process operators and Norcem staff for their assistance during the kiln tests. It would have been impossible to complete the experimental tests without their cooperation and technical support.

Finally, I would like to thank my parents, teachers and friends for their inputs and support during my entire academic endeavour.

Kjøpsvik, 13.05.2018

Umesh Pandey

Contents

Nomenclature

AM	Animal Meal
BP	Bypass System
C	Coal
Calc	Calciner
CF-silo	Continuous Flow silo (controlled flow silo)
CKD	Cement Kiln Dust
Cl	Clinker
COD	Chemical Oxygen Demand
D	Dust
DO	Dissolved Oxygen
DOE	Design of Experiments
EQS	European Quality Standard
F	Fuel
FF	Fabric Filter
FTIR	Fourier Transform Infrared Spectroscopy
G	Gas
GCT	Gas conditioning Tower
GE	General Electric
GSA	Gas Suspension Absorber
HM	Hot Meal
HTC	Heidelberg Technical Centre
ID Fan	Induced Draft Fan
ILC	Inline Calciner
KF	Kiln Feed
PT	Preheater Tower
R	Ratio
RDF	Refused Derived Fuel
RK	Rotary Kiln
RM	Raw Mill
RMF	Rawmill Feed
RM-OFF	Raw Mill Stopped (direct mode)

RM-ON	Raw Mill in Operation (compound mode)
SWFGD	Sea Water Flue Gas Desulphurization
T	Tyre
TOCs	Total Organic Carbons
WO	Waste Oil
XRF	X-Ray Fluorescence
YAGA	Yter Avansert Gass Analyse

1 Introduction

This chapter presents the background for this study, description of the problem, objectives and necessary tasks that must be performed to solve existing problems. The chapter focuses mainly on answering a few questions: What is the problem? Why must this problem be addressed? What are the tasks that should be performed to find a solution to this problem? And, what is the expected outcome? In addition, the chapter also consists of an overview of the report.

1.1 Background

This section gives an overview of a widespread problem of cement plants, sulphur emission problem, and a brief description of Norcem cement plant in Kjøpsvik.

1.1.1 Sulphur Emissions from Cement Plants

Raw materials and fuels used in producing cement consist of a significant amount of sulphur sources, a part of which ends up in the atmosphere as sulphur dioxide (SO_2) and sulphur trioxide (SO_3), collectively identified as SO_x [1]. Sulphur is present in raw materials in the form of pyrrhotite (FeS) and pyrite (FeS_2), along with sulphates in trace amounts. In the fuels, pet coke contains up to 5% of sulphur, and a similar amount is present in the heavy oils. Depending on the source of raw materials, the total sulphur contribution of raw material to the system can be as high as 80-90%. A modern cement plant usually uses coal and other fuel sources with sulphur content as low as 1%, so the contribution of fuels to the emission is insignificant relative to raw materials.

Sulphur present in the fuel and raw material (except in the form of sulphates) oxidises to oxides of sulphur and sulphates. These oxides (SO_2 and SO_3) are emitted to the atmosphere along with the flue gas [1]. In the atmosphere, SO_x react with water in the presence of air to form strong sulphuric acid. This acid contributes to several environmental problems, such as acid rain, reduced visibility, and other health problems. In order to limit sulphur emissions and emissions derived health and ecological hazards, Norwegian Environmental agency (Miljødirektoratet) has set the emission limit for sulphur emissions based on several factors: location of a plant, types of industry and production capacity.

1.1.2 Norcem Cement Plant in Kjøpsvik

Figure 1.1 shows a picture of the plant in Kjøpsvik.

Figure 1.1: A picture of the cement plant and Norwegian fjord in Kjøpsvik.

It is the Northernmost cement plant in the world. The plant was established in 1918, and it is located in Kjøpsvik, Tysfjord commune. Annual cement production from the plant is about 0.5 mil tons/year. The plant uses locally available limestones to produce various qualities of cement and clinker and sale them in the Norwegian market as well as foreign markets.

1.2 Problem Statement

In 2015, the SO_x emissions from Norcem Cement Plant in Kjøpsvik exceeded the limit set at that time (average daily limit- 400 mg/Nm^3 dry @10% O_2. After the audit in 2015, the regulatory body, Norwegian Environment Agency (NEA), enforced the plant to take the necessary measures to reduce sulphur emissions by 2020. Meanwhile, NEA agreed to lift the average daily emission limit to 500 mg/Nm^3 dry gas @10% O_2, and the plant agreed to use low sulphur raw materials as a short-term solution, and seek for a permanent solution to limit sulphur emissions from the plant. However, in 2017, 64 out of 318 daily averaged measurements exceeded the current emission limit. For operating hours of more than 12 hours in a day, 53 daily averages exceeded the emission limit. The plant has planned to tackle this problem by installing Sea Water Flue Gas Desulphurization (SWFGD) installation using easy-to-access seawater from the Tysfjørd. The design uses three pumps with a standard operating volume flow of 3300 m^3/h. The scrubber consumes a considerable amount of electrical power, and the net result is an increase in unit cost of cement production. The increase in the operating cost ultimately reduces the profit margin and the competitiveness of the plant in the market.

A preliminary study shows that there were comparatively higher emissions from the plant in April-June in 2017. The timeframe coincides with the use of waste oil as a partial substitute for coal as a rotary kiln fuel. The coincidence points towards the possible correlation of sulphur emissions with the use of waste oil as rotary kiln fuels. However, there may be other potential factors that can cause substantial variation in sulphur emissions. In order to determine the absolute and relative impact of key factors, it is essential to analyse historical/current data, and sulphur flows in flow streams. Additionally, a detailed study is beneficial to understand sulphur emission characteristics, thus optimising plant operations and scrubber pumping cost in the future.

Questions
In order to find a solution for the aforementioned problem, following set of questions must be answered:

a. What is the current sulphur emission from the plant?
b. Are there significant variations in the emissions? If yes, what are the characteristics of these variations?
c. What factors contribute significantly to the variation in sulphur emissions from the plant?
d. What are the impacts of these factors on sulphur emissions?
e. Why do these factors cause variation in sulphur emissions?
f. Are there specific operating conditions that cause the emission to exceed the limit? If so, what conditions?
g. What is the expected result of the installation of SWFGD and its consequences on the environment, energy consumption and the cement production process?

The signed thesis task description can be found in Appendix A.

1.3 Objectives and Tasks

The goal of this research study is, **"To identify key factors, find their impacts on the variation in sulphur emissions, and describe possible physical and chemical theories behind the variation due to these factors in the Norcem cement plant in Kjøpsvik."**

Figure 1.2 shows three objectives (in blue rectangular boxes) and the tasks (respective branches) that must be accomplished to achieve the goal. Brown box contains the title of the project. The three principal objectives of this study are, to identify the key factors, find their impacts on variation in sulphur emissions, and describe physical and chemical theories behind the variation associated to these factors. The first two objectives are interconnected, as identification of a factor is incomplete without findings its effect and finding its effect is impossible without identifying the potential factor. After identification of key factors and verification of the effect associated with the identified factors, the study aims to describe possible chemical and physical theories behind the influence of identified factors on sulphur emissions from the plant. Additionally, the study aims to describe SWFGD and consequences of installing SWFGD regarding process/operational, energy and environmental aspects.
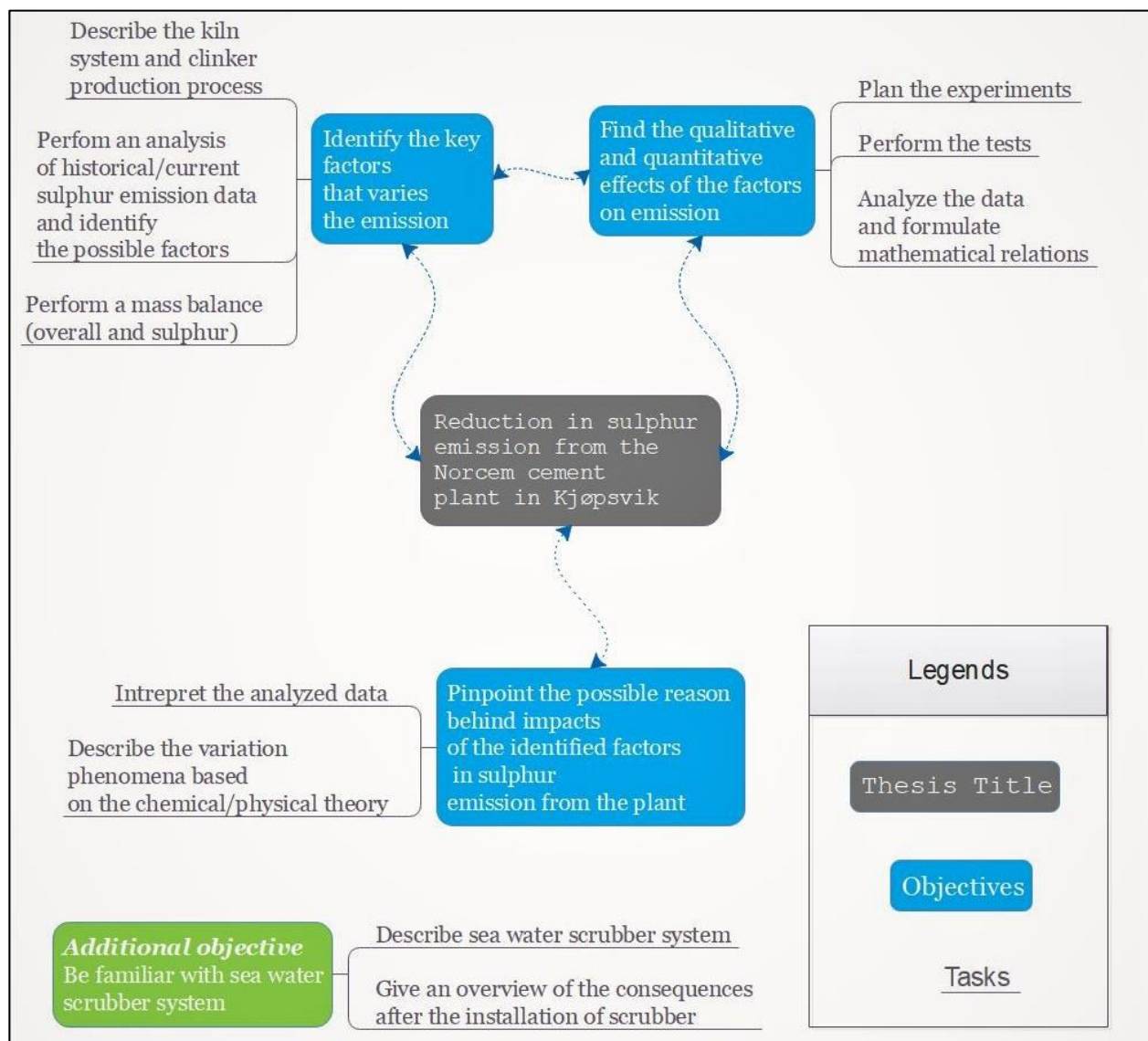
Figure 1.2: A mind-map portrayal of the interlink between objectives and tasks.

1.4 Outline of the Report

The thesis report consists of 8 chapters. The first chapter introduces background of this study and problem statement describing sulphur emission problem of the Norcem cement plant in Kjøpsvik. It also includes objectives and necessary tasks that should be performed to achieve the objectives of this study. The second chapter consists of a description of clinker formation process in the Kjøpsvik plant. The description is based on kiln processes in the Kjøpsvik plant together with a literature review of dry kiln process. The third chapter presents a literature review of sulphur behaviour and sulphur material balance based on kiln process in the Kjøpsvik plant. Sulphur material balance is used in calculating sulphur flow during historical as well as experimental kiln tests. The fourth chapter presents a description of proposed seawater flue gas desulphurization (SWFGD) installation in the Kjøpsvik plant, and its consequences regarding process/operational, energy and environmental aspects.

The fifth chapter presents an analysis of historical emission data. The process and quality data corresponding to two different weeks (22-29 August 2017 and 08-15 December 2017) are analysed using sulphur flow calculation and regression analysis. The sixth chapter presents an experimental plan of kiln tests and a description of the SO_2 measurement system in the stack and bypass system. The process and quality data from the kiln tests are analysed collectively and individually based on sulphur flow calculation and regression model formulation. The results from of the analysis of the experimental results are presented in chapter 7. The final chapter, chapter 8, presents the conclusion of this study and recommendations for future work based on the finding of this study.

2 Description of Clinker Formation process

This chapter describes clinker formation process in the Norcem cement plant in Kjøpsvik. It consists of a description of the material flow, process variables and process equipment used in the kiln. It excludes a discussion about pre-processing of raw materials and postprocessing of the clinker. However, it presents a description of all gas flow streams, rawmill and continuous flow silo (CF-silo), focusing on sulphur inflows and outflows to/from the system. Since the process used in the plant to produce clinker is based on the dry kiln process, all discussions of various components, processes and sub-processes are based on the description of dry kiln process.

2.1 Overview of Clinker and Portland Cement

European Standard defines Portland cement clinker as, "Portland cement clinker is a hydraulic material which shall consist of at least two-thirds by mass of calcium silicates ($3CaO \cdot SiO_2$ and $2CaO \cdot SiO_2$), the remainder consisting of aluminium and iron-containing clinker phases and other compounds. The ratio by mass $(CaO)/(SiO_2)$ shall be not less than 2.0. The content of magnesium oxide (MgO) shall not exceed 5.0 % by mass" [2]. In other words, the clinker consists of a mixture of four crucial cement phases, alites ($3CaO.SiO_2$), belites ($2CaO.SiO_2$), aluminate (Al_2O_3) and ferrite (Fe_2O_3) in specified proportions [3]. The morphology of clinker is nodular with particle size varying from 1 to 25 mm [4]. These nodules are grinded together with gypsum (a hydrated calcium sulphate added to increase setting time of the cement) to produce the Portland cement [2].

2.2 Process Flow Diagram of Clinker Formation Process

Figure 2.1 shows the process flow diagram (PFD) of the clinker production process in the Norcem cement plant in Kjøpsvik. It shows various subprocesses and flow streams along with various process equipment used in the clinker production process. There are four distinct types of streams used in the production of clinker.

A complete process diagram showing cement production process is in Appendix B.

1. **Fuel streams**

Fuel streams refer to the flow of different fuel sources into the kiln and the calciner. The fuels used in the plant are rotary kiln fuels (waste oils and coal) and calciner fuels (refused derived fuel (RDF), tyres, animal meal and coal).

2. **Solid material streams**

Rawmill feed, kiln feed, hot meal and clinker are solid material streams in the PFD.

3. **Water streams**

Water is used in the gas suspension absorber (GSA), cooling tower and rawmill in the clinker production process.

4. **Gas streams**

In the PFD, gas stream refers to the primary air, secondary air, bypass gas, tertiary air and excess clinker cooling air.
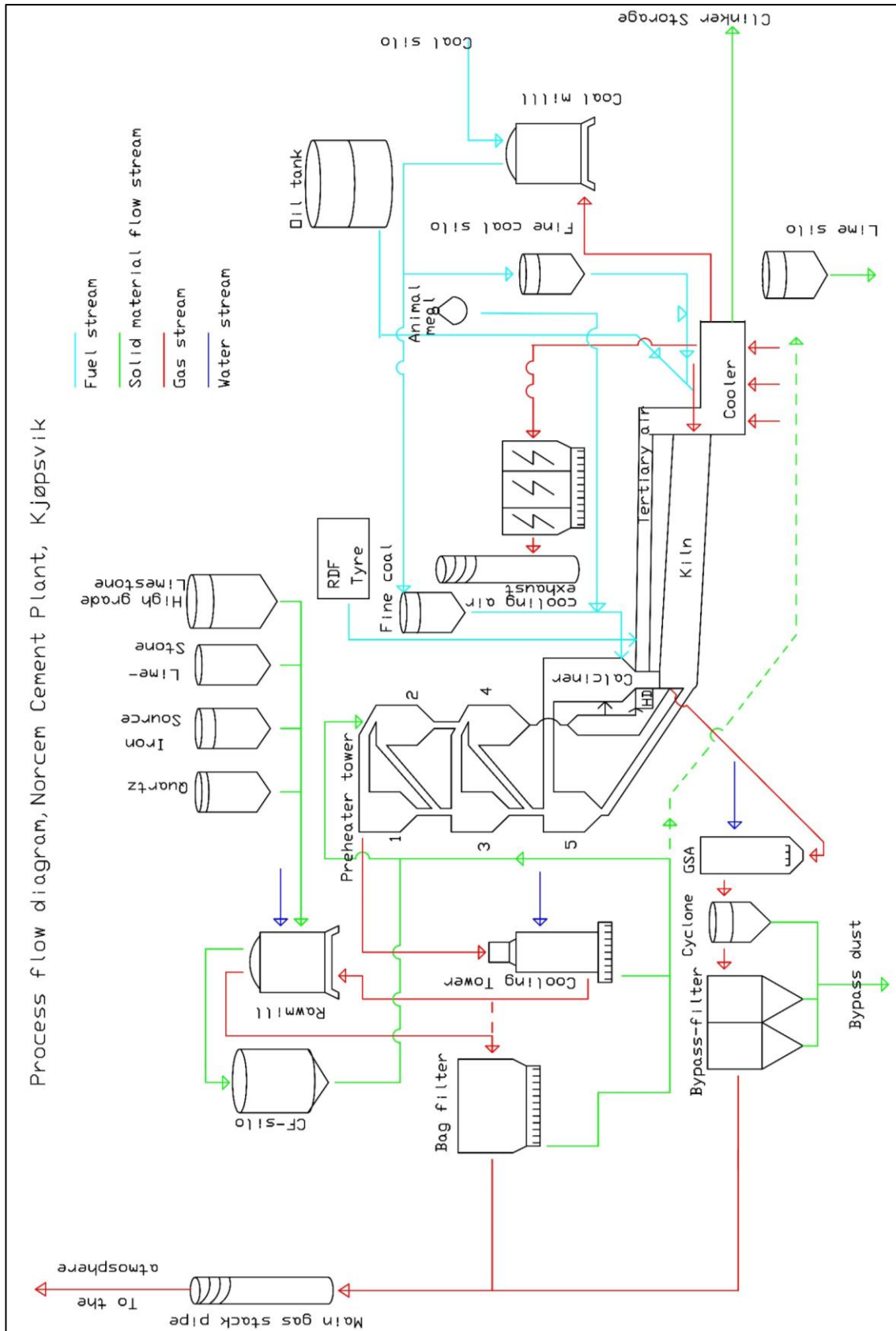
Figure 2.1: Process flow diagram of clinker formation process.

There are four types of cement manufacturing processes based on the water content of the solids entering the kiln from preheater tower [1, 5-7]. These processes are Dry process, Semi-dry process, Semi-wet process, and Wet process. The water content of the hot meal at the kiln inlet for the dry process is about 5%, semi-dry process is 10-15%, semi-wet process is about 20%, and wet process is as high as 30-40%. In the plant in Kjøpsvik, cement is produced using the dry kiln process, so, the description of the clinker formation process is based on the dry process.

In the dry process, the formation of clinker from raw materials occurs via four sub-processes [5]:

a. Drying and preheating
b. Calcining
c. Sintering or clinker formation
d. Clinker cooling process

The remaining section of this chapter describes the clinker formation process and equipment by splitting up into four different subprocesses.

2.3 Drying and Preheating Process

In drying and preheating process, solid materials interact with the preheater exhaust gas in the rawmill and preheater tower, and as a result, rawmill feed loses a part of chemically and physically bound water. At the end of drying and preheating process, a fraction of solid materials is calcined, but the conversion is usually lower than 10%.

2.3.1 Raw Mill and CF-silo

In the rawmill (vertical roller press) in Kjøpsvik plant, the rawmill feed is grinded to a very fine powder (90% particles have a particle size less than 90 μm) using the vertical roller press. The feed consists of a mixture of quartz, limestones, high-grade limestones and iron (mainly iron oxide). The grinded feed is transported to the CF-silo and finally to the preheater tower. An internal cycle in the rawmill ensures that particles are grinded to a desired size distribution. When the kiln is in operation, the temperature of exhaust gas entering into the mill is about 100°C. This heat is utilised partially for drying and preheating of the solid materials.

The significant changes that take place in rawmill are:

- Grinding of rawmill feed to a very fine form and feeding to the preheater tower through CF-silo
- Evaporation of free water present in the rawmill feed
- Absorption of volatile components such as SO_x by reactive CaO formed from the grinding of the rawmill feed [8].

2.3.2 Preheating Process

In most of the modern cement plants with dry kiln system, a series of cyclones along with riser duct (preheater tower) is used in the preheating process. The function of preheater tower is to heat up the solid materials to 850-875°C [9] using hot flue gases from the kiln and calciner. A schematic diagram of 5 cyclones with the calciner is shown in Figure 2.2 [10].
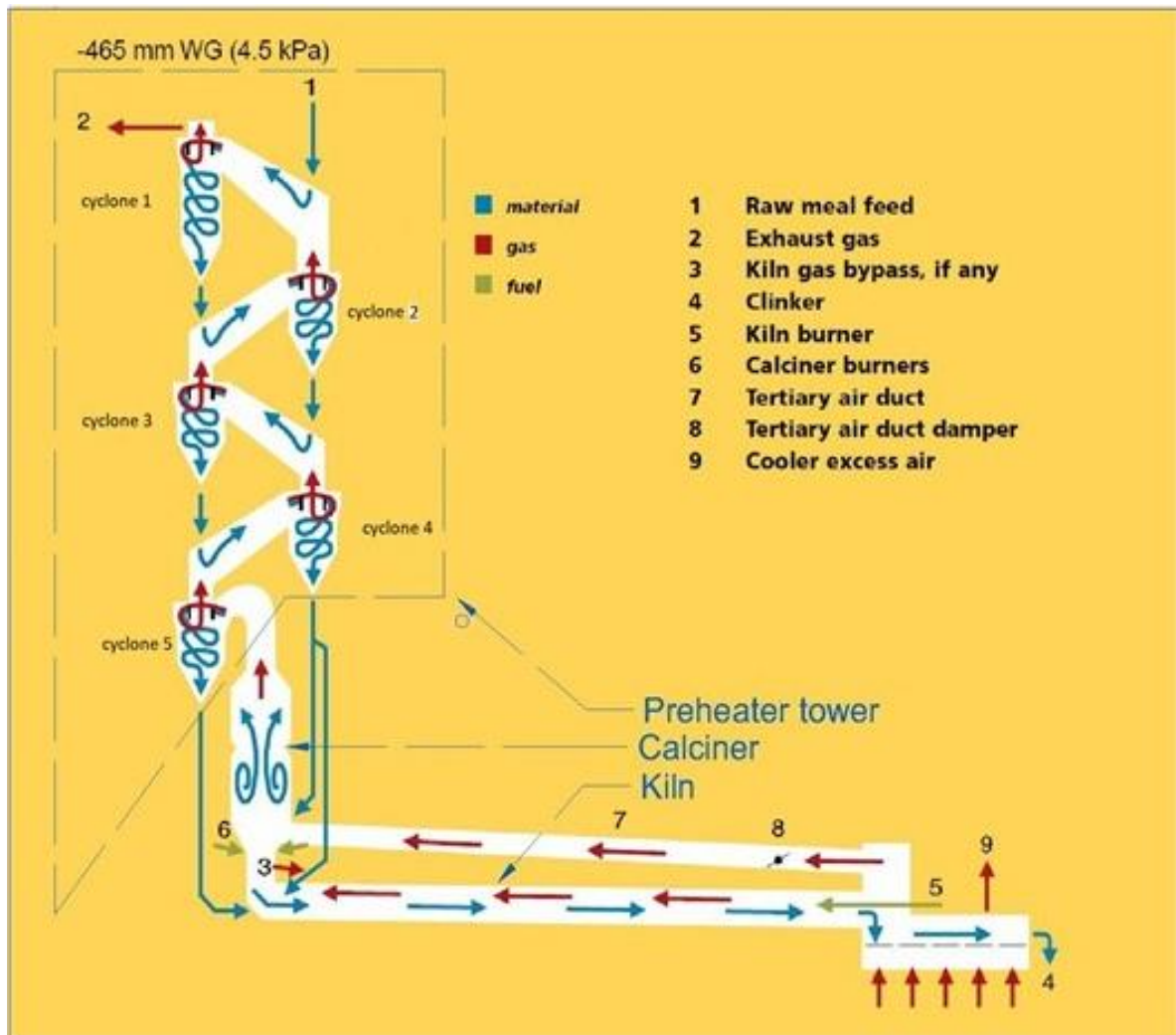
Figure 2.2: A schematic diagram of Inline calciner system similar to the plant in Kjøpsvik [10].

Figure 2.2 shows an inline calciner system (ILC) designed by FLSmidth, similar to the system installed in the Kjøpsvik plant. In the ILC system, the kiln exhaust gas flows into the calciner after mixing with a mixture of combustion gas and hot meal from the hotdisc. Thus, calciner is an integral part of the preheating process in the plant [1, 11].

Description of the Solid and Gas Flows

Solid materials are fed from CF-silo into the riser duct between cyclone 1 and cyclone 2. The exhaust gas from cyclone 2 drags the solids into cyclone 1, where cyclone 1 separates (up to 90% efficiency) solids from the preheater exhaust gas (gas flowing out of the preheater tower). The gas flows into the cooling tower and then to the rawmill. On the other hand, solid particles fall into the riser duct between cyclone 3 and cyclone 2 where the exhaust gas from cyclone 3 drags the solids to cyclone 2. Similarly, solid particles flow from cyclone 2 to cyclone 3 and cyclone 3 to cyclone 4. Solids separated in the cyclone 4 are divided into two parts. The first part (around 20% of the solids separated in cyclone 4) is fed into the kiln riser duct which is dragged back to the calciner by kiln exhaust gases. The main reason behind feeding the solids in the kiln riser duct is to control the kiln exhaust gas temperature entering the calciner, and the secondary reason is to create a restriction in the riser duct which improves the flow of the bypass gas.

The remaining portion (approximately 80% of the solids) flows to the calciner via two routes: directly to the calciner and indirectly after it has passed through the hot disc. In normal

operation with alternative fuels in the hot disc (tyre and RDF), a portion of hot meal enters into the calciner via indirect route after passing through the hotdisc. The fraction of the solids entering into the hotdisc is controlled to obtain stable hotdisc operating temperature. The remaining part flows directly into the calciner. The solids entering into the calciner via three different routes, directly, passing through the hot disc, via kiln riser duct, are calcined in the calciner. The calcining process is discussed separately in section a. The calcined solid particles are forced to flow to cyclone 5 by the swirl of hot flue gases. At the end of preheating process, calcined meal (up to 85-95%) is fed into the kiln.

The most noteworthy process and reactions that occur in the preheating process are:

    a. **Preheating of feed to a calcination temperature.**
    b. Evaporation of free water
    c. Evaporation of physically and chemically bound water
    d. Partial calcination of rawmill feed in the cyclone 4 and 5 (about 10%) via Reaction (2.1) and (2.2):

$$CaCO_3 \xrightarrow{\text{Heat}} CaO + CO_2 \tag{2.1}$$

$$MgCO_3 \xrightarrow{\text{Heat}} MgO + CO_2 \tag{2.2}$$
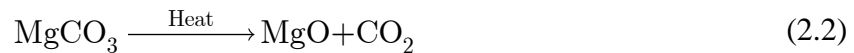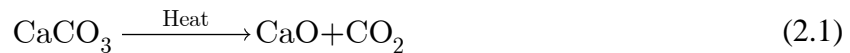
    e. Conversion of metal sulphides to SO_2 via Reaction (2.3):

Schutte et al. point out that metal sulphides present in rawmill feed oxidises to sulphur oxides at 300-600°C in the top cyclone stages in the preheater tower (as cited in Tokeheim, 1999 [6]).

$$-S + O_2 \rightarrow SO_2 \tag{2.3}$$

    f. Absorption of gaseous components by rawmill feed and solidification of volatile components (sodium, potassium, chlorine)

2.4 Calcining Process

CO_2 stripping from the solid materials is known as calcining or decarbonisation process. Reaction 2.3 and 2.4 show the calcination of $CaCO_3$ and $MgCO_3$ in the calciner [11]. In the Kjøpsvik plant, around 85-90% of the calcination takes place in the calciner and preheater tower. Reaction 2.4 and 2.5 show calcination of limestone ($CaCO_3$) and dolomite ($MgCO_3$). To provide additional energy for the calcining process, animal meal, coal, RDF, and tyres are used as fuels in the calciner. As shown in Figure 2.2, a part of clinker cooling air (tertiary air) is used to support secondary combustion in the hotdisc and calciner. RDF and tyres are burnt in the hotdisc, and coal and animal meal are burnt directly in the calciner. A short description of the hotdisc with its schematic drawing is presented in section 2.7.4.

$$CaCO_3 \xrightarrow{\text{Heat}} CaO + CO_2 \tag{2.4}$$

$$MgCO_3 \xrightarrow{\text{Heat}} MgO + CO_2 \tag{2.5}$$
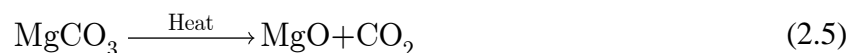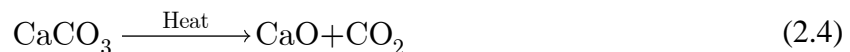
Besides calcination, intermediate clinker phase (belite-C_2S) is also formed via Reaction 2.6 [11].

$$2CaO + SiO_2 \rightarrow C_2S \tag{2.6}$$

2.5 Sintering or Clinkering Process

The sintering or clinkering process is a heating up of the solids up to the melting point of the solid meal to produce clinker. Rotary kiln 5 is used for carrying out sintering process in Kjøpsvik plant.

2.5.1 The Rotary Kiln

Rotary kiln (called Rotary kiln 5 in Kjøpsvik plant) is a long cylinder (drum) rotating at 1-4 rpm in an axial direction. The rotation speed of the kiln is primarily based on the kiln feeding. For instance, the speed is 3 rpm when kiln feed is 115 t/hr. Figure 2.3 shows a pictorial view of the rotary kiln in the plant in Kjøpsvik. The kiln is inclined at a small angle, kiln outlet being at a lower position, which facilitates the flow of clinker towards the grate cooler and the gas-flow towards the preheater tower. The temperature of solid phases reaches up to 1450°C which is higher than the melting point of the steel, so, the kiln is internally protected by bricks (a refractory material).

Figure 2.3: A pictorial view of rotary kiln used in Kjøpsvik plant.

Figure 2.1 and Figure 2.2 shows the gas flow, fuels flow and solid flow into and out of the kiln. The clinker cooling gas is used for the cooling and transport of combustion gases. It is also used for the complete combustion of the fuels. Primary air is responsible for swirling motion and ignition of the fuels in the kiln. In the Kjøpsvik plant, the fuels used in the primary burner is finely grinded coal and waste oil. The temperature is usually around 1000°C in the kiln inlet and 1200°C in the kiln outlet. In the clinkerization zone, the temperature of solids is up to 1450°C [1]. However, the flame temperature can be as high as 2000°C.

Figure 2.4 shows different phases of solid materials in the kiln. Based on the cement phases present in the kiln sections, the kiln can be divided into three distinct zones. The zones are calcining, transition and sintering/clinkerization zone.
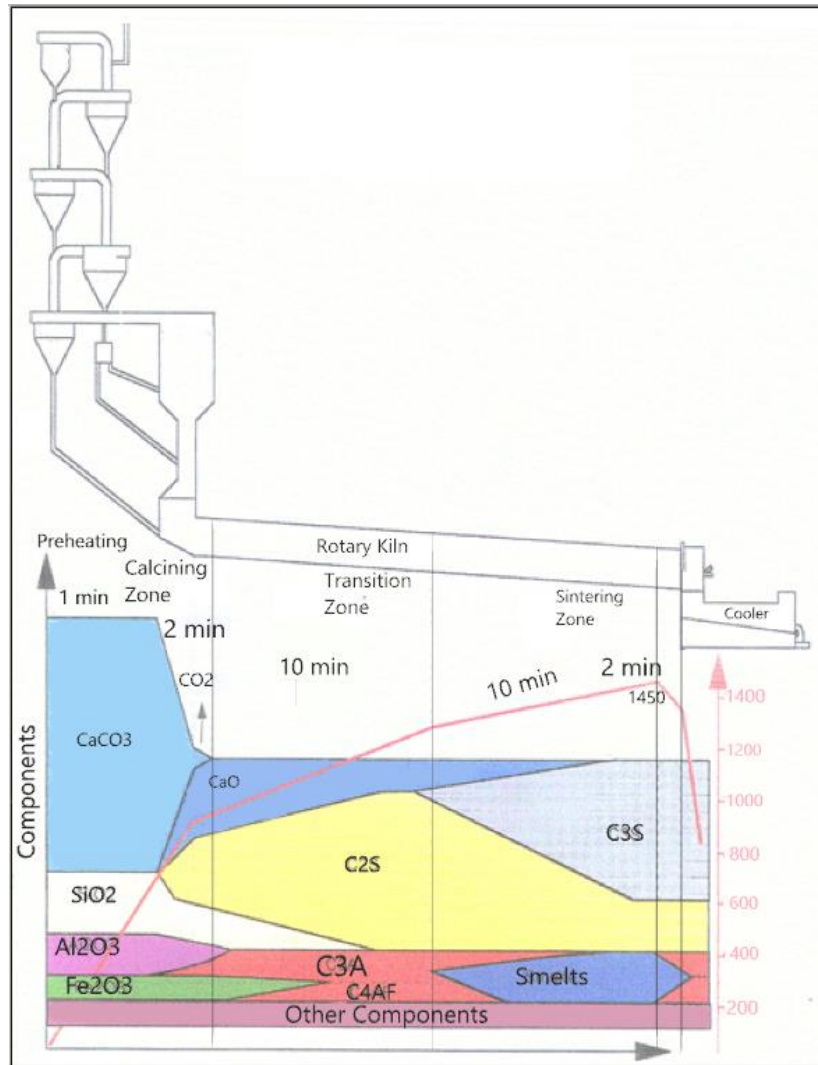
Figure 2.4: Cement clinker formation process in the dry process kiln.

a. Calcining zone

In a preheater system equipped with a calciner, the calcining zone usually occupies one-tenth of the total kiln length. In this zone, a remaining portion of the uncalcined hot meal is calcined [11].

b. Transition zone

In this zone, various solid phases reactions occur, and belite, ferrite and aluminite are formed. Some of the literature mentions this zone as a solid-state reaction zone [12]. The most important reactions occurring in this zone are:

$$2CaO + SiO_2 \longrightarrow C_2S \text{ (Belite)}\,[1] \tag{2.7}$$

$$3CaO + Al_2O_3 \longrightarrow C_3A \text{ (Aluminite)} \tag{2.8}$$

$$4CaO + Al_2O_3 + Fe_2O_3 \xrightarrow{\text{Heat}} C_4AF \text{ (Ferrite)} \tag{2.9}$$

---
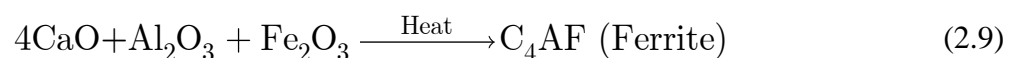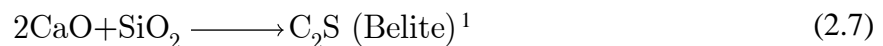
[1] In cement nomenclature, CaO, SiO_2, Fe_2O_3 and Al_2O_3 is represented as C, S, F, and A respectively.

Reaction 2.7 shows formation of belite (C_2S) (one of the vital cement phases out of four cement phases) by the combination of calcium oxide (CaO) and alumina (Al_2O_3) in the transition zone. In addition to belite, intermediate products, such as calcium aluminate (C_3A) and calcium ferrites (C_4AF), are formed via Reaction 2.8 and Reaction 2.9 respectively [12].

  c. Sintering zone

It is the hottest zone in the kiln where belite fuses with free lime (CaO) to form alites (main clinker phase). In this zone, the outer surface of solid materials begins to melt (aluminate and ferrite phases), and agglomerates are forming nodules known as clinker. In the outer layer of these nodules, belite combines with free CaO to form alites via Reaction 2.10. To maintain the clinker quality, the kiln is operated in such a way that there is enough time/temperature for fusion of belites with CaO to form alites and reduce the free lime content in the clinker (less than 1% w/w) [12].

$$C_2S + CaO \rightarrow C_3S \text{ (Alite)} \tag{2.10}$$

2.5.2 The Primary Burner

In the kiln in Kjøpsvik plant, the primary burner is used to combust primary fuels, coal and waste oil. Figure 2.5 shows a cross-sectional view of the burner used in the plant. It is a Duoflex burner supplied by FLSmidth. It has an annular coal duct (1), and the potential for supply of alternative fuels (2,5), liquid fuels (waste oil in this plant) (3), and gaseous fuels (4). It also includes a concentric annular channel for radial air and axial air supply which are mixed in a specified proportion to achieve desired swirl motion [13, 14].

The most notable reaction occurring in the burning zone is combustion of hydrocarbon and sulphides present in the fuels (Reaction 2.11).

$$C_xH_yO_zS_a + \left(x + \frac{y}{4} - \frac{z}{2} + a\right)O_2 \xrightarrow{\text{Combustion}} xCO_2 + \frac{y}{2}H_2O + aSO_2 \tag{2.11}$$

Figure 2.5: A cross-section of the primary burner [14].

2.6 Clinker Cooling Process

After the clinker is formed, it is rapidly cooled by a stream of cold air. Alites, one of the most crucial clinker phases, is unstable below 1200°C, and transform back to belites and free lime. To avoid this problem and maintain clinker morphology, a stream of secondary air cools down the clinker from 1450°C to 1200°C in the kiln outlet. The clinkers are further cooled from 1200°C to less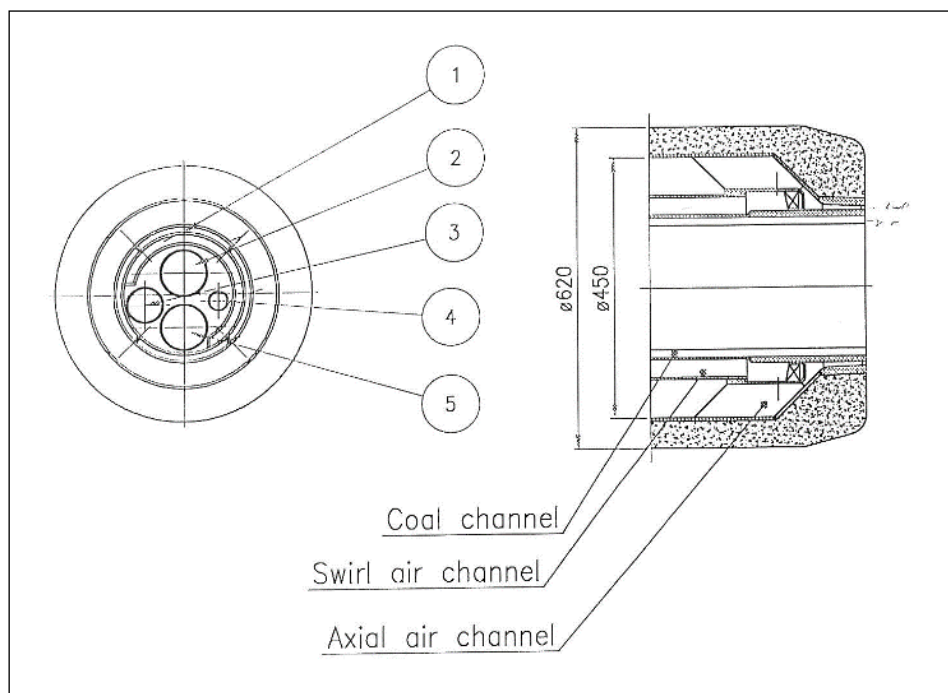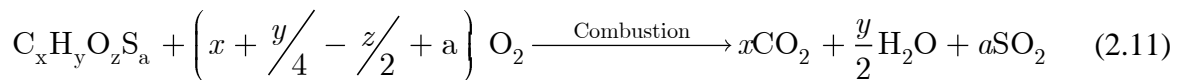 than 100°C in a short period of time using a stream of cold air (clinker cooling air) [15]. The motives behind rapid cooling of clinkers are:

a. Prevent the conversion of alites (C_3S) to belites (C_2S)
b. Preserve the crystal structure of various components in the clinker
c. Recover heat energy
d. Cool the clinker to a sufficiently low temperature before it can be further processed to produce the cement.

2.7 Other Processes

This section describes additional processes: preheater exhaust gas treatment, bypass gas treatment, excess clinker cooling air distribution, and combustion of RDF/tyre in the hotdisc.

2.7.1 Preheater Exhaust Gas Treatment

In the Kjøpsvik plant, the preheater exhaust gas is cooled down in the gas conditioning tower (GCT) to avoid excess thermal load and reduce fan power consumption (as the cooling process reduces volume flow of the gas). In rawmill on mode (RM-ON mode), the gas flows to the fabric filter passing through the rawmill, and in rawmill off mode (RM-OFF mode), the gas flows directly to the fabric filter. In the rawmill, rawmill feed in the presence of moisture absorbs a portion of SO_x, chlorides and volatile metals. The gas is cooled further and then de-dusted in the fabric filter. Some of the volatile compounds, alkali chloride and sulphur compounds, are captured in the dust surface. Finally, the cleaned gas is mixed with the bypass gas and released to the atmosphere via main stack gas pipe.

2.7.2 Bypass System

Alkalis, chloride and sulphur compounds evaporate in the sintering zone of the kiln and cool down in a relatively cold preheater and calciner. The evaporation and condensation process occurs for several cycles before these components leave the system as part of clinker and exhaust gases. The evaporation and condensation processes can lead to a collosal material recirculation phenomenon, decline in product quality, increase the emissions, and can also cause an operational problem such as a blockage. In order to avoid high concentration of these volatile components in the preheater and kiln, part of the kiln gas (maximum designed capacity is 60% total kiln exhaust gas), is purged out of the kiln [15]. This gas is known as bypass gas. The gas is hot and rich in SO_x, alkalis, mercury and chloride pollutants, so, it must be pre-treated before it is released into the atmosphere. Figure 2.6 shows a schematic diagram of bypass system in the Kjøpsvik plant. The system consists of a quench chamber, gas suspension absorber (GSA), cyclone separator, fabric filters, gas recirculation duct, dust recirculation duct, dust storage and transport system.
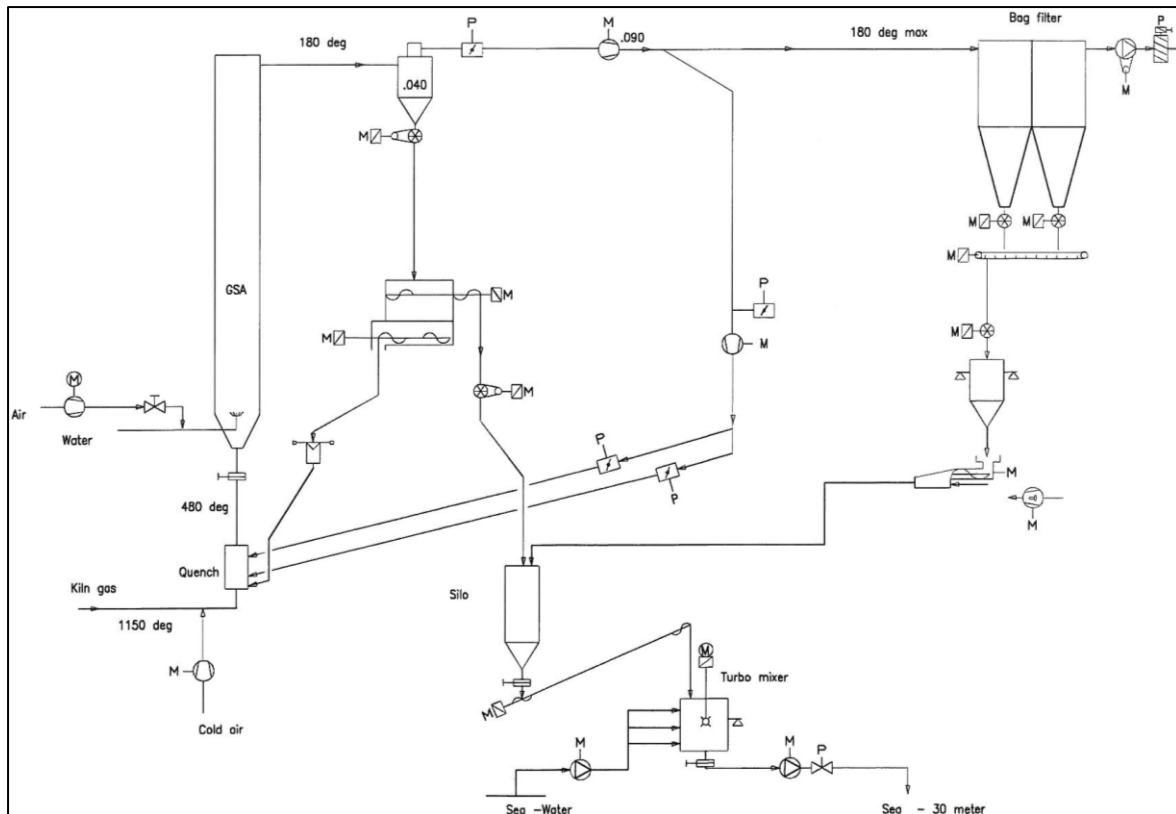
Figure 2.6: Bypass system with GSA, cyclone separator, fabric filters and other accessories [14].

The bypass gas is cooled in the quench chamber by recirculating a portion of bypass gas from the bypass cyclone (roughly temperature of 150-180°C), as shown in Figure 2.6. The recirculated gas is divided into two parts and enters the quench chamber via two separate ducts, thus forming vortex motion in the quench chamber. The vortex increases the effectiveness of gas quenching process. The quenched gas passes through the GSA, where water is sprayed to cool down the gas. In the GSA, suspended dust particles absorb SO_2 and alkalis in the presence of moisture [8]. The gas is then passed through the cyclone separator which separates dust from the bypass gas. A portion of separated dust from the cyclone (usually fine dust) is recirculated back into the quench chamber. The dust grows in size by absorption of alkalis and sulphur in the surface of the dust particles as well as the coalescence of dust particles and then flows back to the cyclone separator with the bypass gas. The absorption efficiency of volatiles by dust particles is increased with the increase in flow rate of bypass water. Coarse dust is then collected and transported to the dust storage. The gas cleaned in the bypass cyclone is further cleaned in the bypass filter (Bag filter) and then mixed with the preheater exhaust gas. The fine dust from bypass filter is also mixed with the coarse dust from the bypass cyclone in the bypass dust silo and sold as cement product. Eventually, mixed gas (Stack Gas) is released into the atmosphere via main gas stack pipe.

2.7.3 Clinker Cooling Air Distribution

In the cooler, air is used to cool down the clinker. The air stream is divided into three parts. The first part, secondary air, is used for exhaust gas transport, and ensure complete combustion of the rotary kiln fuels. The second part, tertiary air, is supplied to hotdisc and calciner to assist the burning of alternative fuels (RDF, Tyre, animal meal and Coal). The remaining part, excess cooler gas, is divided into two substreams. The first substream is used to preheat the coal in the coal mill, and the rest is de-dusted in the ESP and released into the atmosphere.

2.7.4 Combustion in Hotdisc

In the Kjøpsvik plant, hotdisc, a separate combustion chamber, is used to burn RDF and tyres. Tertiary air is used in the combustion process, and then hot combustion gas is transported to the calciner where the gas assists in the calcining process. Figure 2.7 shows a wireframe view of the hotdisc and its internal components. The disc has an inlet for fuel (RDF and tyre) and air (hot tertiary air), and it rotates at a maximum speed of 4.5 rpm. The combusted gas along with the ash leaves the chamber through the kiln riser duct. The scraper is used to remove adhered ash and residues in the chamber. The maximum design capacity of hotdisc is up to 40% of the secondary fuel (196 kJ/kg clinker). The temperature in the disc is controlled by varying the fuel and hot meal flow into the disc [14, 16]. The disc provides long retention time for alternative fuel burning. For this reason, different types of alternative fuels, tyres (whole or shredded), plastics, wood, sludges and other waste fuel can be used in the hotdisc [17].
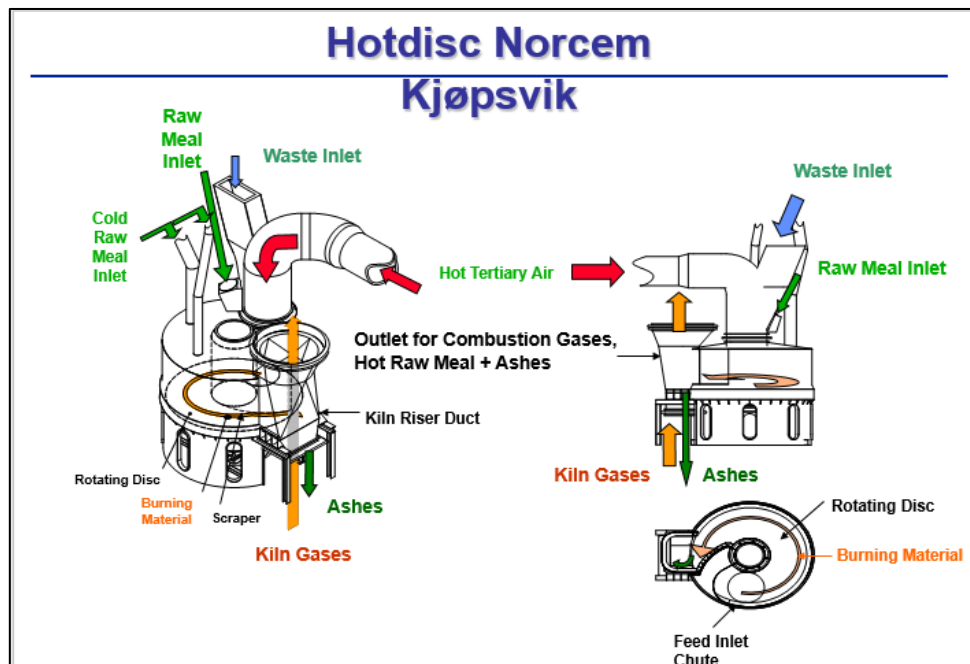

Figure 2.7: A wireframe view of the hotdisc and internal components [14].

3 Sulphur Behaviour in the Kiln System

This chapter presents sulphur behaviour in the kiln; formation of SO_2, circulation of sulphur in the form of sulphates and SO_2, and removal of sulphur in the clinker and exhaust gases. This chapter also includes sulphur material balance model to determine sulphur flow in different streams.

3.1 Admission of Sulphur and Volatiles into the System

Sulphur and other volatile components enter the kiln through fuel and raw materials [18]. Raw materials consist of a variety of inorganic minerals, calcium carbonates, magnesium carbonates, silica, iron oxide, and alumina [1]. Beside these major components, raw materials also consist of alkalis (potassium and sodium), chlorides, sulphur, and heavy metal in trace amounts. Sulphur is predominantly present in the form of pyrite (FeS_2) and pyrrhotite (FeS). It is also present in other forms such as calcium sulphide, and calcium sulphates in trace amounts. The contribution of raw materials is as high as 80-90% of the total sulphur input in the kiln. Table 3.1 shows a typical composition of sulphur, alkalis and chlorine in raw materials [1].

Table 3.1: Typical composition of sulphur, alkalis and chlorine in raw materials, limestones and clay [1].

Components	Raw materials	Clay	Limestone, Limemarl, chalk
	Mass fraction [% w/w]		
SO_3[2]	0-1.5	0.0-4.0	0.0-0.7
Cl	0.0-0.3	0.0-1.0	0.0-0.6
K_2O	0.1-1.5	0.4-5.0	0.0-3.5
Na_2O	0.1-0.5	0.1-1.5	0.0-1.5

Likewise, fuels contain sulphur in various proportions and contribute significantly to the emission of sulphur and other volatile components. Table 3.2 shows typical compositions of sulphur, chlorine, sodium and potassium content in the fuels used in the Kjøpsvik plant. Average sulphur content in the coal is 0.6% w/w, in the waste oil is 0.3% w/w, in the animal meal is 0.5%, and, in the tyre is 1.5% (excluding steel component). However, sulphur in the RDF can vary drastically from 0.2% to 1.3% depending upon the solid waste sources.

Similarly, chlorine and alkalis are introduced into the system from raw materials and fuels. Chlorine is present in raw materials in the form of crystals of metallic chlorides. In the fuel, chlorine is present as organically bound chlorine [19]. The chlorine content in a typical raw material is up to 0.3% w/w (Table 3.1). On the other hand, the composition of chlorine in RDF can be as high as 0.8% w/w in comparison to 0.1% w/w in the coal, and 60 ppm in the waste oil. Alkalis, sodium and potassium, are present in raw materials in the form of crystalline alkali salts. Clay consists of a significant amount of potassium (5% w/w) and sodium (1.5% w/w) (Table 3.1) and contributes significantly to total potassium input in the kiln. In the fuels, alkalis are either present as organic crystalline salts or organically bound potassium. Potassium content in the coals is as high as 1.5% w/w K_2O equivalent and in trace amounts in other fuels (Table 3.2). In case of sodium, it is present in a significant amount in RDF (1.1% w/w Na_2O equivalent), while relatively low amounts in the coal, RDF and animal meal.

---

[2] Sulphur content expressed in terms of SO_3

Table 3.2: Typical composition of sulphur, chlorine, alkalis in different types of fuel used in Kjøpsvik.

Components	Coal	Waste oil	RDF	Animal meal	Tyre Without Steel
	Mass fraction (% w/w)				
S	0.5	0.3	1.3 (non-pellets) 0.3 (pellets)	0.0-0.5	1.5
Cl	0.1	0.007	0.8	………	0.08
K_2O	0.1-1.5	……....	0.0-0.5	0.5-0.7	……..
Na_2O	0.1-0.5	……..	0.2-1.1	0.6-0.9	……..
Moisture	<1.0	9.8	………	………	……..
Calorific Value (MJ/kg)	27.8	37.2	20.7	………	32

3.2 Fate of Sulphur and Other Volatiles

Sulphur entrained to the kiln system end up in various forms, SO_2, alkali sulphates, calcium sulphates and mixed sulphates. The fate of sulphur depends upon the location of SO_2 formation in the kiln, the presence of free CaO, and the composition of alkalis and chlorine. Upcoming sections discuss the fate of sulphur in the clinker formation process.

3.2.1 Formation of SO_2 in the Preheater

Sulphur in raw materials (pyrite and pyrrhotite) reacts with oxygen to produce SO_2 at a temperature range of 300-600°C. Pyrite yields SO_2 through a two-step reaction mechanism. In the first step, pyrite yields FeS and SO_2 via Reaction 3.1. The favourable temperature for this reaction is 300-600°C; This temperature corresponds to the temperature in the first and second cyclone stages. In the next step, pyrrhotite oxidises to iron oxide (Fe_2O_3) and SO_2 via reaction 3.2. It occurs at a higher temperature (>600°C); Almost complete conversion of sulphide to SO_2 occurs at this temperature. This reaction occurs mainly in 2nd, 3rd and 4th cyclone stages in the preheater tower [8].

$$FeS_2(s) + O_2(g) \rightarrow FeS(s) + SO_2(g) \tag{3.1}$$

$$FeS(s) + 1.75O_2(g) \rightarrow 0.5Fe_2O_3(s) + SO_2(g) \tag{3.2}$$
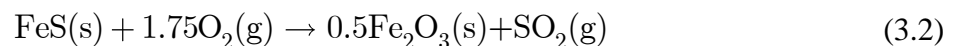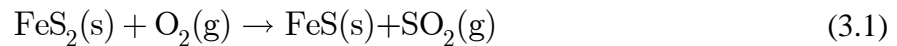
In the case of fuel-sulphur, organically bound sulphur oxidises to SO_2 as soon as fuel is injected in the calciner and kiln. Reaction 3.3 shows combustion of fuel-sulphur to SO_2.

$$-S(fuel) + O_2(g) \rightarrow SO_2(g) \tag{3.3}$$

3.2.2 Emission of SO_2 from the Preheater

A portion of SO_2 formed in the preheater is transported with the preheater exhaust gas. Another part is absorbed by freshly formed reactive CaO and alkalis and enters the kiln in the form of calcium sulphates and alkali sulphates. Capture of SO_2 by the solids in the top cyclone stages is less effective due to insufficient CaO[3]. The effluent SO_2 present in the preheater exhaust gas is further absorbed by suspended dust particles in the gas conditioning tower (GCT) and rawmill feed in the rawmill. The dust (cement kiln dust) is separated in a fabric filter and transported back to the preheater tower. Along with the dust, sulphur and other volatiles

---

[3] Calcination requires a temperature about 895°C while sulphide oxidation occurs at 300-600°C.

absorbed by the cement kiln dust (CKD) are also circulated back to the preheater. The unabsorbed SO_x in the gas flowing out of the fabric filter is then released into the atmosphere.

3.2.3 Sulphur Capture in the Clinker and Recirculation Phenomena

In the calciner and lower cyclone stages (cyclone 4 and 5), SO_2 released from the oxidation of sulphides present in solid materials and calciner fuels is transported by kiln exhaust gas and absorbed by freshly formed reactive CaO as well as alkalis. The absorption of SO_2 by reactive CaO takes place via reaction 3.4 and 3.5 [1].

$$CaO(s) + SO_2(g) \rightarrow CaSO_3(s) \tag{3.4}$$

$$CaSO_3(s) + \frac{1}{2}O_2(g) \rightarrow CaSO_4(s) \tag{3.5}$$
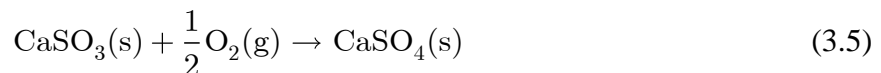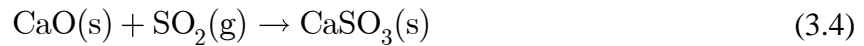
Alkalis react with sulphur in the inlet and the transition zone of the rotary kiln. Reaction 3.6 and 3.7 shows a capture of SO_2 by alkalis. Thus formed alkali sulphates, and calcium sulphates are transported to the burning zone along with solid materials [8].

$$2KCL(s) + SO_2(g) + O_2(g) \rightarrow K_2SO_4(s) + Cl_2(g) \tag{3.6}$$

$$2NaCl(s) + SO_2(g) + O_2(g) \rightarrow Na_2SO_4(s) + Cl_2(g) \tag{3.7}$$
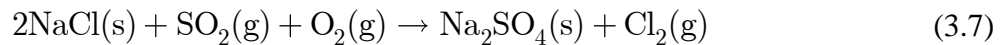
In the burning zone, a portion of the alkali sulphates, trace amounts of calcium sulphate and mixed sulphates leave the kiln in the clinker. The concentration of SO_3 in the clinker is 1.0-1.5% w/w. Generally, alkalis leave the system in the clinker as alkali chlorides or alkali sulphates, but alkalis might leave the clinker in other forms as well. The degree of sulphatization measures the efficiency of sulphur capture by excess[4] alkalis, and it indicates the intensity of the volatile circulation (sulphur, alkalis and chlorine) between the preheater, calciner and kiln. Equation 3.8 is an equation to calculate the degree of sulphatization in the clinker [6].

$$SD_{out} \triangleq \frac{\dot{n}_{SO_3,CL}}{\dot{n}_{K_2O,CL} + \dot{n}_{Na_2O,CL} - 2\dot{n}_{Cl,CL}} 100\% \tag{3.8}$$

A sulphatization degree of 100% means almost all sulphur in the clinker is chemically combined with alkalis. If it is below 100%, excess alkalis leave the clinker in other forms rather than only as alkali sulphates or alkali chlorides and above 100% means excess sulphur leaves the clinker in other forms rather than just alkali sulphates. In the Kjøpsvik plant, average sulphatization degree in December 2017 was 79%. It indicates that excess alkalis are leaving the clinker in other forms rather than only as sulphates or chlorides.

In the sintering zone, another part of alkali sulphates and most of the alkali chlorides evaporate which are transported back to the preheater and calciner with the kiln exhaust gas. Calcium sulphate decomposes to free lime (CaO) and SO_2 in the burning zone, and thus formed SO_2 flows back to the preheater tower with the kiln gas. Reaction 3.9 is a decomposition reaction of calcium sulphate to SO_2 at a higher temperature (>1200°C).

---

[4] Difference between total moles of alkalis and moles of alkalis combined with the chlorides

$$CaSO_4 \rightarrow CaO + SO_2 + \frac{1}{2}O_2 \qquad (3.9)$$
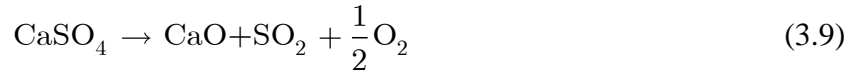
The stability of calcium sulphate is drastically reduced with rising temperature; Almost complete decomposition of $CaSO_4$ occurs at a temperature higher than 1200°C [20]. Swift et al. suggested that the decomposition of calcium sulphate begins at 800°C (0.33% decomposition) and is completed at 1375°C (99.5°C). The rate of decomposition is enhanced by the presence of fuel radicals (carbon and hydrocarbon radicals) which are formed during combustion of fuels [20]. Reaction 3.10 and 3.11 show decomposition of calcium sulphates in the presence of reducing radicals.

$$CaSO_4 + CO\cdot \rightarrow CO_2 + CaO + SO_2 \qquad (3.10)$$

$$CaSO_4 + 2H\cdot \rightarrow H_2O + CaO + SO_2 \qquad (3.11)$$
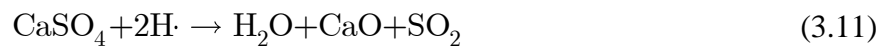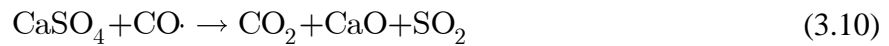
In addition to the reducing fuel radicals, the SO_2 concentration drops in the bypass gas with the available O_2 level in the kiln inlet [8]. Figure 3.1 shows the SO_2 in the bypass gas at specific oxygen composition in the kiln inlet [8]. It shows that the SO_2 level in the bypass gas drastically decreases with the increase in oxygen composition in the kiln exhaust gas. 3% O_2 in the rotary kiln exhaust gas is a favourable condition for excellent sulphur capture by solid materials.
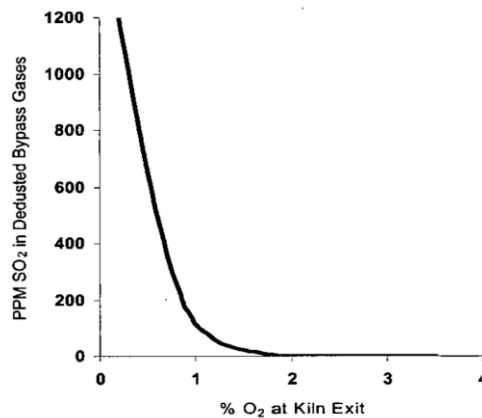
Figure 3.1: A plot of sulphur (ppm in bypass gas)) in the bypass to the O_2 (% of bypass gas) in the bypass.

In addition to O_2 level and temperature, the circulation of sulphur depends on the chloride circulation in the kiln. Experimental tests have shown that sulphur emissions decreased from 375 ppm to as low as 100 ppm by addition of chloride salt in raw materials [19].

Recirculation Phenomena

The process of formation and decomposition of $CaSO_4$ occurs several times due to the transport of sulphur by solid materials from the preheater tower to the kiln and back to the preheater tower by the kiln gas. It occurs several times before sulphur leaves the system in the clinker, bypass dust (mainly as alkali sulphates and mixed sulphates) and stack gas. Similar phenomena occur with alkalis and chlorides due to their volatile nature at higher temperatures.

Figure 3.2 shows the circulation of volatiles in the preheater, calciner and kiln and the removal of volatiles from the system.
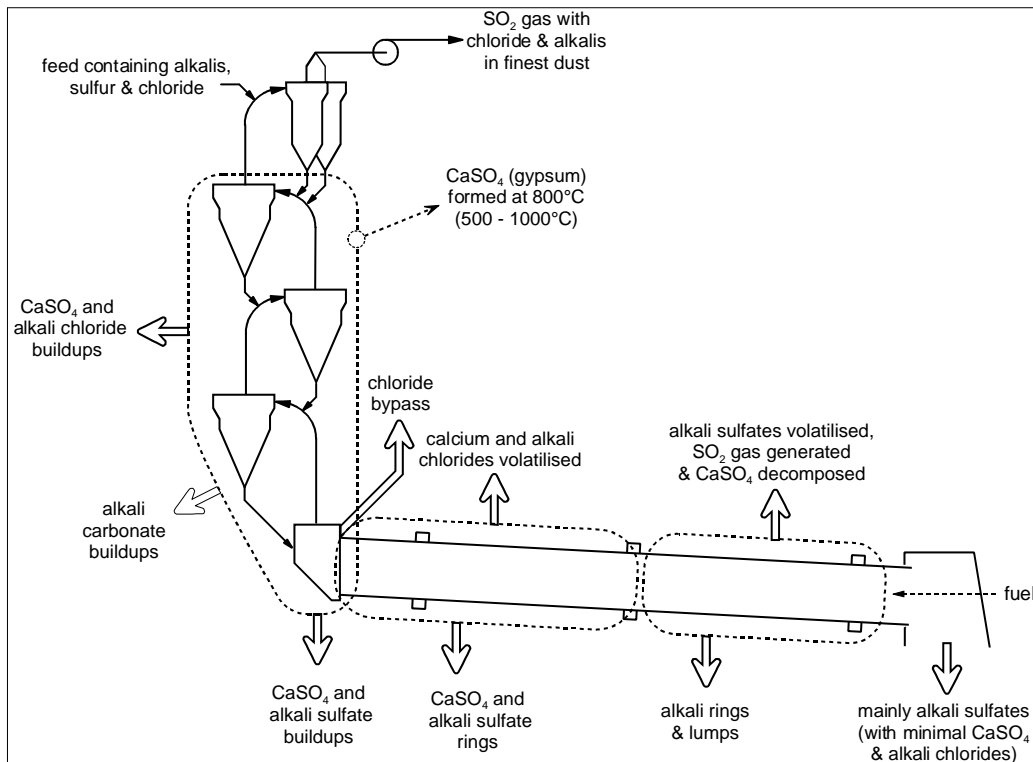
Figure 3.2: Recirculation of volatile components, alkalis, chlorides, and sulphur in the kiln system [14].

3.2.4 Sulphur in the Bypass Gas

In order to avoid high concentrations of alkali and chloride due to the recirculation phenomena, bypass gas is purged out from the kiln inlet. Along with alkalis and chlorine, sulphur in the form of SO_2 and traces of sulphates leaves the kiln with bypass gas. Suspended dust particles in the gas capture a part of SO_2 and rest is emitted to the atmosphere [8]. The average concentration of sulphur in the bypass dust in 2017 was 4.5% w/w in the plant in Kjøpsvik.

3.3 Sulphur Material Balance in Clinker Formation Process

This section together with remaining sections presents a formulation of sulphur flow model in the clinker formation process.

3.3.1 Block Diagram

Figure 3.3 shows a block diagram representation of the clinker formation process focusing on inflow and outflow of sulphur. It consists of flow streams that either introduce sulphur into the system or emit out of the system. These streams are gas streams (red), fuel streams (blue), feed stream (brown), product stream (green), dust streams (magenta), and internal solid streams (black). Gas streams represent all fresh air streams, preheater exhaust gas, kiln exhaust gas, bypass gas and stack gas. Fuel streams represent feeding of the tyre, RDF (both non-pellets and pellets type), animal meal, and coal into the calciner, and waste oil and coal into the rotary kiln. The feed stream is rawmill feed into the rawmill. Dust flow streams represent cement kiln dust (CKD), and bypass dust. Internal solid streams are flow streams of the kiln feed and hot meal, and product flow stream represents the flow of clinker. Flow variables associated with these streams which are required to establish sulphur material balance is described in section 3.2.
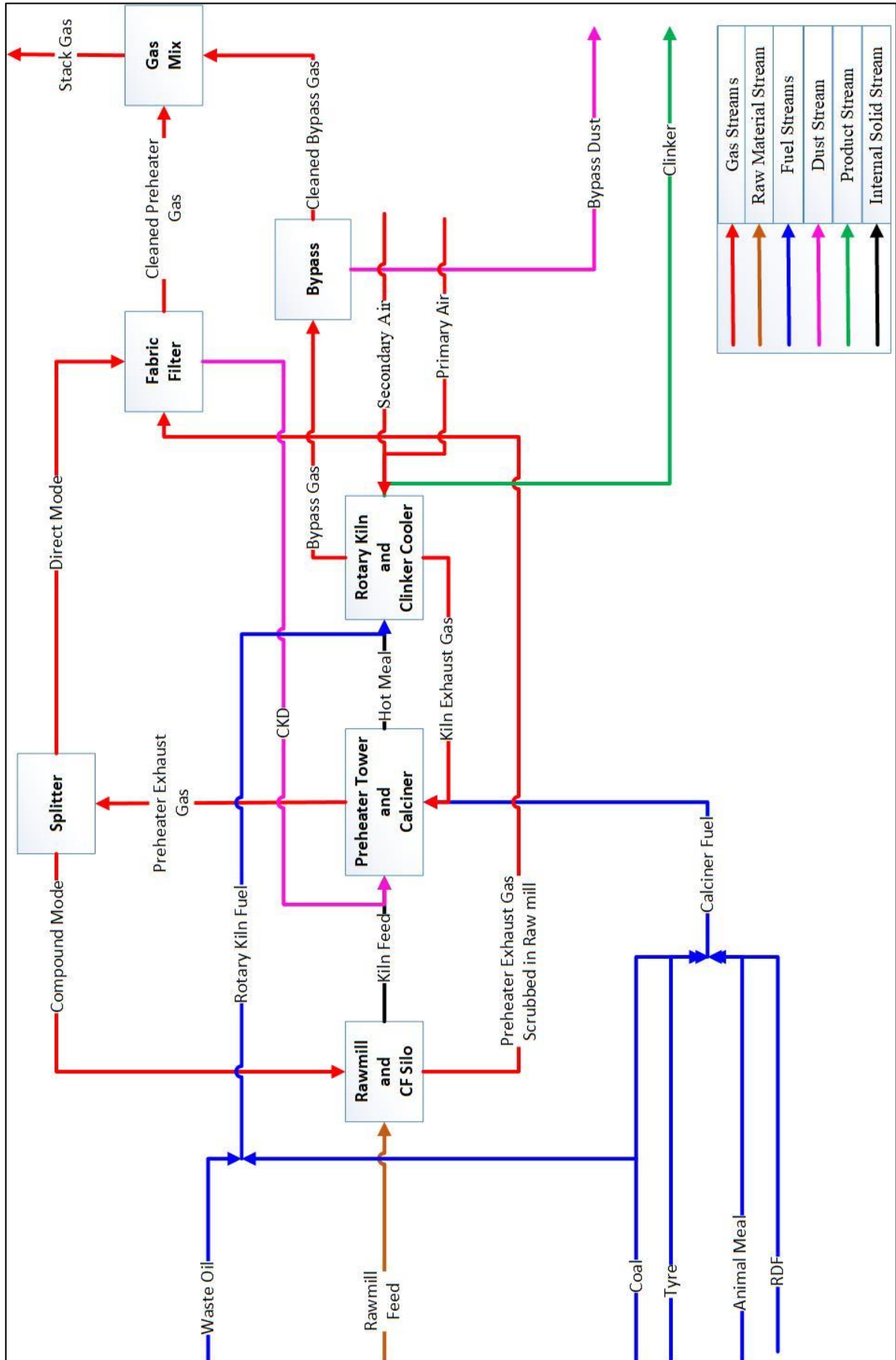
Figure 3.3: Block diagram representation of sulphur inflows and outflows in the clinker formation process.

3.3.2 Description of Flow Variables

Table 3.3 shows a list of flow variables associated with solid material flow streams. In the block diagram, solid material flow streams refer to rawmill feed, kiln feed, hot meal, clinker, bypass dust and cement kiln dust.

Table 3.3: List of flow variables and their description associated with solid material flow streams.

| Variables	Units	Description	Type
Rawmill feed			
$\dot{m}_{RMF,RM,in}$	[kg/h]	Mass flow rate of rawmill feed into the rawmill	Input
$w_{SO_3,RMF,RM,in}$	[-]	Weight fraction of sulphur in terms of SO_3 equivalent in rawmill feed	Input
$\dot{m}_{SO_3,RMF,RM,in}$	[kg/h]	Flow rate of sulphur in terms of SO_3 equivalent in rawmill feed	Calculated
$\dot{m}_{S,RMF,RM,in}$	[kg/h]	Flow rate of sulphur in rawmill feed	Calculated
Accumulation in CF-silo			
$\Delta\dot{m}_{CF}$	[kg/h]	Average accumulation rate of kiln feed in the CF-silo	Input
$\Delta\dot{m}_{SO_3,CF}$	[kg/h]	Accumulation rate of sulphur in terms of SO_3 equivalent in the CF-silo	Calculated
$\Delta\dot{m}_{S,CF}$	[kg/h]	Accumulation of sulphur in the CF-silo	Calculated
Kiln Feed			
$\dot{m}_{KF,PT,in}$	[kg/h]	Mass flow rate of kiln feed into the preheater tower	Input
$w_{SO_3,KF,PT,in}$	[-]	Weight fraction of sulphur in terms of SO_3 equivalent in the kiln feed flowing into the preheater tower	Measured
$\dot{m}_{SO_3,KF,PT,in}$	[kg/h]	Mass flow rate of sulphur in terms of SO_3 equivalent in the kiln feed flowing into the preheater tower	Calculated
$\dot{m}_{S,KF,PT,in}$	[kg/h]	Mass flow rate of sulphur in the kiln feed flowing into the preheater tower	Calculated
Hot Meal			
$R_{KF\_2\_HM}$	[-]	Kiln feed to hot meal ratio	Calculated
$\dot{m}_{HM,RK,in}$	[kg/h]	Hot meal feeding rate in the kiln inlet	Calculated
$w_{SO_3,HM,RK,in}$	[-]	Weight fraction of sulphur in terms of SO_3 equivalent in the hot meal flowing into the rotary kiln	Measured
$\dot{m}_{SO_3,HM,RK,in}$	[kg/h]	Mass flow rate of sulphur in terms of SO_3 equivalent in the hot meal flowing into the rotary kiln	Calculated
$\dot{m}_{S,HM,RK,in}$	[kg/h]	Mass flow rate of sulphur in the hot meal flowing into the rotary kiln	Calculated
Clinker			
$\dot{m}_{CL,RK,out}$	[kg/h]	Mass flow rate of the clinker product out of the rotary kiln	Measured
$w_{SO_3,CL,RK,out}$	[-]	Weight fraction of sulphur in terms of SO_3 equivalent in the clinker flowing out of the rotary kiln	Measured
$\dot{m}_{SO_3,CL,RK,out}$	[kg/h]	Mass flow rate of sulphur in terms of SO_2 equivalent in the clinker flowing out of the rotary kiln	Calculated
$\dot{m}_{S,CL,RK,out}$	[kg/h]	Mass flow rate of sulphur in the clinker flowing out of the rotary kiln	Calculated
Bypass Dust			
$\dot{m}_{D,BP,out}$	[t/h]	Mass flow rate of the dust flowing out of the bypass	Measured
$w_{SO_3,D,BP,out}$	[-]	Weight fraction of sulphur in terms of SO_3 equivalent in the bypass dust flowing out of the bypass	Measured
$\dot{m}_{SO_3,D,BP,out}$	[kg/h]	Mass flow rate of sulphur in terms of SO_2 equivalent in the dust flowing out of the bypass	Calculated
$\dot{m}_{S,D,BP,out}$	[kg/h]	Mass flow rate of sulphur in the dust flowing out of the bypass	Calculated

		Cement Kiln Dust (CKD)	
$\dot{m}_{SO_3,CKD,FF,out}$	[t/h]	Mass flow rate of sulphur in terms of SO_2 equivalent in CKD flowing out of the fabric filter	Calculated
$w_{SO_3,CKD,FF,out}$	[-]	SO_3 content in the CKD	Measured
$\dot{m}_{S,CKD,FF,out}$	[kg/h]	Mass flow rate of sulphur in CKD	Calculated
$\dot{m}_{CKD\_RaM}$	[kg/h]	CKD contribution from the rawmill	Calculated
$\dot{m}_{CKD\_G\_PT}$	[kg/h]	CKD contribution from the preheater exhaust gas	Approx.

Table 3.4 shows a list of variables associated with fuel flow streams. Fuel streams are divided into two main streams based on the fuel supply in the calciner (calciner fuels) and fuel supply in the kiln (rotary kiln fuels). There are four types of fuel used in the calciner (RDF, Tyre, Animal meal and coal) and two types of fuel in the rotary kiln (waste oil and coal).

Table 3.4: List of flow variables and their description associated fuel streams.

Variables	Units	Description	Types
		Coal in calciner and Rotary Kiln	
$\dot{m}_{C,Calc,in}$	[kg/h]	Mass flow rate of coal into the calciner	Measured
$\dot{m}_{C,RK,in}$	[kg/h]	Mass flow rate of coal into the rotary kiln	Measured
$w_{S,C}$	[-]	Weight fraction of sulphur in the coal	Measured
$\dot{m}_{S,C,Calc,in}$	[kg/h]	Mass flow rate of sulphur in the coal flowing into the calciner	Calculated
$\dot{m}_{S,C,RK,in}$	[kg/h]	Mass flow rate of sulphur in the coal flowing into the rotary kiln	Calculated
		Waste oil	
$\dot{m}_{WO,RK,in}$	[kg/h]	Mass flow rate of waste oil into the rotary kiln	Measured
$w_{S,WO}$	[-]	Weight fraction of sulphur in the waste oil	Measured
$\dot{m}_{S,WO,RK,in}$	[kg/h]	Flow rate of sulphur in the waste oil flowing into the rotary kiln	Calculated
		Animal Meal	
$\dot{m}_{AM,Calc,in}$	[kg/h]	Mass flow rate of the animal meal into the calciner	Measured
$w_{S,AM}$	[-]	Weight fraction of sulphur in the animal meal	Measured
$\dot{m}_{S,AM,Calc,in}$	[kg/h]	Flow rate of sulphur in the animal meal flowing into the calciner	Calculated
		Tyre	
$\dot{m}_{T,Calc,in}$	[kg/h]	Mass flow rate of the tyre into the calciner	Measured
$w_{S,T}$	[-]	Weight fraction of sulphur in the tyre	Measured
$\dot{m}_{S,T,Calc,in}$	[kg/h]	Flow rate of sulphur in the tyre flowing into the calciner	Calculated
		RDF	
$\dot{m}_{RDF,Calc,in}$	[kg/h]	Mass flow rate of RDF in the calciner	Measured
$w_{S,RDF}$	[-]	Weight fraction of sulphur in the RDF	Measured
$\dot{m}_{S,RDF,Calc,in}$	[kg/h]	Flow rate of sulphur in the RDF flowing into the calciner	Calculated

Table 3.5 shows a list of variables associated with the gas stream. In Table 3.5, gas streams are preheater exhaust gas (compound mode and direct mode), kiln gas, bypass gas, cleaned preheater gas, cleaned bypass gas and stack gas.

Table 3.5: List of flow variables and their description associated with gas streams.

Variables	Units	Description	Type
Preheater Exhaust Gas			
$\dot{m}_{SO_2,G,PT,out}$	[kg/h]	Mass flow rate of SO_2 in the preheater exhaust gas flowing out of the preheater tower	Calculated
$\dot{m}_{S,G,PT,out}$	[kg/h]	Mass flow rate of sulphur in the preheater exhaust gas flowing out of the preheater tower	Calculated
Kiln Exhaust Gas			
$\dot{m}_{SO_2,G,RK,out}$	[kg/h]	Mass flow rate of SO_2 in the preheater exhaust gas flowing into the preheater tower	Calculated
$\dot{m}_{S,G,RK,out}$	[kg/h]	Mass flow rate of sulphur in the preheater exhaust gas flowing into the preheater tower	Calculated
Preheater Exhaust Gas Direct Mode (directly to the fabric filter)			
$\dot{m}_{SO_2,G,FF,Dir,in}$	[kg/h]	Mass flow rate of SO_2 in the gas flowing directly into the fabric filter from the preheater tower (Direct Mode)	Calculated
$\dot{m}_{S,G,FF,Dir,in}$	[kg/h]	Mass flow rate of sulphur in the gas flowing directly into the fabric filter from the preheater tower (Direct Mode)	Calculated
Preheater Exhaust Gas Compound Mode (through Rawmill)			
$\dot{m}_{SO_2,G,RM,in}$	[kg/h]	Mass flow rate of SO_2 in the gas flowing into the rawmill from the preheater tower (Compound mode)	Calculated
$\dot{m}_{S,G,RM,in}$	[kg/h]	Mass flow rate of sulphur in the gas flowing into the rawmill from the preheater tower (Compound mode)	Calculated
Bypass Gas			
$\dot{m}_{SO_2,G,BP,in}$	[kg/h]	Mass flow rate of SO_2 in the bypass gas leaving the kiln	Calculated
$\dot{m}_{S,G,BP,in}$	[kg/h]	Mass flow rate of sulphur in the bypass gas leaving the kiln	Calculated
Preheater Exhaust Gas Scrubbed in the rawmill			
$\dot{m}_{SO_2,G,RM,out}$	[kg/h]	Mass flow rate of SO_2 in the gas flowing out of the rawmill	Calculated
$\dot{m}_{S,G,RM,out}$	[kg/h]	Mass flow rate of sulphur in the gas flowing out of the rawmill	Calculated
Cleaned Preheater Exhaust Gas			
$\dot{m}_{SO_2,G,FF,out}$	[kg/h]	Mass flow rate of SO_2 in the gas flowing out of the fabric filter	Calculated
$\dot{m}_{S,G,FF,out}$	[kg/h]	Mass flow rate of sulphur in the gas flowing out of the fabric filter	Calculated
Cleaned Bypass Gas			
$\dot{V}_{G,BP,out}$	[Nm³/h]	Volume flow rate of the gas flowing out of the bypass system	Estimated
$C_{SO_2,G,BP,out}$	[mg/Nm³]	SO_2 concentration in the gas flowing out of the bypass system	Measured
$\dot{m}_{SO_2,G,BP,out}$	[kg/h]	Mass flow rate of SO_2 in the gas flowing out of the bypass system	Calculated
$\dot{m}_{S,G,BP,out}$	[kg/h]	Mass flow rate of sulphur in the gas flowing out of the bypass system	Calculated
$T_{BP,out}$	[°C]	Temperature in the bypass gas flowing out of the bypass system	Measured

Stack Gas			
$\dot{V}_{G,Stack}$	[Nm^3/h]	Volume flow rate of the stack gas	Output
$C_{SO_2,G,Stack}$	[mg/Nm^3]	SO$_2$ concentration in the stack gas	Output
$\dot{m}_{SO_2,G,Stack}$	[kg/h]	Mass flow rate of SO$_2$ in the stack gas	Calculated
$\dot{m}_{S,G,Stack}$	[kg/h]	Mass flow rate of sulphur in the stack gas	Calculated

Table 3.6 shows sulphur inflow and outflow variables associated with the blocks.

Table 3.6: List of sulphur inflow and outflow in the blocks.

Variables	Units	Description	Type
$\dot{m}_{S,PT,in}$	[Nm^3/h]	Sulphur flow rate into the preheater tower	Calculated
$\dot{m}_{S,F,PT,in}$	[kg/h]	Sulphur flow rate of fuels into the calciner	Calculated
$\dot{m}_{S,PT,out}$	[mg/Nm^3]	Sulphur flow rate out of the preheater tower	Calculated
$\dot{m}_{S,RK,in}$	[kg/h]	Sulphur flow rate into the rotary kiln	Calculated
$\dot{m}_{S,F,RK,in}$	[kg/h]	Sulphur flow rate of fuels into the rotary kiln	Calculated
$\dot{m}_{S,RK,out}$	[Nm^3/h]	Sulphur flow rate out of the rotary kiln	Calculated
$\dot{m}_{S,RM,in}$	[mg/Nm^3]	Sulphur flow rate into the rawmill	Calculated
$\dot{m}_{S,RM,out}$	[kg/h]	Sulphur flow rate out of the rawmill	Calculated
$\dot{m}_{S,FF,in}$	[Nm^3/h]	Sulphur flow rate into the fabric filter	Calculated
$\dot{m}_{S,FF,out}$	[kg/h]	Sulphur flow rate out of the fabric filter	Calculated
$\dot{m}_{S,BP,out}$	[Nm^3/h]	Sulphur flow rate out of the bypass	Calculated
x	[-]	A split ratio of the gas stream to the rawmill and fabric filter	Input

3.4 Model Development

This section presents a model formulation of sulphur flow in the kiln system. It presents sulphur material balances on different blocks based on the general material balance.

3.4.1 General Material Balance

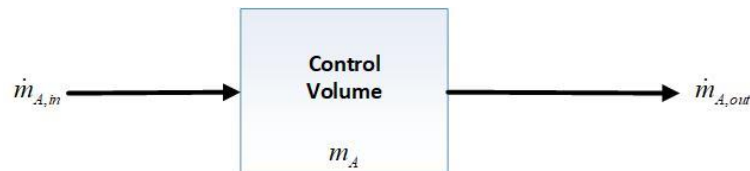Figure 3.4 is a control volume (CV) considered for the material balance of component A.

Figure 3.4: A block diagram representation of the control volume.

Symbol	Units	Description
m_A	[kg]	Mass of A in the CV

$\dot{m}_{A,in}$ [kg/h]   Mass flow rate of A into the CV

$\dot{m}_{A,out}$ [kg/h]   Mass flow rate of A out of the CV

Assuming only stoichiometric reactions take place in the CV, Equation 3.12 represents a general material balance of component A in the CV.

$$\frac{dm_A}{dt} = \dot{m}_{A,in} - \dot{m}_{A,out} \tag{3.12}$$

3.4.2 Assumptions

A list of assumptions for simplifying and achieving closure property in the model are:

    a. There is always steady-state flow in each block except in rawmill and CF-silo block. In steady state flow of component A, the general material balance of A (Equation 3.12) transforms into Equation 3.13. Upcoming sulphur material balance model is based on Equation 3.13.

$$\dot{m}_{A,in} = \dot{m}_{A,out} \tag{3.13}$$

       It is a theoretically invalid assumption as the sulphur deposition takes place in the preheater tower and kiln system. The deposition rate is insignificant in comparison to overall sulphur flows in the system. Therefore, any error in flow estimation based on this assumption is insignificant.

    b. All the solid material streams, gas streams and fuel streams are homogeneous regarding material distribution and sulphur composition.

    c. In the calculation of sulphur flow in the bypass gas, a linear interpolation method (Equation 3.13) is used to approximate bypass gas volume flow out of the bag filter. The reference data is based on prior measurements of the flow rate of bypass gas. The reference data from process audit in 2017 is in Appendix C.

$$\dot{V}_{G,BP,out,wet} = \frac{\dot{V}_{G,BP,out,wet,ref}}{\dot{V}_{G,stack,wet,ref}} \cdot \dot{V}_{G,stack,dry} \tag{3.14}$$

    d. Due to a lack of flow measurement system to measure hot meal flow, kiln feed to hot meal ratio is approximated based on the loss of ignition (LOI) of hot meal. The data was not available for the reference period, so it is approximated that average LOI data of the hot meal is unchanged for the plant in calculation period with reference period. The ratio calculation is presented in Appendix D, and hot meal flow is calculated using Equation 3.15.

$$\dot{m}_{HM,RK,in} = \dot{m}_{KF,PT,in} \cdot \frac{1}{R_{KF\_2\_HM}} \tag{3.15}$$

    e. In the calculation of cement kiln dust (CKD) recirculation, it is assumed that the CKD contribution from the flue gas varies linearly (Equation 3.16) with the total gas flow and kiln feed. Reference data (Table E.1, Appendix E) provided by technical support (HTC) is used to calculate CKD recirculation in the preheater tower.

$$\dot{m}_{CKD\_G\_PT} = \dot{m}_{CKD,FF,out,ref} \cdot \frac{\dot{m}_{KF,PT,in}}{\dot{m}_{KF,PT,in,ref}} \cdot \frac{\dot{V}_{G,Stack}}{\dot{V}_{G,Stack,ref}} \tag{3.16}$$

3.4.3 Sulphur Material Balance in the Preheater Tower

Figure 3.5 is a block diagram of preheater tower and calciner along with inflows and outflow streams of materials. The inflows in this block are kiln feed, cement kiln dust (CKD), kiln exhaust gas and tertiary air, and outflows are preheater exhaust gas and hot meal.
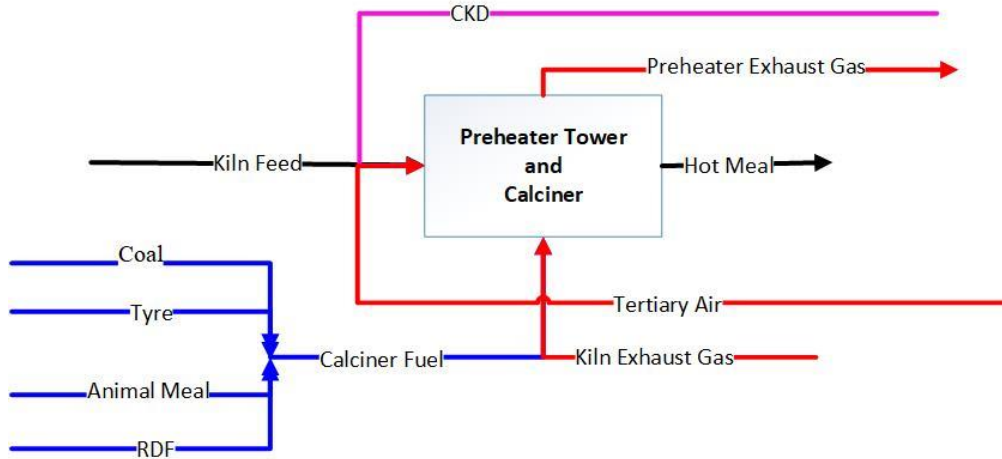
Figure 3.5: Block diagram of preheater tower.

Equation 3.17 is the steady state sulphur material balance in the preheater tower.

$$\dot{m}_{S,PT,in} = \dot{m}_{S,PT,out} \tag{3.17}$$

Equation 3.18 is an equation for calculating sulphur inflow into the system.

$$\dot{m}_{S,PT,in} = \dot{m}_{S,CKD,FF,out} + \dot{m}_{S,KF,PT,in} + \dot{m}_{S,F,PT,in} + \dot{m}_{S,G,RK,out} \tag{3.18}$$

Equation 3.19-3.23 are equations to calculate sulphur in the CKD, kiln feed, and kiln exhaust gas respectively.

$$\dot{m}_{SO_3,CKD,FF,out} = \dot{m}_{CKD,FF,out} w_{SO_3,CKD,FF,out} \tag{3.19}$$

$$\dot{m}_{S,CKD,FF,out} = \dot{m}_{SO_3,CKD,FF,out} \cdot \frac{Mw_S}{Mw_{SO_3}} \tag{3.20}$$

$$\dot{m}_{SO_3,KF,PT,in} = \dot{m}_{KF,PT,in} \cdot w_{SO_3,KF,PT,in} \tag{3.21}$$

$$\dot{m}_{S,KF,PT,in} = \dot{m}_{SO_3,KF,PT,in} \cdot \frac{Mw_S}{Mw_{SO_3}} \tag{3.22}$$

$$\dot{m}_{S,G,RK,out} = \dot{m}_{SO_2,G,RK,out} \cdot \frac{Mw_S}{Mw_{SO_2}} \tag{3.23}$$

Equation 3.24 is an equation for calculating sulphur flow in the calciner fuels, and Equation 3.25-3.28 are equations to calculate sulphur contribution from coal, tyre, RDF and animal meal respectively.

$$\dot{m}_{S,F,PT,in} = \dot{m}_{S,C,Calc,in} + \dot{m}_{S,T,Calc,in} + \dot{m}_{S,RDF,Calc,in} + \dot{m}_{S,AM,Calc,in} \qquad (3.24)$$

$$\dot{m}_{S,C,Calc,in} = \dot{m}_{C,Calc,in} \cdot w_{S,C} \qquad (3.25)$$

$$\dot{m}_{S,T,Calc,in} = \dot{m}_{T,Calc,in} \cdot w_{S,T} \qquad (3.26)$$

$$\dot{m}_{S,RDF,Calc,in} = \dot{m}_{RDF,Calc,in} \cdot w_{S,RDF} \qquad (3.27)$$

$$\dot{m}_{S,AM,Calc,in} = \dot{m}_{AM,Calc,in} \cdot w_{S,T} \qquad (3.28)$$

Equation 3.29 is an equation for calculating sulphur outflow from the preheater tower. Equation 3.30 and 3.31 are equations to calculate sulphur flow and sulphur flow in terms of SO_3 equivalent in the hot meal respectively. Equation 3.32 is an equation for calculating sulphur outflow in the preheater exhaust gas.

$$\dot{m}_{S,PT,out} = \dot{m}_{S,HM,RK,in} + \dot{m}_{S,G,PT,out} \qquad (3.29)$$

$$\dot{m}_{SO_3,HM,RK,in} = \dot{m}_{HM,RK,in} \cdot w_{SO_3,HM,RK,in} \qquad (3.30)$$

$$\dot{m}_{S,HM,RK,in} = \dot{m}_{SO_3,HM,RK,in} \cdot \frac{Mw_S}{Mw_{SO_3}} \qquad (3.31)$$

$$\dot{m}_{SO_2,G,PT,out} = \dot{m}_{S,G,PT,out} \cdot \frac{Mw_{SO_2}}{Mw_S} \qquad (3.32)$$

3.4.4 Sulphur Material Balance in the Rotary Kiln

Figure 3.6 is a block diagram of rotary kiln and clinker cooler together with inflows and outflow of materials. The inflows in the block are hot meal and rotary kiln fuels, and outflows are the clinker, kiln exhaust gas and bypass gas.
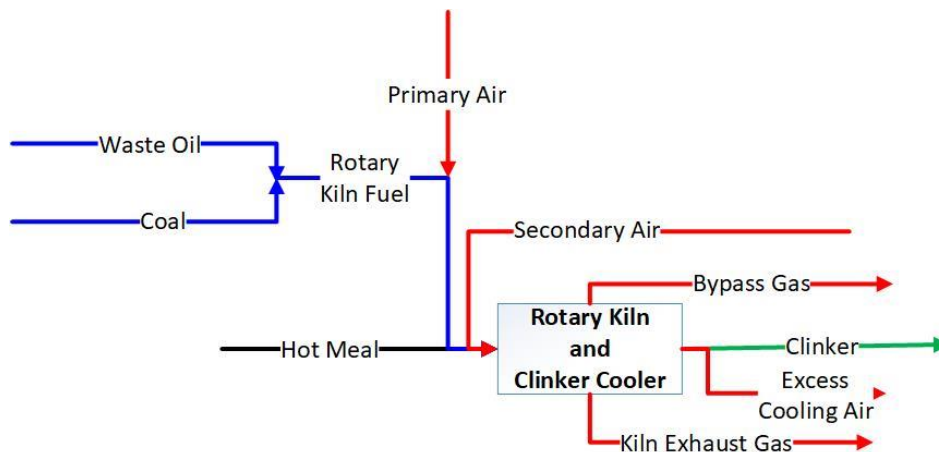
Figure 3.6: Block diagram of the rotary kiln and clinker cooler.

Equation 3.33 is the steady state sulphur material balance in the rotary kiln.

$$\dot{m}_{S,RK,in} = \dot{m}_{S,RK,out} \tag{3.33}$$

Equation 3.34 is an equation for calculating sulphur inflow into the system.

$$\dot{m}_{S,RK,in} = \dot{m}_{S,HM,RK,in} + \dot{m}_{S,F,RK,in} \tag{3.34}$$

Equation 3.35 is an equation for calculating sulphur flow in the hot meal and 3.36-3.37 are equations to calculate sulphur flow in the rotary kiln fuels.

$$\dot{m}_{S,F,RK,in} = \dot{m}_{S,C,RK,in} + \dot{m}_{S,WO,RK,in} \tag{3.35}$$

$$\dot{m}_{S,C,RK,in} = \dot{m}_{C,RK,in} \cdot w_{S,C} \tag{3.36}$$

$$\dot{m}_{S,WO,RK,in} = \dot{m}_{C,WO,in} \cdot w_{S,WO} \tag{3.37}$$

Equation 3.38 is an equation for calculating sulphur outflows from the rotary kiln. Equation 3.23 is an equation for calculating sulphur flow in the kiln exhaust gas, and Equation 3.39-3.40 are equations to calculate sulphur flow in the clinker. Equation 3.41 is an equation for calculating sulphur flow in the bypass gas flowing out of the rotary kiln.

$$\dot{m}_{S,RK,out} = \dot{m}_{S,CL,RK,out} + \dot{m}_{S,G,RK,out} + \dot{m}_{S,G,BP,in} \tag{3.38}$$

$$\dot{m}_{SO_3,CL,RK,out} = \dot{m}_{CL,RK,out} \cdot w_{SO_3,CL,RK,out} \tag{3.39}$$

$$\dot{m}_{S,CL,RK,out} = \dot{m}_{SO_3,CL,RK,out} \cdot \frac{Mw_S}{Mw_{SO_3}} \tag{3.40}$$

$$\dot{m}_{SO_2,G,BP,in} = \dot{m}_{S,G,BP,in} \cdot \frac{Mw_{SO_2}}{Mw_S} \tag{3.41}$$

3.4.5 Sulphur Material Balance in the Raw Mill and CF-silo

Figure 3.7 is a block diagram of the rawmill and CF-silo along with inflows and outflow streams of materials. The inflows in this block are rawmill feed, preheater exhaust gas (compound mode operation), and outflow is kiln feed and gas out of the rawmill.
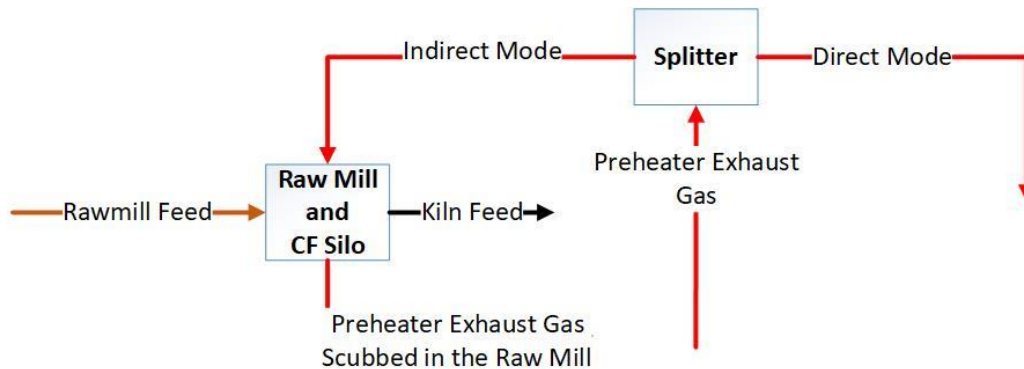
Figure 3.7: Block diagram of the raw mill and CF-silo.

Equation 3.42 is a steady state sulphur material balance in the Raw mill.

$$\dot{m}_{S,RM,in} = \dot{m}_{S,RM,out} + \Delta\dot{m}_{CF,AC} \tag{3.42}$$

Equation 3.43 is an equation for calculating sulphur inflow into the system.

$$\dot{m}_{S,RM,in} = \dot{m}_{S,RMF,RM,in} + \dot{m}_{S,G,RM,in} \tag{3.43}$$

Equation 3.44-3.45 are equations to calculate sulphur and SO_3 flow in the rawmill feed. Equation 3.46 is an equation to calculate sulphur flow in the preheater exhaust gas entering the rawmill.

$$\dot{m}_{SO_3,RMF,RM,in} = \dot{m}_{RMF,RM,in} \cdot w_{SO_3,RMF,RM,in} \tag{3.44}$$

$$\dot{m}_{S,RMF,RM,in} = \dot{m}_{SO_3,RMF,RM,in} \cdot \frac{Mw_S}{Mw_{SO_3}} \tag{3.45}$$

$$\dot{m}_{SO_2,G,RM,in} = \dot{m}_{S,G,RM,in} \cdot \frac{Mw_{SO_2}}{Mw_S} \tag{3.46}$$

Equation 3.47 is an equation for calculating sulphur outflows from the rawmill. Equation 3.22 is an equation for calculating sulphur flow in the kiln feed, and Equation 3.48 is an equation for calculating SO_2 flow in the preheater exhaust gas scrubbed in the rawmill.

$$\dot{m}_{S,RM,out} = \dot{m}_{S,KF,PT,in} + \dot{m}_{S,G,RM,out} \tag{3.47}$$

$$\dot{m}_{SO_2,G,RM,out} = \dot{m}_{S,G,RM,out} \cdot \frac{Mw_{SO_2}}{Mw_S} \tag{3.48}$$

Sulphur accumulation in the CF-silo is calculated using Equation 3.49 and 3.50.

$$\Delta\dot{m}_{SO_3,CF} = \Delta\dot{m}_{CF} \cdot w_{SO_3,KF,PT,in} \tag{3.49}$$

$$\Delta\dot{m}_{S,CF} = \Delta\dot{m}_{SO_3,CF} \cdot \frac{Mw_S}{Mw_{SO_3}} \tag{3.50}$$

CKD contribution from the rawmill feed is calculated using total material balance (Equation 3.51) in the rawmill.

$$\dot{m}_{CKD\_RaM} = \dot{m}_{RaM,RM,in} - \dot{m}_{KF,PT,in} - \Delta\dot{m}_{CF,AC} \tag{3.51}$$

The total CKD contribution is calculated using Equation 3.52, where CKD contribution from the preheater exhaust gas is calculated using Equation 3.15.

$$\dot{m}_{CKD,FF,out} = \dot{m}_{CKD\_RaM} + \dot{m}_{CKD\_G\_PT} \tag{3.52}$$

3.4.6 Sulphur Material Balance in the Fabric Filter

Figure 3.8 is a block diagram of preheater tower along with inflows and outflow streams of the materials. The inflows in the block are hot meal and rotary kiln fuels, and outflows are clinkers, kiln exhaust gas, and bypass gas.
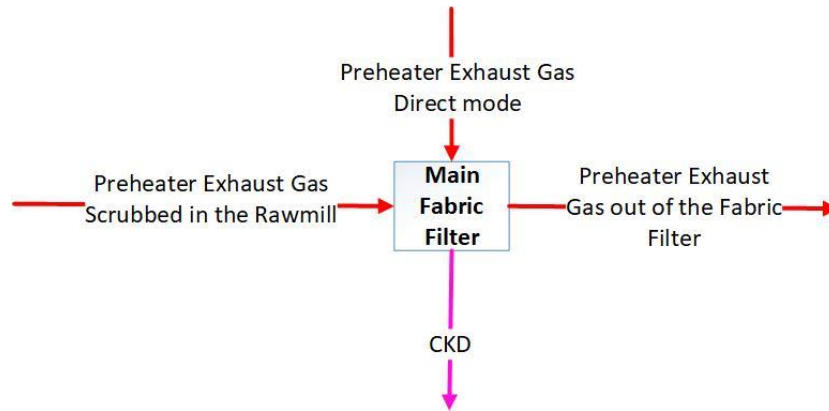

Figure 3.8: Block diagram representation of the fabric filter.

Equation 3.53 is a steady state sulphur material balance in the fabric filter.

$$\dot{m}_{\mathrm{S},FF,in} = \dot{m}_{\mathrm{S},FF,out} \tag{3.53}$$

Equation 3.54 is an equation for calculating sulphur inflow into the fabric filter.

$$\dot{m}_{\mathrm{S},FF,in} = \dot{m}_{\mathrm{S},G,RM,out} + \dot{m}_{\mathrm{S},G,FF,Dir,in} \tag{3.54}$$

Equation 3.55 and Equation 3.48 are equations to calculate sulphur inflow into the fabric filter through the direct and compound mode of operation respectively.

$$\dot{m}_{\mathrm{SO_2},G,FF,Dir,in} = \dot{m}_{\mathrm{S},G,FF,Dir,in} \cdot \frac{Mw_{\mathrm{SO_2}}}{Mw_{\mathrm{S}}} \tag{3.55}$$

Equation 3.56 is an equation for calculating sulphur outflows from the fabric filter. Equation 3.57 and Equation 3.58 are equations to calculate sulphur and SO_3 outflows in the CKD and Equation 3.59 is an equation for calculating SO_2 flow in the cleaned preheater gas.

$$\dot{m}_{\mathrm{S},FF,out} = \dot{m}_{\mathrm{S},CKD,FF,out} + \dot{m}_{\mathrm{S},G,FF,out} \tag{3.56}$$

$$\dot{m}_{\mathrm{SO_3},CKD,FF,out} = \dot{m}_{CKD,FF,out} \cdot w_{\mathrm{SO_3},CKD,FF,out} \tag{3.57}$$

$$\dot{m}_{\mathrm{S},CKD,FF,out} = \dot{m}_{\mathrm{SO_3},CKD,FF,out} \cdot \frac{Mw_{\mathrm{S}}}{Mw_{\mathrm{SO_3}}} \tag{3.58}$$

$$\dot{m}_{\mathrm{SO_2},G,FF,out} = \dot{m}_{\mathrm{S},G,FF,out} \cdot \frac{Mw_{\mathrm{SO_2}}}{Mw_{\mathrm{S}}} \tag{3.59}$$

3.4.7 Sulphur Material Balance in the Bypass

Figure 3.9 is a block diagram of the bypass system that includes quench chamber, GSA, bypass cyclone and bag filter as a single block. The inflow stream is bypass gas flowing out of the kiln and outflow streams are bypass dust and cleaned bypass gas.
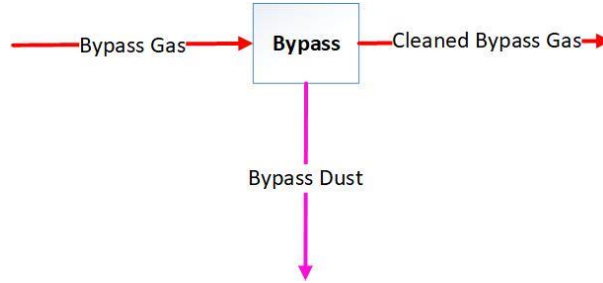
Figure 3.9: Block diagram of the Bypass.

Equation 3.60 is a steady state sulphur material balance in the bypass.

$$\dot{m}_{S,G,BP,in} = \dot{m}_{S,BP,out} \tag{3.60}$$

Equation 3.61 is an equation for calculating sulphur outflow in the bypass.

$$\dot{m}_{S,BP,out} = \dot{m}_{S,G,BP,out} + \dot{m}_{S,D,BP,out} \tag{3.61}$$

Equation 3.62-3.63 are equations to calculate SO_2 and sulphur flow in the bypass gas and Equation 3.64-3.65 are equations to calculate sulphur flow in the cleaned bypass gas and bypass dust respectively.

$$\dot{m}_{SO_2,G,BP,out} = \dot{V}_{G,BP,out} \cdot C_{SO_2,G,BP,out} \tag{3.62}$$

$$\dot{m}_{S,G,BP,out} = \dot{m}_{SO_2,G,BP,out} \cdot \frac{Mw_S}{Mw_{SO_2}} \tag{3.63}$$

$$\dot{m}_{SO_3,D,BP,out} = \dot{m}_{D,BP,out} \cdot w_{SO_3,D,BP,out} \tag{3.64}$$

$$\dot{m}_{S,D,BP,out} = \dot{m}_{SO_3,D,BP,out} \cdot \frac{Mw_S}{Mw_{SO_3}} \tag{3.65}$$

3.4.8 Sulphur Material Balance in the Splitter

Figure 3.10 is a block diagram representation of splitting up of the preheater exhaust gas in the direct and compound mode of operation.
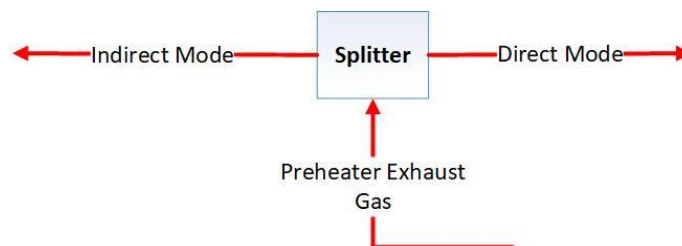
Figure 3.10: Block diagram of the splitter.

Equation 3.66 is a sulphur material balance in the splitter. Equation 3.67 is used for calculating sulphur outflow in the preheater exhaust gas flowing into the rawmill. x is the split ratio of gas flowing into the rawmill to the gas flowing directly into the fabric filter. In the cement plant in Kjøpsvik, the ratio is either 1 (RM-ON) or 0 (RM-OFF).

$$\dot{m}_{S,G,PT,out} = \dot{m}_{S,G,RM,in} + \dot{m}_{S,G,FF,out} \tag{3.66}$$

$$\dot{m}_{S,G,PT,out} = x \cdot \dot{m}_{S,G,RM,in} \tag{3.67}$$

3.4.9 Sulphur Material Balance in the Gas Mix

Figure 3.11 is a block diagram representation of a mixing process of dedusted preheater exhaust gas flowing out of the fabric filter and bypass gas flowing out of the bypass filter.
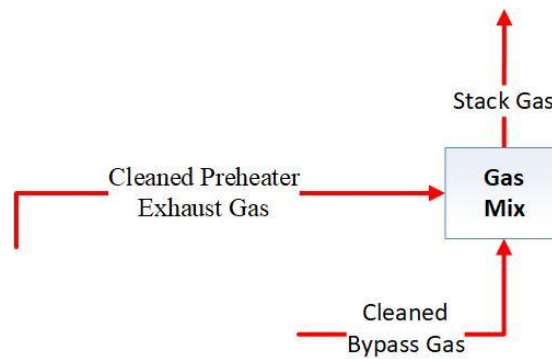
Figure 3.11: Block diagram of mixing of preheater exhaust gas and the bypass gas.

Equation 3.68 is a steady state sulphur material balance in the Gas mix. Equation 3.69-3.70 are equations to calculate SO_2 and sulphur outflows in the stack gas.

$$\dot{m}_{S,G,BP,out} + \dot{m}_{S,G,FF,out} = \dot{m}_{S,G,Stack} \tag{3.68}$$

$$\dot{m}_{SO_2,G,Stack} = \dot{V}_{G,Stack} \cdot C_{SO_2,G,Stack} \tag{3.69}$$

$$\dot{m}_{S,G,Stack} = \dot{m}_{SO_2,G,Stack} \cdot \frac{Mw_S}{Mw_{SO_2}} \tag{3.70}$$

3.4.10   Model Summary

Table 3.7 is a summary of sulphur material balances in the clinker formation process. In the model, the total number of equations and measured/approximated values is equal to the total number of unknown variables. Hence, the flow model can be used in sulphur flow calculations.

Table 3.7: List of sulphur inflow and outflow in the blocks.

Description	Total
Total number of independent equations	57
Total number of variables	54
Total number of measured variables	23

4 Seawater Flue Gas Desulphurization Installation

Proven environmental and health hazards of SO_x emissions has prompted countries around the globe in formulating emission regulation with the aim of limiting the emissions from the respective country. A fundamental approach of most of the industries to abide emission regulation of their country has been replacing high sulphur fuels with low sulphur fuels thereby reducing the overall input of sulphur and subsequently SO_x emissions [21]. However, in many industries like cement plants, it is impossible to avoid sulphur entrainment to the system as sulphur enters predominantly with raw materials rather than just with combustion fuels. At the same time, the availability of sulphur rich raw materials and fuels near a plant and at a relatively low cost motivates industries to use these sulphur rich raw materials and fuels. Henceforth, industries prefer alternative approach to control their emission problem while the plant and country can benefit utilizing these sulphur rich resources.

Many transportation industries (marine), and plants located near to the coastal area have successfully implemented sea water flue gas desulphurization (SWFGD) technology to reduce SO_x emissions and comply with the regulations [22, 23]. The Norcem cement plant in Kjøpsvik aims to install SWFGD installation utilising readily available water from Tysfjørd to deal with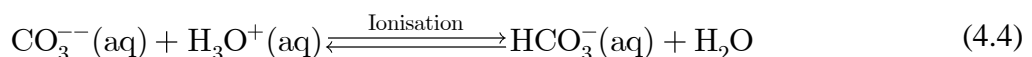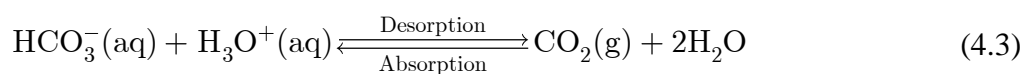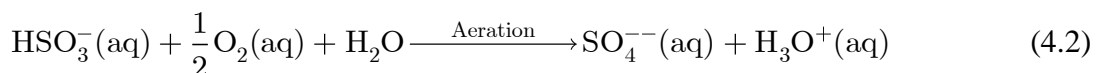 its emission problem. This chapter presents a description of SWFGD technology and a description of proposed SWFGD installation. The chapter also discusses its consequences based on process, plant operations and energy aspects, and environmental aspects.

4.1 Working Principle of SWFGD Technology

SWFGD technology is one of the promising technologies to reduce SO_x emissions along with emissions of other acidic gases like HCl and HF from exhaust gases. In the SWFGD technology, SO_2, an acidic oxide, is absorbed by seawater and then it ionises to produce bisulphite ion and hydronium ion via Reaction 7.1. As it is an equilibrium reaction, the forward reaction rate (absorption of SO_2) is favoured by a lower concentration of hydronium ions. Seawater is naturally alkaline due to the basic buffer created by the interaction between carbonate and bicarbonate ions. It results in a pH of 7.5-8.5, and thus seawater can neutralise the considerable amount of ionised hydronium ions without substantial fall in pH level of seawater. The neutralisation of hydronium ions takes place via Reaction 7.3 and 7.4 and consequently increases absorption efficiency of SO_2 by seawater. In the end, bisulphite ion oxidises to sulphate ion (neutral and already a major component of seawater) in the presence of dissolved O_2 via Reaction 7.2 [24].

$$SO_2(g) + 2H_2O(aq) \xrightleftharpoons[\text{Desorption}]{\text{Absorption}} HSO_3^-(aq) + H_3O^+(aq) \tag{4.1}$$

$$HSO_3^-(aq) + \frac{1}{2}O_2(aq) + H_2O \xrightarrow{\text{Aeration}} SO_4^{--}(aq) + H_3O^+(aq) \tag{4.2}$$

$$HCO_3^-(aq) + H_3O^+(aq) \xrightleftharpoons[\text{Absorption}]{\text{Desorption}} CO_2(g) + 2H_2O \tag{4.3}$$

$$CO_3^{--}(aq) + H_3O^+(aq) \xrightleftharpoons{\text{Ionisation}} HCO_3^-(aq) + H_2O \tag{4.4}$$

4.2 Description of SWFGD Installation Design

This section presents a description of proposed design and working mechanism of the SWFGD installation in the Kjøpsvik plant.

4.2.1 Description of Absorber Design

Figure 5.1 shows an SWFGD absorber designed by M/S Doosan Lentjes. The design length of the absorber is 78700 mm with a diameter of 5000 mm in absorption section (bottom section) and 2800 mm in stack section (top section). It consists of an inlet for kiln gas (2), three water spray banks with a series of nozzles (3, 4, and 5) and a water outlet in the bottom (1). It includes a mist eliminator (6) and an inlet for relatively hot excess clinker cooling air (8). Beside absorber, the design consists of three pumps with a maximum capacity of 3300 m^3/h to pump water and a pump house (10). The design includes a bypass valve (7) between discharge and inlet pipe. A booster fan is incorporated in the downstream of mixing zone of bypass gas flowing out of the bypass filter and gas flowing out of the main filter (Not shown in Figure 7.1).
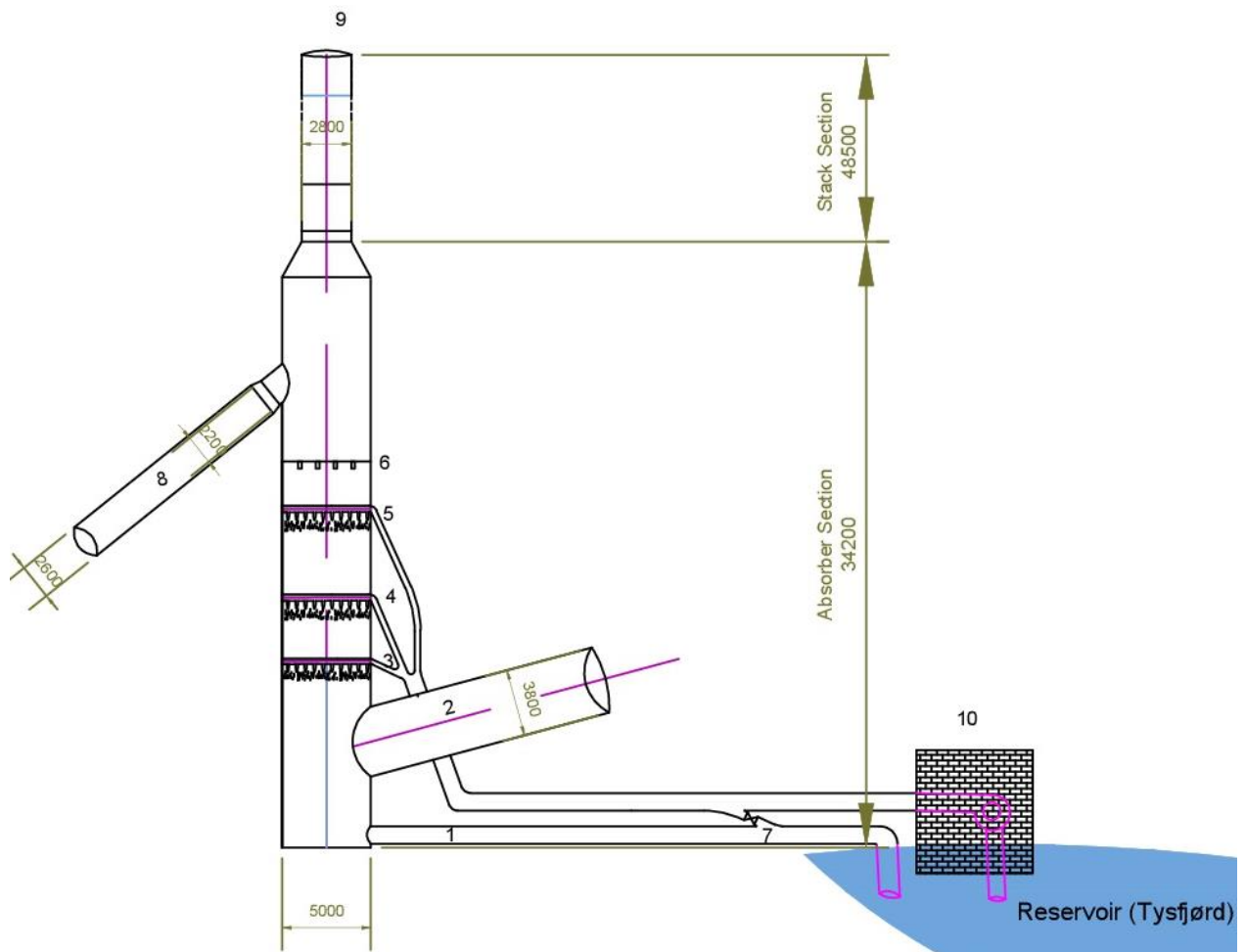

Figure 4.1: A schematic drawing of the absorber (Source: **Technical offer-Doosan Lentjes**).

4.2.2 Working Mechanism of SWFGD Installation in Kjøpsvik

A booster fan propels the kiln gases (a mixture of preheater gas flowing out of the fabric filter and the bypass gas flowing out of the bypass filter) to the absorption tower. The absorber is

43

divided into two sections, absorption section and stack section. In the absorption section, three nozzles spray Tysfjørd water, where SO_x, as well as other pollutants, come into extensive contact with the water. In the due process, SO_x is absorbed as described in section 7.1. Trace amounts of HCl and other components are also absorbed in absorption section. The gas then flows through the mist eliminator which reduces the moisture from the kiln gas. During the entire process, the gas gets cooled and results in a decrease in the buoyancy force associated with the stack gas. A relatively hot and clean excess clinker cooling air is mixed with scrubbed flue gas to compensate for the decrease in gas temperature and thus enhances the flow of stack gas in the stack section. The design temperature of the gas after mixing process is 60 ℃. If the temperature of the excess clinker cooling air is substantially high (more than 300 ℃), lake water is used to quench the cooling air and subsequently control the temperature of cooling air. The mixed gas (stack gas), is then released into the atmosphere through the stack section. In the case of effluent water, the outlet pipe discharges effluent water with design pH of 5.0 or higher at 10 m depth in the Tysfjørd. However, if the pH level of the effluent water is less than 5.0, a part of the pumped water (water bypass valve) is mixed with effluent water before it is discharged into the Tysfjørd. The typical design data and expected pH and temperature in the effluent water are shown in Table 4.1.

Table 4.1: Design data and water flow rate in the inlet pipe (Source: **Technical offer-Doosan Lentjes**).

Design Parameter	Compound mode (RM-ON mode)		Direct Mode (RM-OFF mode)	
	Normal SO$_2$ emission	High SO$_2$ emission	Normal SO$_2$ level	High SO$_2$ level
Design SO$_2$ level in the stack gas [mg/Nm^3 dry @10% O$_2$]	286	386	515	818
Design volume flow rate of stack gas [Nm^3/h dry @10% O$_2$]	226471	245883	213889	232222
Calculated volume flow rate of water in the inlet pipe [m^3/h]	1600	1600	2200	3000
Calculated effluent water temperature [ºC]	21.0	22.4	17.4	15.0
Expected pH level in the effluent water [-]	≤5.0	≤5.0	≤5.0	≤5.0

4.3 Consequences of SWFGD Installation

This section presents significant modifications to the existing process and the consequences of SWFGD installation based on process, operational and energy aspects. It also includes the environmental impact of SWFGD installation.

4.3.1 Process, Operational and Energy Aspects

Figure 7.2 shows a process flow diagram of clinker formation process. It shows the non-functional process (existing process but non-functional after scrubber installation) and a new scrubber process with accessories. A major modification regarding process and operational aspects is the replacement of main stack pipe, and subsequent piping from the fabric filter and bypass filter with the absorber tower, booster fan and essential piping ducts. Beside stack gas exhaust system, there will be a modification in the clinker cooling air exhaust system. At present, excess cooling air is released into the atmosphere via cooling gas exhaust pipe. In a

future design with SWFGD installation, cooling air will be primarily used to raise the temperature of cooled stack gas in the absorber. Existing cooling exhaust pipe will still be in operation in the case of emergencies (clinker cooling gas temperature higher than 300°C), and a damper will control the flow to the existing cooling exhaust pipe in the case of emergencies. In the case of emergencies, lake water will be used to control the temperature of the cooling gas. Table 4.2 shows the process equipment and their design capacity in the SWFGD installation.

Table 4.2: Description of process equipment and design capacity (Source: **Technical offer-Doosan Lentjes**).

Equipment Description	Maximum Design Capacity	Quantity
Absorber spray pump	1100 m^3/h (head 40.6 m)	3
Mist eliminator	50 mg/m^3 (pressure drop 2.5 mbar	1
Booster fan	300523 m^3/h (max pressure 32.5 mbar)	1

The additional process equipment in Table 4.2 and processes associated with scrubber operation will require control system installation, safety monitoring, scheduled maintenances and breakdown maintenances. There will not be any modifications in GasMet CEMs II (stack gas analyser) operation. It will be reinstalled in the stack section of the absorber tower with identical equipment, instrument air supply and control systems as in the current operation. Regular maintenance and calibration of stack gas analyser system will also be unaltered. However, additional process equipment and processes (booster fan, water pumps, bypass water valve operation, pH measurement system in the effluent water and clinker cooling gas damper) will require regular monitoring, scheduled maintenance, and breakdown maintenances in critical scenarios.

In addition to process/operational modification and its consequences associated with scrubber operation, SWFGD installation will substantially increase the total power consumption from the plant. For normal operation mode, overall electrical energy consumption (by booster fan and seawater pumps) will be increased by 850 kW in RM-OFF mode and 750 kW in RM-ON mode. In RM-ON mode, sulphur emission is significantly lower, and thus requires relatively lesser pump water and subsequently results in lower pump electrical power consumption. The estimation of required power is based on normal operation scenarios; however, the power consumption can be higher than this with higher emissions and higher volume flow in the stack gas.
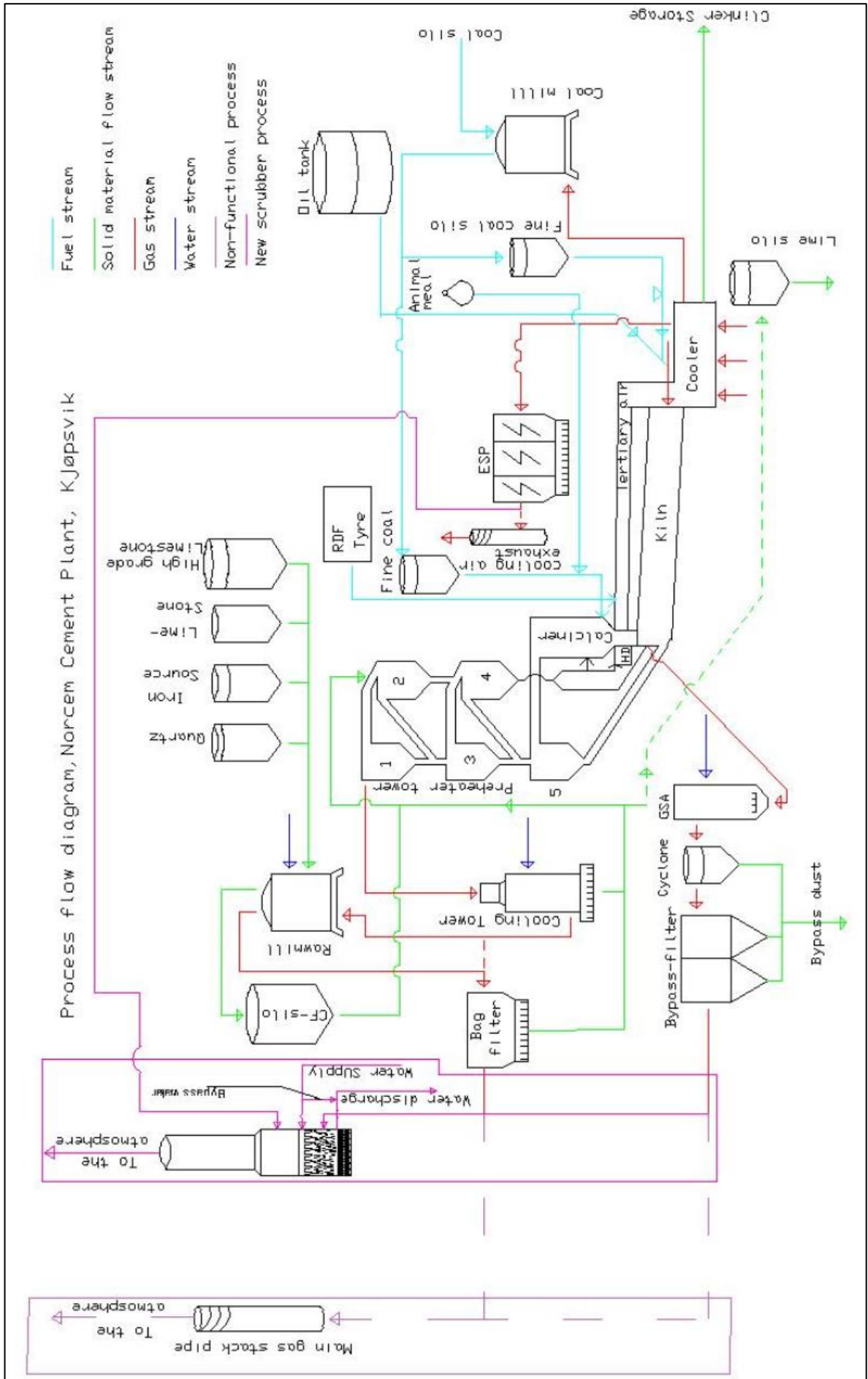
Figure 4.2: Process flow diagram with sea water scrubber installation.

4.3.2 Environmental Aspects

The proposed SWFGD installation in Kjøpsvik plans to utilise seawater to absorb SO_2 from the flue gas and recirculate back it to Tysfjørd. As absorbed SO_2 oxidises to neutral sulphates in the presence of dissolved O_2, SO_2 removal using seawater is an environmentally friendly and sustainable solution. However, the oxidation process consumes available dissolved oxygen (DO) and increases the chemical oxygen demand (COD) in the water thereby adversely affecting the balance in a marine ecosystem [24]. In addition, absorbed SO_2 causes a localised drop in pH level. The most favourable pH for sea flora and fauna is in the range of 6.5-9.0. Any deviation of pH level from this value negatively impacts the breeding as well as the survival of living organisms. An increase in pH level also increases the solubility of harmful chemicals which will ultimately affect the survivability of marine organisms [25]. In the current SWFGD design, pH of effluent water at the outlet of discharge pipe will be 5.0 or higher (in extreme scenarios lower than 5.0), which is relatively different from normal pH (7.5-8.0) of the water in the Tysfjørd. The design has a provision to treat acidic effluent water with fresh Tysfjørd water via bypass valve if the pH of effluent water is lower than 5.0. Besides, the design doesn't have any additional provision for neutralisation of effluent water using alkalis or limewater.

In addition to a drop in pH level and reduction in DO, absorption of heavy metals (especially mercury) and dioxins are identified as a critical concern during internal environmental impact assessment of SWFGD installation. Environmental concerns related to water pollution due to the emission of heavy metals are expressed in numerous studies that were conducted to determine the possible environmental impact of heavy metals on the marine ecosystem. A study on exposure of mercury with various concentration level on three aquatic plants, hydrilla, water lettuce, and karbia weed by Mhatre et al. pointed out that exposure to mercury severely affects aquatic plants and causes foliar injury, and affect the chlorophyll content. In the case of floating plants, exposure to high doses of mercury increases leaf injury index [26]. In birds and fishes (tertiary consumers in the food chain), bioaccumulation of mercury occurs due to assimilation, and it can be fatal to these aquatic animals or animals that depend on these animals for food [27]. Another detrimental group of pollutants, dioxins, are a group of several hundred organic compounds, which are commonly referred to as persistent chemical compounds due to their inert and stable nature. Due to their stability, accumulation of dioxins occurs in tertiary consumers, fish, birds and humans, and causes adverse effects on these organisms. In human, even exposure to very low dioxin level is carcinogenic and has an adverse impact on the reproductive system. In fishes, exposure to dioxins causes an adverse impact on embryo-larval developments and other behavioural responses [28]. Thus, in the long term, dioxins emitted from the plant can have a negative impact on local fishing industries as well as human health.

To address aforementioned problem, Norcem cement plant in Kjøpsvik conducted environmental impact assessment by evaluating possible emission to the water and potential impact of emissions on the Tysfjørd ecosystem. The study shows that other pollutants except pH, dioxins and mercury are well within the accepted limit of emissions even if almost 100% of other pollutants in the kiln gases are absorbed in the water. As per design calculations, the emission will be critical to a moderate level at 50 m radius from the discharge end, and beyond 50 m, pollutant will be diluted to the same concentration as in the rest of the Tysfjørd. Moreover, the total discharged water during normal operation is negligible in comparison to the total expected natural replacement of the water in the Tysfjørd which results in further dilution as well as transport of deposited heavy metals and dioxins. The study also claims that dioxins level in the Tysfjørd water will be well within European Quality Standard (EQS) as dioxins are feebly soluble in water.

In the case of mercury emission, an internal study conducted by General Electric (GE) at the request of Kjøpsvik plant has claimed that mercury emissions to the Tysfjørd water will be insignificant during the scrubber operations. In their study, they measured oxidised mercury as 10% and free mercury as 90% of the total mercury emission in the stack gas. Based on the measurement and prior experiences, the study claims that mercury level will be merely 0.046 µg/l (accepted EQS level), as only about 28% of total mercury (20% of free mercury and 100% of oxidised mercury) currently emitted to the atmosphere will end up in the effluent water [29, interanl study]. Similar to pH and other pollutants, rapid dilution and natural replacement of seawater will reduce mercury level and expected to nullify the potential negative impact on flora and fauna.

Henceforth, it can be concluded that possible emission of volatile components and heavy metals and dioxins in the water has insignificant harmful impact on the Tysfjørd ecosystem. However, a periodic Tysfjørd assessment of water quality is essential in the future to evaluate possible alteration of the Tysfjørd ecosystem.

5 Analysis of Historical Emission Data

This chapter discusses sulphur emissions in the stack gas in 2017 and correlates the emission with important kiln variables based on statistical correlation analysis. The analysis is performed for two weeks, Week-1 (8th to 15th December) and Week-2 (22nd to 29th August). Moreover, it presents a comparison of sulphur flows in different streams and subsequent representation of flows in the Sankey Diagram. The flow calculation is performed for two periods, Period-1 in Week-1 and Period-2 in Week-2. Furthermore, the chapter presents a regression model formulation of SO_2 emission in the stack gas using odd serial number data from both weeks, Week-1 and Week-2, (in rawmill on mode (RM-ON mode)) and model validation using data from Week-3 and Week-4 (in RM-ON mode). The analysis presented in this chapter is the basis for design and analysis of kiln tests.

5.1 Historical Trend of Sulphur Emissions in 2017

Figure 5.1 shows averaged daily sulphur emissions in the stack gas and bypass gas in 2017. SO_2 emissions in the bypass gas (secondary axis, mg/m^3) as well as in the stack gas (primary axis, mg/Nm^3 dry @10% O_2) have been higher than normal operating mode several times in that year. The emission level was highest in last week of April to 2nd week of June. After maintenance in the primary burner in June, sulphur emissions were expected to decrease, but the emission peaked further in July, October and December. Upcoming sections present analysis of SO_2 emissions in two different weeks Week-1 (8th to 15th December-high emission week) and Week-2 (22nd to 29th August-low emission week)[5] after maintenance in the primary burner.
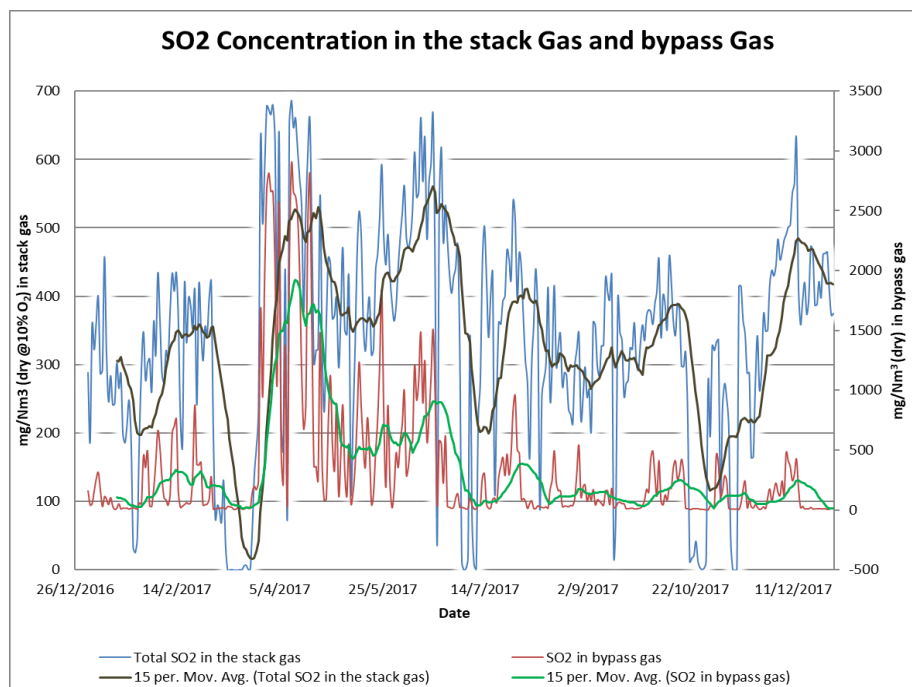
Figure 5.1: Sulphur emissions in the stack gas and bypass gas in 2017.

---

[5] Both periods correspond to the timeline after maintenance of the primary burner.

5.2 Analysis Period and Data Collection

5.2.1 Analysis Period

Figure 5.2 shows trends of SO_2 emissions in the bypass gas (red) and stack gas (blue) in Week-1 (8th December 2017, 00:00 to 15th December 2017, 00:00). Figure 5.3 shows trends of SO_2 emission in the stack gas (blue) and bypass gas (red) in Week-2 (22nd August 2017, 00:00 to 29th August 2017, 00:00). These periods include two different scenarios, critical SO_2 level in the stack gas (Week-1) and normal SO_2 level in the stack gas (Week-2). The remaining sections of this chapter focus on comparing these weeks regarding the impact of kiln parameters and sulphur flows. Additionally, a single regression model with a combined data of these weeks is formulated for RM-ON mode and validated using data of two separate weeks (in RM-ON mode) (24th September 2017, 8:43 to 1st October 2017, 8:42 and 20th October 2017, 00:00 to 27th October 2017, 00:00).
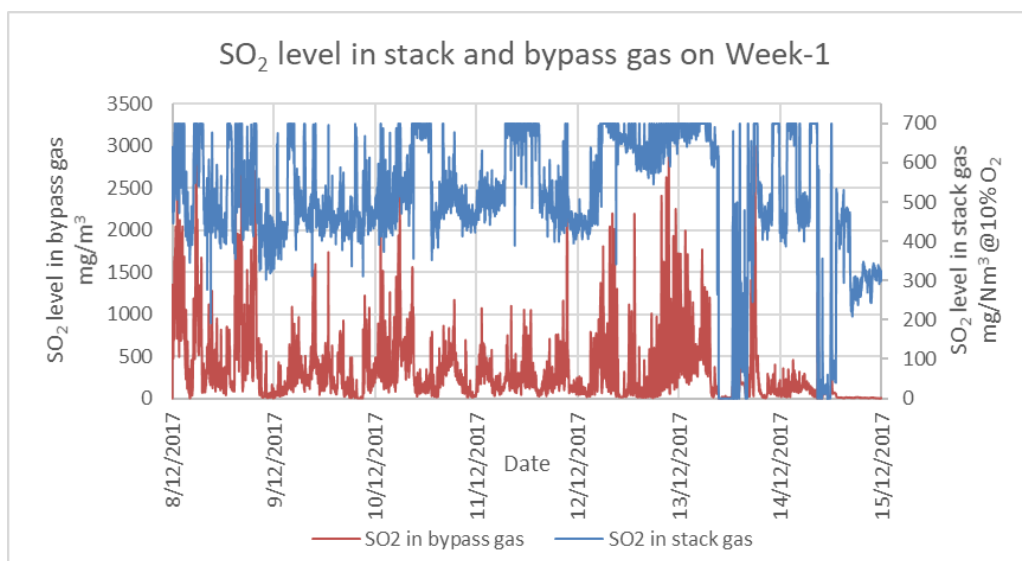
Figure 5.2: Trends of sulphur emissions in the stack gas ([mg/Nm³ dry @10% O_2]) (magenta) and bypass gas (red) (mg/m³) in Week-1.
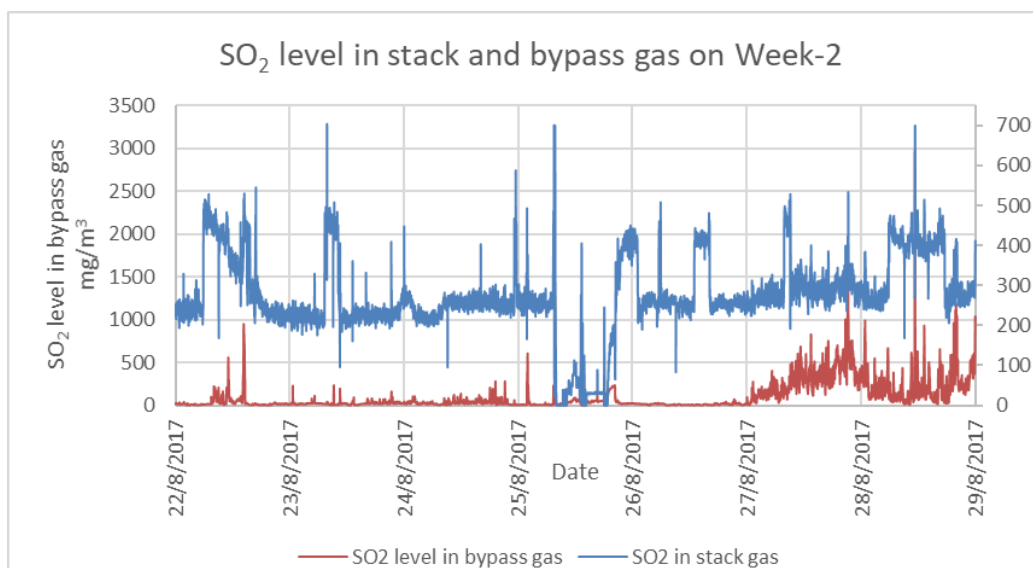
Figure 5.3: Trends of sulphur emissions in the stack gas (magenta) ([mg/Nm³ @10% O_2]) (secondary axis) and bypass (red) ([mg/m³]) in Week-2.

5.2.2 Data Collection

10080 raw timestamps data of important kiln parameters for each week, Week-1 and Week-2, are collected for further analysis. The data points are further filtered to ensure normal operating conditions; bypass water flow rate is filtered to 1 m^3/h or higher, and kiln feed is filtered to 80 t/h or higher. In addition, the SO$_2$ level in the stack gas is set to lower than 650 mg/Nm^3 and in the bypass gas lower than 2900 mg/m^3 to avoid errors arising from limitations of measuring equipment[6]. When rawmill is turned off, most of the time, measurement shows randomly varying value in the vicinity of 0 t/h but not precisely 0 t/h. To deal with this issue, 60 t/h is chosen as a transition between rawmill on mode (RM-ON) and rawmill off mode (RM-OFF). It can introduce error due to the presence of the transition data between 60 t/h to 110 t/h[7], but the total number transition data is insignificant in comparison to the total number of normal operation mode data (1% of the total timestamps data). Table 5.1 presents the total number of timestamp data after the filtration.

Table 5.1: Total number of data of each parameter after filtration in respective weeks.

Rawmill mode	Numbers of timestamp data (Week-1)	Number of timestamp data (Week-2)
RM-OFF	1086	1811
RM-ON	5735	7231

Table 5.2 presents a description of independent/controllable kiln parameters.

Table 5.2: Independent kiln parameters.

Description of kiln parameters	Symbol	Graph symbol	Units
% ID fan power	$p_{\%,ID}$	p_%ID	[%]
Tyre feeding in the hotdisc	$\dot{m}_{T,Calc,in}$	m_T_Calc_in	[kg/h]
RDF feeding in the hotdisc	$\dot{m}_{RDF,Calc,in}$	m_RDF_Calc_in	[kg/h]
Waste oil feeding in the kiln	$\dot{m}_{WO,RK,in}$	m_WO_RK_in	[kg/h]
Coal feeding in the kiln	$\dot{m}_{C,RK,in}$	m_C_RK_in	[t/h]
Total alternative fuel (Tyre, RDF, and waste oil)	$\dot{m}_{Alt\_Fuel}$	m_Alt_Fuel	[kg/h]
Kiln feed into the preheater tower	$\dot{m}_{KF,PT,in}$	m_KF_PT_in	[t/h]
Opening % of the tertiary air damper	$O_{\%,D,TA}$	O_%_D_TA	[%]
Kiln rotating speed (% of maximum speed)	$\omega_{\%,RK}$	Omega_%RK	[%]
Rawmill feed rate into the rawmill	$\dot{m}_{RaM,RM,in}$	m_RaM_RM_in	[kg/h]
Bypass water supply rate in the bypass	$\dot{V}_{W,BP,in}$	V_W_BP_in	[m^3/h]
Energy input per unit ton of clinker from the rotary kiln fuels	$\hat{E}_{F,UTC,RK,in}$	E_F_UTC_RK_in	[MJ/t clinker]

Energy input per unit ton of clinker from rotary kiln fuels is a function of rotary kiln fuel flow, and it is calculated using Equation 5.1. The clinker production rate is estimated using kiln feed to clinker ratio (experience based constant factor). The Kjøpsvik plant uses 1.56 as a factor to calculate clinker production rate from the plant. Data collection and filtration for other parameters are discussed at the beginning of this section.

---

[6] Maximum SO$_2$ measurement limit is 700 mg/Nm^3 in the stack gas and 3000 mg/m^3 in the bypass gas.

[7] The plant is usually operated at rawmill feed of 110 t/h or higher.

$$\hat{E}_{F,RK.in} = \frac{H_C \cdot \dot{m}_{C,RK,in} + {H_{WO} \cdot \dot{m}_{WO,RK,in}}\Big/{1000}}{\dot{m}_{CL,RK,out}} \tag{5.1}$$

Where,

$\hat{E}_{F,RK.in}$	Energy input per ton of clinker from rotary kiln fuels	[MJ/t clinker]
H_C	Calorific value of the coal	[MJ/kg]
H_{WO}	Calorific value of the waste oil	[MJ/kg]
$\dot{m}_{C,RK,in}$	Coal feeding rate into the rotary kiln	[t/h]
$\dot{m}_{WO,RK,in}$	Waste oil feeding rate into the rotary kiln	[kg/h]
ρ_{WO}	Density of waste oil	[kg/l]
$\dot{m}_{CL,RK,out}$	Clinker production rate	[t/h]

Table 5.3 shows a list of supplier's data of thermal properties of coal and waste oil used during Week-1 and Week-2.

Table 5.3: Rotary kiln fuel properties.

Fuel Properties	Value	
	Week-2	Week-1
H_C	27.6 MJ/kg	29.2 MJ/kg
H_{WO}	37 MJ/kg	37 MJ/kg

The independent/controllable parameters in Table 5.2 generally control the operating condition and the fuel/feed inputs in the kiln process. As a result, any variation in the independent parameters results in process alterations and subsequent variation in emissions in the stack gas. Among independent parameters, fuel in the rotary kiln and the calciner (RDF/tyre in the hotdisc, and coal/waste oil in the rotary kiln) significantly vary sulphur behaviour in the process. These fuels introduce sulphur into the system and provide a suitable environment for the SO_2 formation, SO_2 capture and sulphate decomposition. Alternative fuels such as RDF and tyre burn less efficiently than coal and waste oil causing reducing environment in the kiln inlet, potentially increasing the rate of sulphur decomposition in the kiln. Similarly, variation in ID fan speed significantly varies gas flow rate which eventually changes gas/solid residence time in the kiln. Another important parameter, kiln feed, is the primary source of sulphur input in the kiln and any variation in the kiln feed varies sulphur input and subsequently sulphur emissions from the plant. Any variation in tertiary air supply varies the air flow in the hotdisc consequently varying O_2 level in the kiln inlet and temperature in the calciner. The energy input per ton of clinker in the rotary kiln varies kiln temperature which ultimately affects sulphur decomposition in the sintering zone of the kiln. Besides these parameters, rawmill feed (when raw mill in operation) is expected to capture SO_2 present in the preheater exhaust gas, thereby decreasing emission in the preheater exhaust gas as well as in the stack gas.

Table 5.4 shows a list of dependent/process parameters. The variation in process parameters such as pressure and temperature in the cyclones and hot meal feeding to the hotdisc directly or indirectly influences SO_2 formation and SO_2 capture by solid materials in the preheater tower. Cyclone temperature primarily controls the formation and absorption of SO_2 in different cyclone stages. The effect of temperature is more noticeable in top cyclone stages. It is

potentially due to the fact that the temperature in top cyclone stages is sufficient for oxidation of sulphides present in the feed, but the temperature is significantly lower than the temperature required for a calcining process. Correspondingly, pressure variations in the cyclone stages vary gas flow and gas residence time in cyclone stages. The variation in gas flow and subsequently gas residence time control the solid-gas interaction thereby affecting the SO_2 absorption in the preheater tower. Furthermore, the O_2 level and CO level in the kiln inlet can be used to detect potential reducing environment in the rotary kiln.

Table 5.4: Dependent kiln parameters.

Kiln Parameters Description	Symbol	Graph Symbol	Units
Temperature of flue gas in cyclone 1	$T_{G,Cy1,out}$	T_G1_out	[°C]
Outlet pressure in cyclone 1	$P_{Cy2,out}$	P_2_out	[mbar]
O_2 concentration in the preheater exhaust gas	$w_{O_2,G,PT,out}$	w_O2_G_PT_out	[% wt/wt]
Temperature of the flue gas in cyclone 2	$T_{G,Cy2,out}$	T_G2_out	[°C]
Outlet pressure in cyclone 2	$P_{Cy2,out}$	P_2_out	[mbar]
Temperature of the flue gas in cyclone 3	$T_{G,Cy3,out}$	T_G3_out	[°C]
Outlet pressure in cyclone 3	$P_{Cy3,out}$	P_3_out	[mbar]
Temperature of the flue gas in cyclone 4	$T_{G,Cy4,out}$	T_G4_out	[°C]
Outlet pressure in cyclone 4	$P_{Cy4,out}$	P_4_out	[mbar]
Inlet pressure in cyclone 5	$P_{Cy5,out}$	P_5_in	[mbar]
Inlet temperature in cyclone 5	$T_{G,Cy5,in}$	T_G5_in	[°C]
Outlet temperature in cyclone 5	$T_{HM,RK,in}$	T_HM_RK_in	[°C]
Inlet pressure in the kiln	$P_{RK,in}$	P_RK_in	[mbar]
CO concentration in the kiln inlet	$w_{CO,RK,inlet}$	w_CO_RK_inlet	[%]
O_2 concentration in the kiln inlet	$w_{O_2,RK,inlet}$	W_O2_RK_inlet	[%]
O_2 concentration in preheater exhaust gas	$w_{O_2,G,PT,out}$	W_O2_G_PT_out	[%]
Moment in the kiln	τ_{RK}	tau_RK	[Nm]
Hot meal feeding to hotdisc	$m_{\%,HM\_Hotdisc}$	m_%_HM_Hotdisc	[%]

As discussed in this section, independent kiln parameters in Table 5.2 control the dynamics of the process, sulphur input to the system and sulphur output from the system. On the other hand, dependent kiln parameters in Table 5.4 indicates the influence of changes in independent kiln parameters. For instance, variation in %ID Fan power varies fan speed subsequently varying pressure and to some degree temperature in the preheater tower thereby varying sulphur capture and formation phenomena in the tower. Henceforth, all independent/dependent kiln parameters mentioned above are chosen for further statistical analysis. Clinker production rate is omitted in the analysis as it is linearly related to the kiln feed (100% correlation).

5.3 Correlation of SO$_2$ Level in the Stack Gas with Kiln Parameters

Correlation coefficient is a statistical tool for determining the linear relationship between two random variables. The coefficient between two random variables x & y is calculated using Equation 4.2. The coefficient is between -1 to 1, and it measures the strength of one to one linear relationship between two random variables. The coefficient value in the vicinity of +1 indicates a strong linear relationship between two variables and a variable is expected to increase with an increase in another variable or vice versa. The coefficient value in the vicinity of -1 indicates a strong linear relationship between two variables. However, a variable is expected to decrease with an increase in another variable or vice versa. The coefficient value in the vicinity of 0 means that two variables do not have a linear relationship or a weak linear relationship. Correlation coefficient calculation is a useful tool to determine the potential positive/negative relationship between two variables. For this reason, it is used to compare relation between kiln variables and SO$_2$ level in the stack gas.

$$r_{xy} = \frac{n\sum x \cdot y - \sum x \sum y}{\sqrt{\left[n\sum x^2 - \left(\sum x\right)^2\right]\left[n\sum y^2 - \left(\sum y\right)^2\right]}} \tag{5.2}$$

Where,

r_{xy} Correlation coefficient between x and y

n Sample size

Figure 5.4 and Figure 5.5 show a bar chart of the correlation coefficient between SO$_2$ level in the stack gas and important kiln parameters. Both compare coefficients between Week-1 and Week-2 in two different rawmill operation mode, RM-ON (Figure 5.5), and RM-OFF (Figure 5.5). Calculated correlation coefficients are significantly far from ±1, especially in RM-ON mode. However, the plot can be used to compare relative significance of the parameters. Among the parameters, the most significant parameters with a positive correlation in RM-ON mode in both weeks are kiln feed, kiln speed and hot meal feeding to the hotdisc, and with significant negative correlations are bypass water supply rate, rawmill feed, and volume fraction of tertiary air. Interestingly, there is a very high correlation between process parameters (pressure and temperature) with the SO$_2$ level in the stack gas in Week-1 (especially in RM-OFF mode), but the correlation in Week-2 in RM-OFF mode is relatively lower. Beside bypass water supply, other parameters have different correlations in 4 different cases, Week-1: RM-OFF mode, Week-1: RM-ON mode, Week-2: RM-OFF mode and Week-2: RM-ON mode. The inconsistent correlations between emission level and the kiln parameters are probably due to non-uniform variation of the parameters in chosen data and lack of identical raw materials and fuels.

Figure 5.4: Comparison plot of correlation coefficients between SO2 in the stack gas and other important kiln parameters in Week-1 (blue) and Week-2 (red) (RM-ON mode).
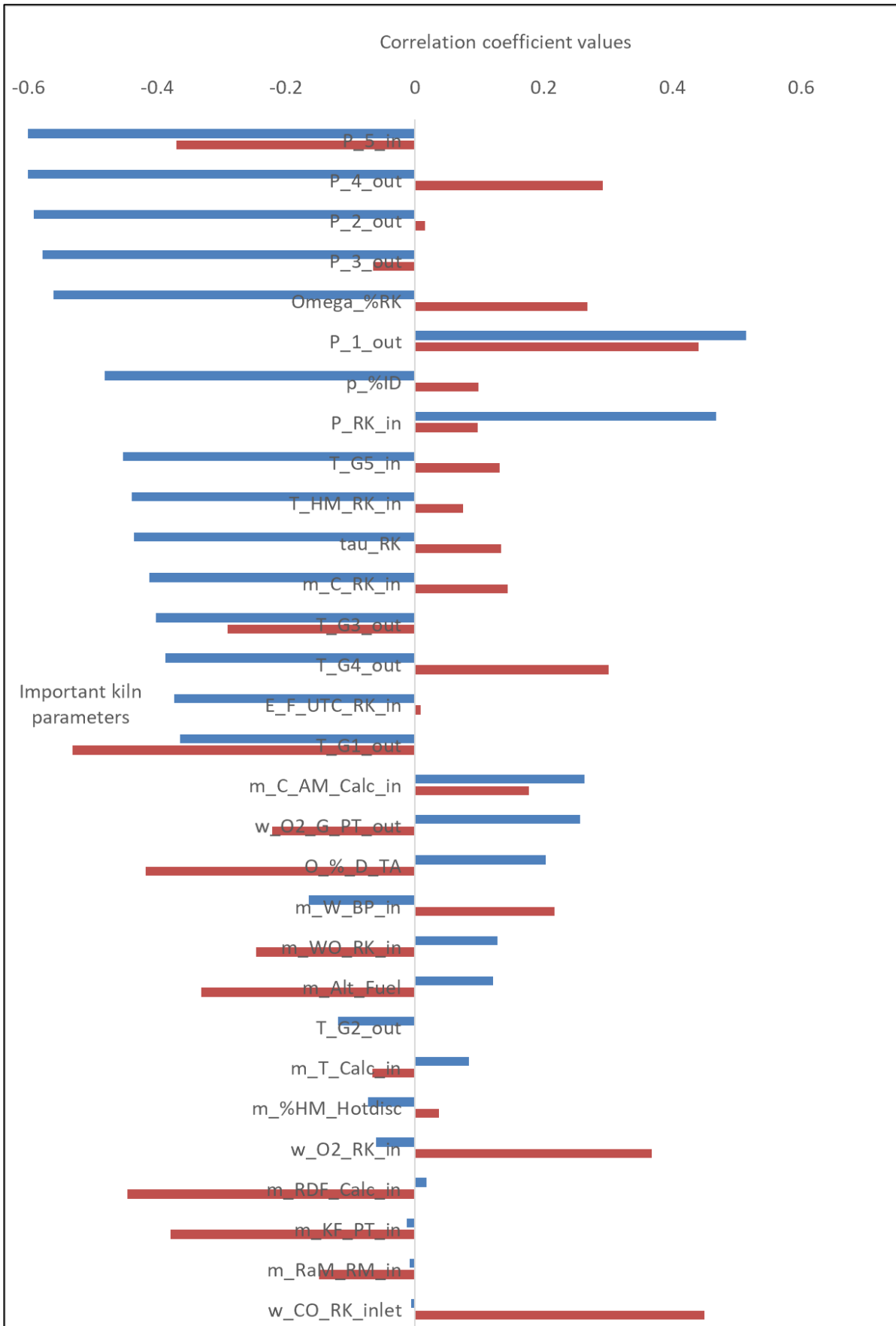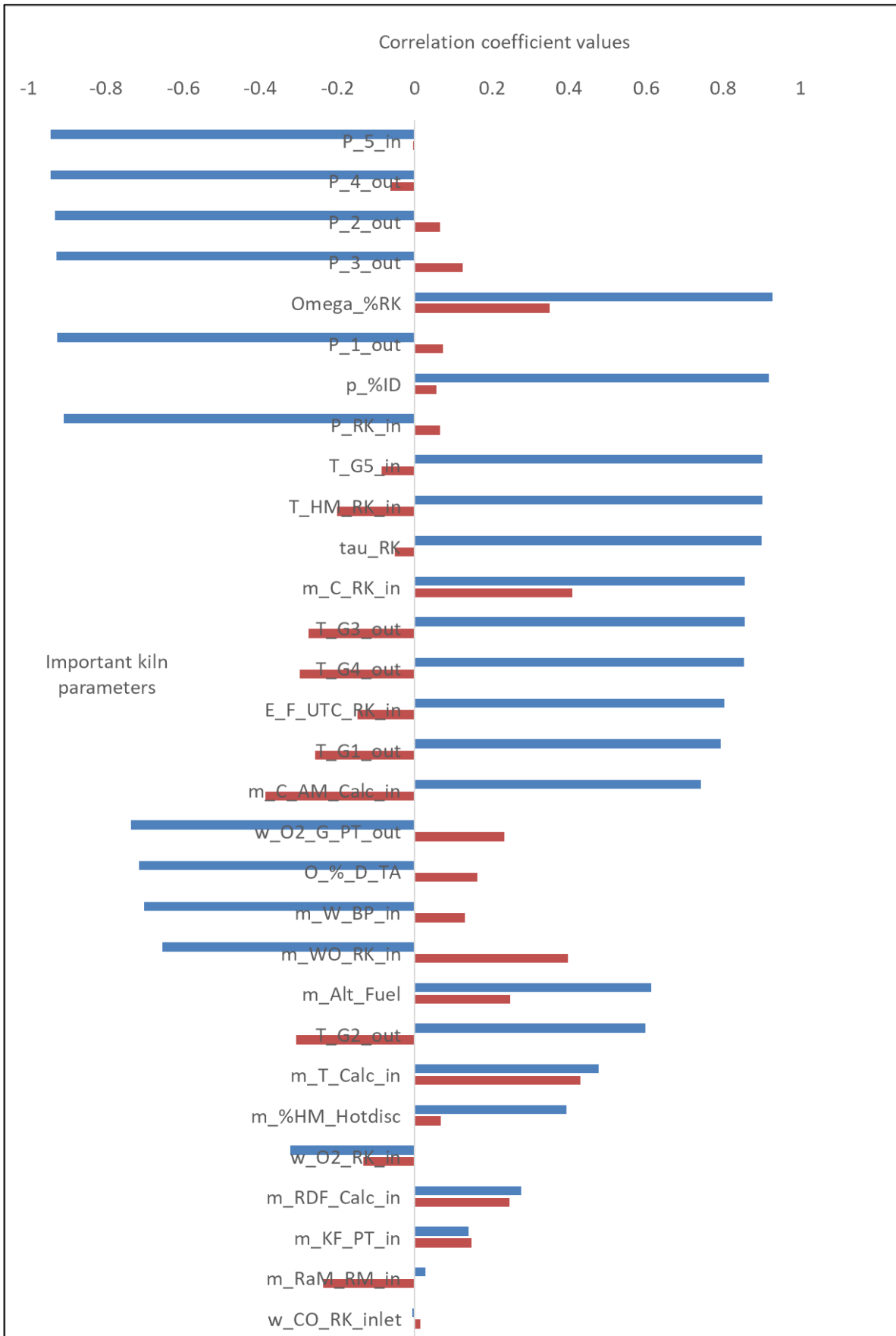
Figure 5.5: Comparison plot of correlation coefficients between SO_2 in the stack gas and other important kiln parameters in Week-1 (blue) and Week-2 (red) (RM-OFF mode).

5.4 Sulphur Material Flow Calculation and Sankey Diagram

This section presents a summary of data used for calculation of sulphur flow in different streams, and subsequent sulphur flow representation in Sankey Diagram.

5.4.1 Data Summary

Sulphur flow calculation using model formulation in Chapter 3 is performed in two different periods, Period-1 (11 December 22:00 to 12 December 05:00), and Period-2 (24 August 00:00 to 24 August 22:00). Period-1 and Period-2 represent the longest rawmill operating period in Week-1 and Week-2 respectively. Table 5.5 and Table 5.6 present a summary of averaged flow data and sulphur concentration data in the respective periods.

Table 5.5: Summary of collected flow and sulphur composition data in Period-1.

Variables	Value	Type of data	Start Time	End Time	Number of data points
$\dot{m}_{RMF,RM,in}$	129.8 t/h	Averaged Raw Data	11 December 22:00	12 December 5:00	420
$w_{SO_3,RaM,RM,in}$	0.77%	Averaged Lab Data	2017 Averaged Lab Data obtained from the Lab Department		
$\dot{m}_{KF,PT,in}$	99 t/h	Averaged Raw Data	11 December 22:00	12 December 5:00	420
$w_{SO_3,KF,PT,in}$	1.0%	Averaged Lab Data	11 December 23:34	12 December 03:37	2
$w_{SO_3,HM,RK,in}$	4.35%	Averaged Lab Data	12 December 00:32	12 December 05:12	2
$\dot{m}_{CL,RK,out}$	63.5 t/h	Approx.	11 December 22:00	12 December 5:00	420
$w_{SO_3,CL,RK,out}$	1.2%	Averaged Lab Data	12 December 00:14	12 December 06:23	4
$w_{SO_3,CKD,FF,out}$	0.96%	Historical Lab Data	2016-03-04	2016-03-04	1
$w_{SO_3,D,BP,out}$	8.8%	Single lab data sampled on 15th December 2017			
$\dot{m}_{D,BP,out}$	0.24 t/h	Average bypass dust collected in Period-1			
$\dot{m}_{C,Calc,in}$	3.4 t/h	Averaged raw Data	11 December 22:00	12 December 5:00	420
$\dot{m}_{C,RK,in}$	3.3 t/h	Averaged Raw Data	11 December 22:00	12 December 5:00	420
$w_{S,C}$	0.76%	As received quality data of the coal delivered at the plant on 14th September			
$\dot{m}_{AM,Calc,in}$	0 kg/h	Averaged Raw Data	11 December 22:00	12 December 5:00	420
$w_{S,AM}$	0.34%	As received quality data of the oil delivered at the plant from 25th September 2017 to 23rd January 2018			
$\dot{m}_{T,Calc,in}$	47 kg/h	Averaged Raw Data	11 December 22:00	12 December 5:00	420
$w_{S,T}$	0.5%	Measured	Suppliers Sampled Data		
$\dot{m}_{RDF,Calc,in}$	1230 kg/h	Averaged Raw Data	11 December 22:00	12 December 5:00	420

Variables	Value	Type of data	Start Time	End Time	Number of data points
$w_{S,RDF}$	1.5%	Measured	Suppliers Data		
$\dot{m}_{RDF,Calc,in}$	435 kg/h (pellets)	Averaged Raw Data	11 December 22:00	12 December 5:00	420
$w_{RDF,Pel}$	0.21 (Pellets)	Measured	Approximated value		
$C_{SO_2,G,BP,out}$	170 mg/Nm^3 (wet)	Averaged Raw Data	11 December 22:00	12 December 5:00	420
$\dot{V}_{G,Stack}$	170000 Nm^3/h	Averaged Raw Data	11 December 22:00	12 December 5:00	420
$T_{G,BP,out}$	142.6°C	Averaged Raw Data	24 August 00:00	24 August 22:00	1320
$C_{SO_2,G,Stack}$	464 mg/Nm Dry @10% O$_2$	Averaged Raw Data	11 December 22:00	12 December 5:00	420
M_{CF,T_1}	90.71%	Raw Data	CF-silo level at 22:00, 11 December		
M_{CF,T_2}	91.78%	Raw Data	CF-silo level at 05:00, 12 December		
$M_{CF,AC}$	18.3 t/h	Calculated	---		

Table 5.6: Summary of collected flow and sulphur composition data of Period-2.

Variables	Value	Type of data	Start Time	End Time	Number of data points
$\dot{m}_{RMF,RM,in}$	130.1 t/h	Averaged Raw Data	24 August 00:00	24 August 22:00	1320
$w_{SO_3,RaM,RM,in}$	0.59%	Averaged Lab Data	2017 Averaged Lab Data obtained from the Lab Department		
$\dot{m}_{KF,PT,in}$	103.5 t/h	Averaged Raw Data	24 August 00:00	24 August 22:00	1320
$w_{SO_3,KF,PT,in}$	0.83%	Averaged Lab Data	24 August 3:12	24 August 19:23	5
$w_{SO_3,HM,RK,in}$	4.1%	Averaged Lab Data	Average of three samples from 11th August and one sample from 9th September		
$\dot{m}_{CL,RK,out}$	67.2 t/h	Approx.	24 August 00:00	24 August 22:00	1320
$w_{SO_3,CL,RK,out}$	1.27%	Averaged Lab Data	24 August 02:04	24 August 20:32	10
$w_{SO_3,CKD,FF,out}$	0.96%	Past Sampled Lab Data	2016-03-04	2016-03-04	1
$w_{SO_3,D,BP,out}$	13.4 %	Single lab data sampled on 15th December 2017			
$\dot{m}_{D,BP,out}$	0.24 t/h	Average bypass dust collected in Period-2			
$\dot{m}_{C,Calc,in}$	3.4 t/h	Averaged raw Data	24 August 00:00	24 August 22:00	1320
$\dot{m}_{C,RK,in}$	2.51 t/h	Averaged Raw Data	24 August 00:00	24 August 22:00	1320
$w_{S,C}$	0.60%	As received quality data of the coal delivered at the plant on 14th September			
$\dot{m}_{WO,RK,in}$	437 kg/h	Averaged Raw Data	24 August 00:00	24 August 22:00	1320
$w_{S,WO}$	0.34%	As received quality data of the oil delivered at the plant from 25th September 2017 to 23rd January 2018			
$\dot{m}_{AM,Calc,in}$	0 kg/h	Averaged Raw Data	24 August 00:00	24 August 22:00	1320

Variables	Value	Type of data	Start Time	End Time	Number of data points
$w_{S,AM}$	0.5%	Measured	Suppliers Sampled Data		
$\dot{m}_{T,Calc,in}$	2791 kg/h	Averaged Raw Data	24 August 00:00	24 August 22:00	1320
$w_{S,T}$	1.5%	Measured	Suppliers Data		
$\dot{m}_{RDF,Calc,in}$	530 kg/h (pellets)	Averaged Raw Data	24 August 00:00	24 August 22:00	1320
$w_{RDF,Pel}$	0.21 (Pellets)	Measured	Approximated value		
$C_{SO_2,G,BP,out}$	38 mg/m^3 (wet)	Averaged Raw Data	24 August 00:00	24 August 22:00	1320
$\dot{V}_{G,Stack}$	168000 Nm^3/h	Averaged Raw Data	24 August 00:00	24 August 22:00	1320
$T_{G,BP,out}$	149°C	Averaged Raw Data	24 August 00:00	24 August 22:00	1320
$C_{SO_2,G,Stack}$	249 mg/Nm^3 Dry @10% O_2	Averaged Raw Data	24 August 00:00	24 August 22:00	1320
M_{CF,T_1}	90.56%	Raw Data	CF silo level at 00:00, 24 August		
M_{CF,T_2}	93.61%	Raw Data	CF silo level at 22:00, 24 August		
$M_{CF,AC}$	18.9 t/h	Calculated	---		

5.4.2 Sulphur Flow Calculations and Sankey Diagrams

Sankey Diagram is a graphical presentation of flow quantities such as material and energy flows. The width of a line in the diagram is proportional to the flow rate. Therefore, it enables direct comparison of relative flow of material/energy in the different flow streams and assesses critical flow streams. In this section, sulphur flows in different flow streams for Period-1 and Period-2 are presented in Sankey Diagram. The procedures for reference sulphur flow calculation for Period-1 are presented in Appendix F. The results for both periods are summarised in Table F.1 in Appendix G. Figure 5.6, and Figure 5.7 are Sankey Diagrams representing sulphur flows in the respective periods.

Period-1 represents the higher sulphur emission period with an average sulphur flow of *39.4 kg/h*, and Period-2 represents the lower sulphur emission period with an average sulphur flow of *20.9 kg/h* in the stack gas. In both periods, the sulphur flow in the hot meal *(1171.8 kg/h in Period-1 and 1154.7 kg/h in Period-2)* and kiln exhaust gas *(877.7 kg/h in Period-1 and 813.7 kg/h in Period-2)* are significantly higher than sulphur flow in the kiln feed *(396.0 kg/h in Period-1 and 343.6 kg/h in Period-2)* and fuel *(67.8 kg/h in Period-1 and 73.6 kg/h in Period-2)*. The sulphur flow in the hot meal is almost 3 times sulphur input from the kiln feed in respective periods indicating very high internal recirculation between the preheater, calciner and rotary kiln. The recirculation in Period-1 is relatively higher than in Period-2, which coincides with comparatively higher emission in Period-1. At the same time, sulphur capture in bypass dust in Period-2 is relatively higher than in Period-1.
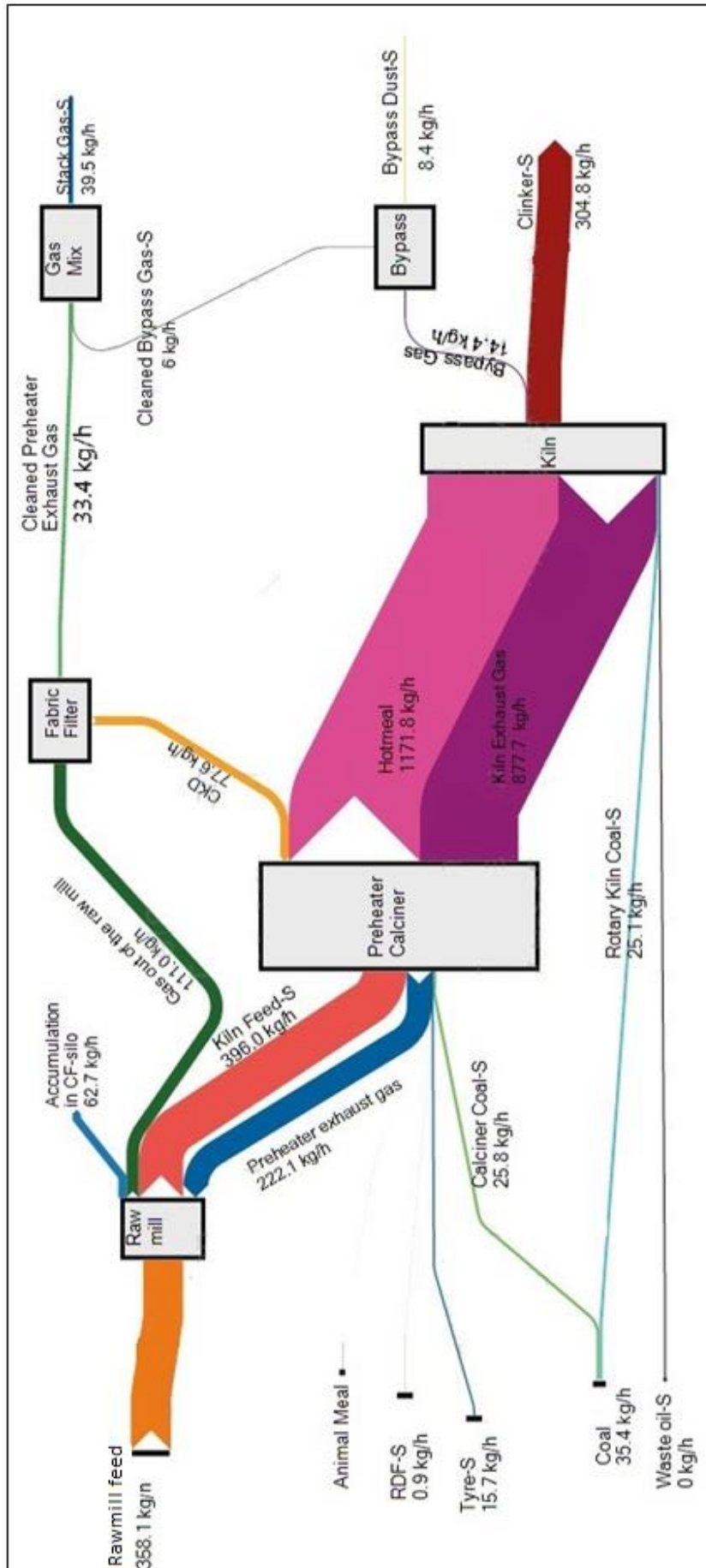
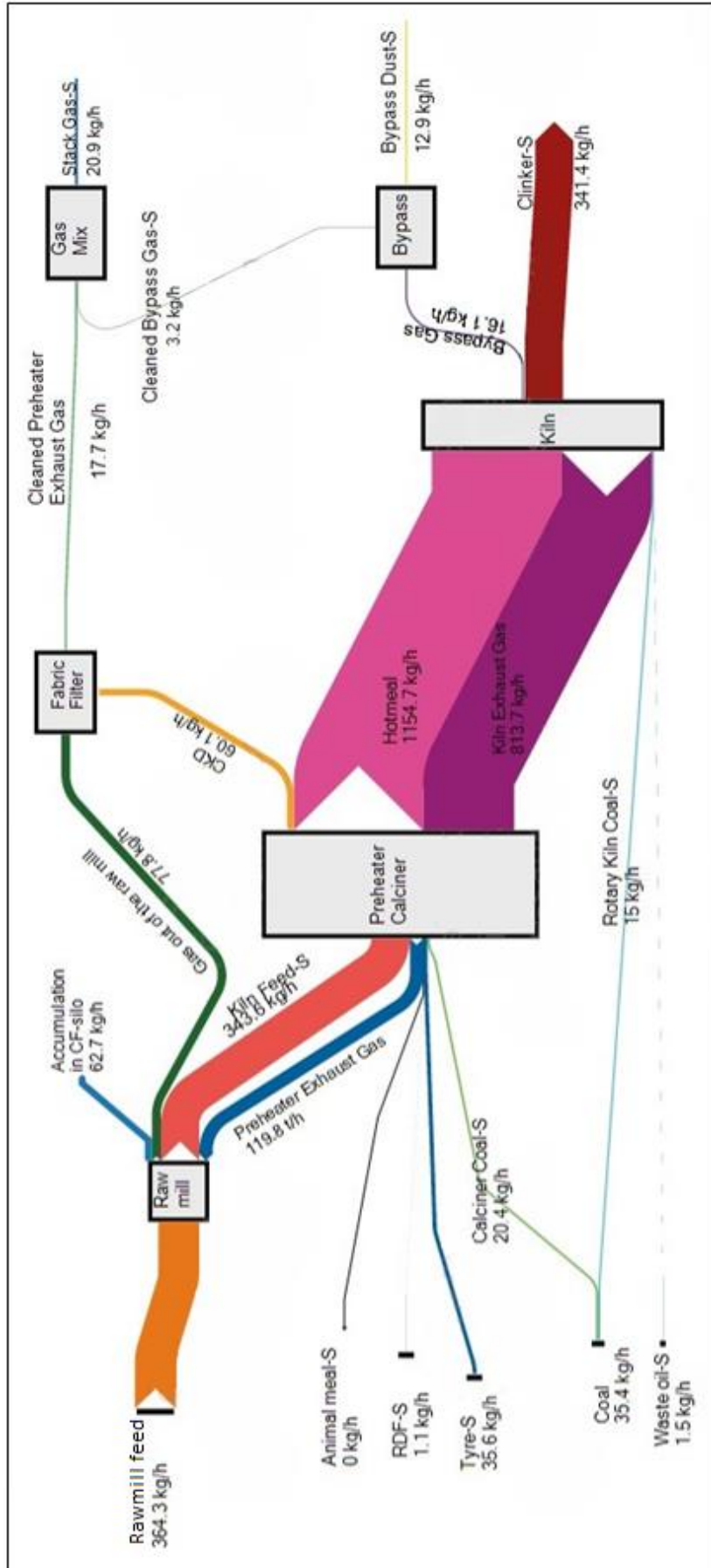Figure 5.6: Sankey diagram representing sulphur flows on Period-1.

Figure 5.7: Sankey diagram representing sulphur flows on Period-2.

5.5 Multivariate Regression Analysis

In this section, multiple regression analysis is used to formulate SO_2 regression model (in RM-ON mode) and compare relative significance of the parameters on the variation in sulphur emissions. Additionally, the model is validated using RM-ON mode data in two separate weeks.

5.5.1 Data Processing

A single model using odd serial number data of independent parameters of both weeks (RM-ON mode) is used to formulate the regression model. The data from both weeks in RM-ON mode, Week-1 and Week-2 are merged followed by separation of odd/even serial number data to reduce total data. After filtration of odd/even serial number data, odd serial number data group has 6484 timestamps data points, and even serial number data group has 6483 timestamp data points of all parameters. The parameter values are normalised using the maximum and minimum values of respective parameters (Equation 4.3). The normalised values are non-dimensional and are in the range of -1 to 1. The main benefit of model formulation using normalised parameter values is that the relative significance of the parameters can be found by direct comparisons of coefficient values in the model.

$$X_{\text{normalized}} = 2 \cdot \frac{X_{\text{actual}} - X_{\text{min}}}{X_{\text{max}} - X_{\text{min}}} - 1 \tag{5.3}$$

Where,

$X_{\text{normalized}}$	Normalized value of variable X
X_{actual}	Actual value of X
X_{max}	Maximum value of variable X
X_{min}	Minimum value of variable X

The maximum and minimum values of independent kiln parameters in typical plant operations in 2017 is summarised in Table 5.7.

Table 5.7: Maximum and minimum value of independent kiln parameters in RM-ON mode.

Kiln Parameters Description	Symbol	Units	Max value	Min Value
Tyre feeding in the hotdisc	$\dot{m}_{T,Calc,in}$	[kg/h]	4495	0
RDF feeding in the hotdisc	$\dot{m}_{RDF,Calc,in}$	[kg/h]	4067	0
Coal feeding in the kiln	$\dot{m}_{C,RK,in}$	[kg/h]	3.7	2.45
Kiln feed into the preheater tower	$\dot{m}_{KF,PT,in}$	[t/h]	105.7	89.2
Volume fraction of tertiary air	$\dot{V}_{\%,TA}$	[-]	44.2	24.1
Raw material feeding into the raw mill	$\dot{m}_{RaM,RM,in}$	[t/h]	150.4	63.6
Bypass water supply rate in the bypass	$\dot{V}_{W,BP,in}$	[m³/h]	7.6	1.73
Energy input per ton of clinker from the rotary kiln fuels	$\hat{E}_{F,UTC,RK,in}$	[MJ/t clinker]	2053	1070
SO_3 composition in the kiln feed	$w_{SO_3,KF,PT,in}$	[% w/w]	1.0	0.81

In the model formulation, independent parameters, kiln rotating speed, % ID Fan power and calciner gas temperature set-points, are omitted. These parameters are usually constant, and they are only changed to maintain the quality of the clinker (reduce free lime and increase alites content) and operability of the kiln.

5.5.2 Regression Model

Equation 4.4 is a regression model (Model-1) formulated using odd serial number data of both weeks (RM-ON mode). The goodness of fit[8] R^2_{M1} is significantly high (88%) which shows that the model parameters are the primary cause of variation in sulphur emissions in the chosen week. It is also evident in the trends of measured and predicted SO_2 level as shown in Figure 5.8. The measured level and predicted level are overlapping to a certain degree which confirms that the kiln parameters included in the model cause variation in sulphur emission and the model is quite efficient to predict SO_2 level in both weeks.

$$
\begin{aligned}
C_{SO_2,g,stack} = {} & 344.7 + 132.5 w_{SO_3,KF,PT,in} - 89.0 \dot{V}_{W,BP,in} + 82.6 \dot{E}_{F,RK.in} \\
& - 56.8 \dot{m}_{RaM,RM,in} + 28.0 \dot{m}_{KF,PT,in} + 24.4 \dot{m}_{C,RK,in} + 11.4 \dot{m}_{T,Calc,in} \quad (5.4) \\
& - 5.8 \dot{m}_{RDF,Calc,in} - 3.0 O_{\%,D,TA}
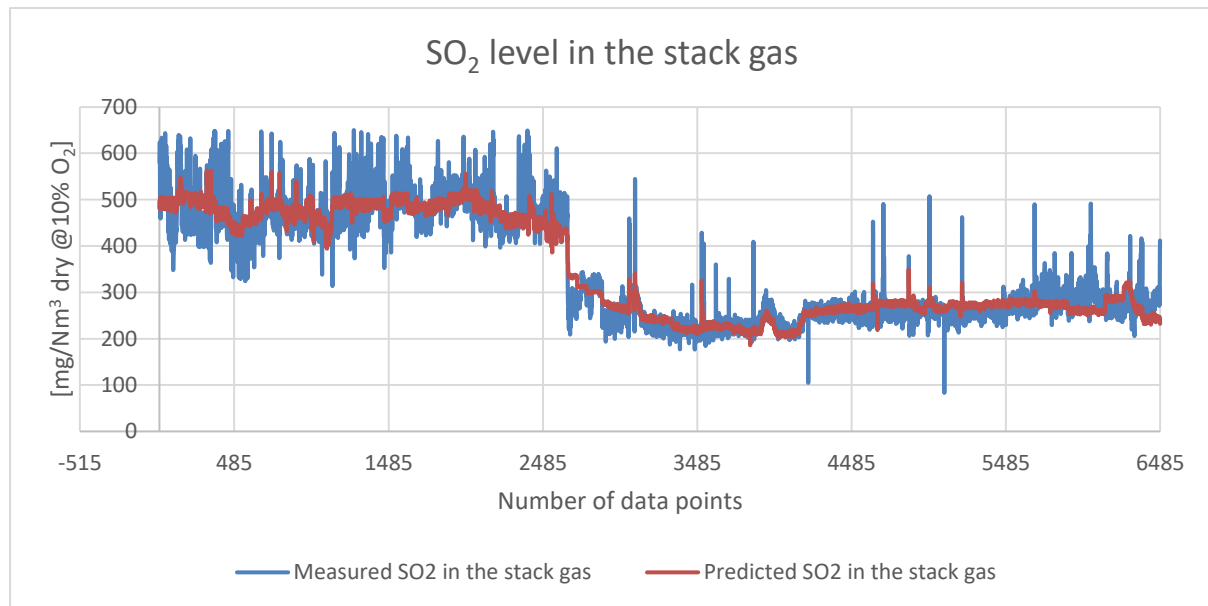\end{aligned}
$$

$$ R^2_{M1} = 0.88 \tag{5.5} $$

Figure 5.8: Trends of measured and predicted SO_2 level in the stack gas ([mg/Nm^3 @10% O_2]) of odd serial number data of both weeks.

Figure 5.9 shows a chart of coefficients in the model. The parameters are sorted in descending order of coefficient values. Among all independent parameters, SO_3 content in kiln feed (w_SO3_KF_PT_in) and energy input per unit ton of clinker by rotary kiln fuels

---

[8] Goodness of fit measures how well the model represents the data used for model formulation. A 100% (1) or close to 100% fit means that the model predicted data and actual data used to build the model are statistically identical and hence the model parameters are primary cause of variation in the output variable. A 0% or close to 0% fit means that the model predicts entirely different data than the actual data used to build the model, and the chosen parameters in the model have no influence in the variation of output variable.

(E_F_UTC_RK_in) have a significant positive effect[9] on the emission level in the stack gas. In addition to these parameters, kiln feed (m_KF_PT_in), coal feeding in the kiln (m_C_RK_in) and tyre feeding (m_T_Calc_in) have a positive effect on the emission level. In contrast, bypass water supply rate (V_W_BP_in) and rawmill feed (m_RMF_RM_in) have a significant negative[10] effect on the emission level. RDF feeding (m_RDF_Calc_in) has relatively low but negative effect on the SO_2 emission level, and tertiary air supply has a negligible impact on the SO_2 emissions. The impact of tertiary air supply rate in the model might have been impacted by the fact that tertiary air damper was operated manually in Week-1 and Week-2.
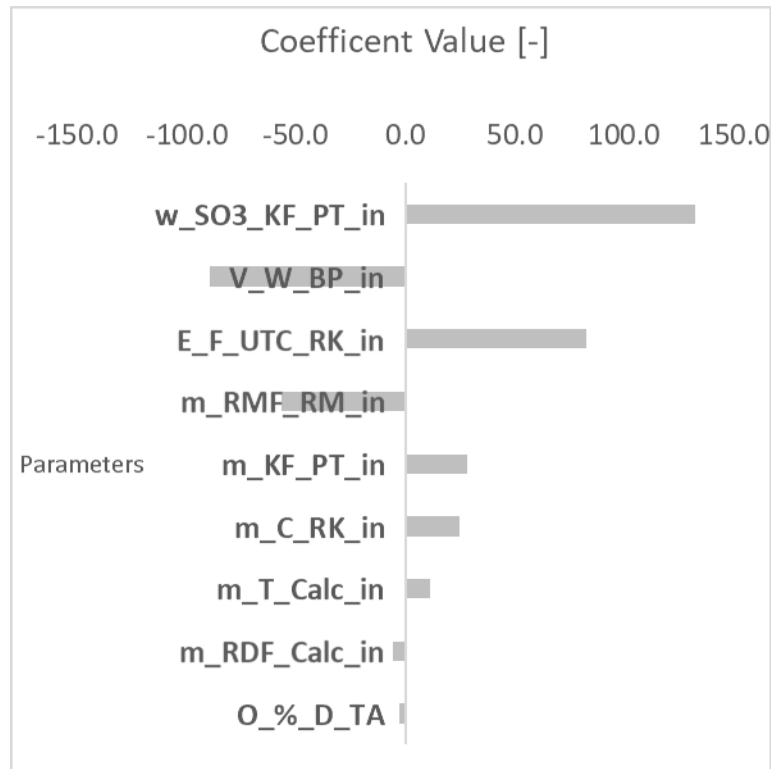

Figure 5.9: Coefficients of the regression model.

5.5.3 Model Validation

To check the validity of the sulphur emission model, Equation 5.4, data from 24th September 2017, at 08:43 to 1st October 2017, at 08:42 (Week-3) and 8th March 2018, at 23:55 to 15th March 2018, at 23:55 (Week-4) are used. Both weeks contain 10080 raw timestamps data points of all model parameters along with SO_2 emission level in the stack gas. After filtration of kiln feeding to 80 t/h or higher, bypass water supply 1 m³/s or higher, and SO_2 level in stack gas 650 mg/Nm³ or lower, filtered dataset consists of 8155 and 8256 timestamps dataset of Week-3 and Week-4 (in RM-ON mode) respectively. These data are normalised using maximum and minimum value in Table 5.7 (as the model is formulated using normalised parameters values of odd serial number data from Week-1 and Week-2) and then SO_2 emission for each timestamps data in RM-ON mode is predicted using Equation 5.4.

---

[9] Positive effect means an increase in a parameter results in an increase in a output variable or vice versa.

[10] Negative effect means a increase in a parameter results in a decrease in output variable or vice versa.

Figure 5.10 shows a comparison plot of the predicted SO_2 emission level and measured SO_2 level in the stack gas. The first half of the curve in Figure 5.10 corresponds to the predicted and measured SO_2 level in Week-3, and next half corresponds to the predicted and measured SO_2 level in Week-4. The model efficiently predicts general trends of the emission in Week-3. In the prediction of SO_2 level in Week-4, the model is unable to reproduce peaks in measured SO_2 emission curve. It is since the data used for model formulation does not contain a systematic variation of model parameters. On the other hand, the model (Equation 5.4) omits potential influences of types of RDF (pellets or non-pellets) used in Week-1 and Week-2. Besides these reasons, the model might have been affected by other parameters such as preheater exhaust gas flow (controlled by % ID Fan Power parameter), tertiary air supply and clinker quality[11]. Nevertheless, the model can still be used to predict a general trend of sulphur emission in stack gas and compare the relative impact of the model parameters on the variation in sulphur emission.
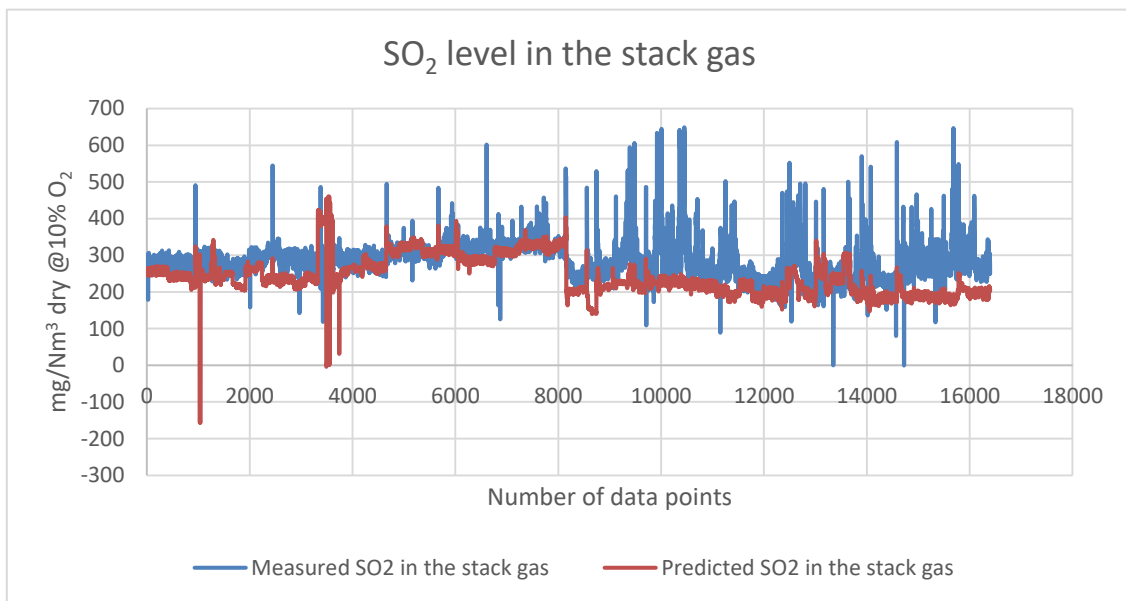

Figure 5.10: Measured SO_2 in the stack gas and model predicted SO_2 level in the stack gas ([mg/Nm^3 @10% O_2]) on validation period.

5.6 Summary of Data Analysis

Correlation analysis, regression analysis, and sulphur flow calculation and subsequent representation in the Sankey Diagram show that kiln parameters, independent or dependent parameters directly or indirectly influences SO_2 emissions from the plant. Emission level in Week-1 was higher than in Week-2. The significant difference between these weeks apart from emission level was that the SO_3 content in the kiln feed was substantially different between Week-1 and Week-2 (1% w/w in Week-1 to 0.83% w/w in Week-2). Other parameters show inconclusive and inconsistent correlations (significantly far from ±1) in different scenarios (Week-1: RM-ON mode, Week-1: RM-OFF mode, Week-2: RM-ON mode, and Week-2 RM-OFF mode) suggesting that sulphur emission behaviour is a complex thermochemical process.

In case of regression model formulated using odd serial number data of Week-1 and Week-2, the model has fairly high R^2 value and indicates that model parameters are the primary cause of variation in sulphur emissions from the plant. The model is formulated using 9 controllable

---

[11] Calciner gas temperature setpoint is varied based on the free lime content in the clinker.

kiln parameters. The model suggests that SO_3 content in the kiln feed and Energy input per unit ton of clinker from rotary kiln fuels have the largest positive impact, and bypass water supply has the largest negative impact on the emission level. Other parameters, kiln feed, coal feeding in the kiln and tyre feeding, have a positive impact while RDF feeding and tertiary air supply has a relatively low negative impact on the emission level. The model could reproduce emission behaviour in Week-1 and Week-2 and to some degree in Week-3, but it is unable to predict emission levels (in Week-4) with reasonable accuracy.

The inconsistent correlation between emission level with kiln parameters in different scenarios and the inability of the model to predict emission level with sufficient accuracy can be potentially related to a lack of systematic variation of the parameters, time lag between changes in emission level and kiln parameters and limitations of SO_2 measuring instruments. Furthermore, it is difficult to measure exact sulphur content in the rawmill feed, and the plant does not have provision to measure sulphur content in the preheater exhaust gas, cleaned preheater exhaust gas flowing out of the fabric filter and cement kiln dust. Hence, it is deemed necessary to perform kiln test in the controlled environment and measure sulphur content in various streams to formulate a fairly representative statistical SO_2 model and analyse sulphur flow in different streams.

6 Experimental Tests of Kiln Process

Sulphur emission model (Model-1) formulated using historical emission data in Chapter 4 shows that the lack of systematic and uniform variation of kiln parameters is the main reason behind the inability of the model to predict sulphur emissions in Week-3 and Week-4. Furthermore, the lack of live sampling or at least frequent spot sampling of SO_3 content in the cement kiln dust, preheater exhaust gas flowing out of the preheater tower and gas flowing out of the rawmill have caused difficulties in determining sulphur flow in these streams as well as in the rawmill feed with reasonable accuracy. Thus, an experimental plan is prepared to test sulphur behaviour in the kiln with the aim of finding out impacts of kiln parameters on the emissions and formulating a sulphur emission model. This chapter presents an overview of the design of experiments (DOE) as well as a description of SO_2 measurement systems in the stack and bypass. Additionally, it presents a summary of the experimental responses of SO_2 emissions and sulphur content in various streams.

6.1 Design of Experiments in the Kiln Tests

Oxford Dictionary defines Experiments as "A scientific procedure undertaken to make a discovery, test a hypothesis, or demonstrate a known fact" [30]. In general, experiments are planned, performed and analysed to determine the impact of variables (factors) on dependent variables (response variable) by varying factor to distinct predetermined values (levels of the factor). Figure 6.1 shows the interaction of experimental factors, constraints and random noise on the response variable [31, 32]. In the kiln tests, SO_2 level in the stack gas is a response variable, and kiln parameters are experimental factors. The variability in ambient temperature, feeding of fuels and rawmill/kiln feed, and faulty operations introduces random noise in the response variable while calciner exhaust gas temperature setpoints, ID fan speed, kiln rotating speed and tertiary air supply are constraints to maintain clinker quality and operability of the kiln.
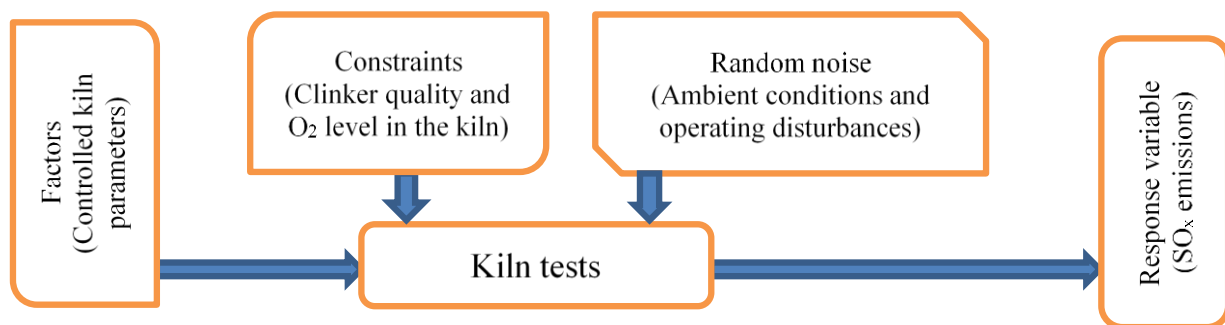

Figure 6.1: Interaction between factors, constraints and random noise and their impact on the response variable.

In this study, DOE is used to plan, perform and analyse the experiments systematically. It aims to identify the effect of factors on the response variables. There are diverse types of DOEs based on a total number of runs, the scope of experiments, objectives and time/cost factors. Among many designs, a full factorial design of experiments is a design where test runs are a combination of all factors at all levels. It consists of the largest possible number of runs thereby requires huge time and cost. A full factorial design with n factors each at 2 levels has total experimental runs of 2^n without any replications. The main advantage of this design is that it can be used to determine linear effects of the factors on the response variable as well as higher order interactions effects between the experimental factors. In real industrial experimental tests, it is impractical, expensive and time-consuming to perform a large number of test. Instead,

alternatives design such as fractional factorial design and screening design with a fewer number of tests are preferred [31, 32].

The fractional factorial design is a subset of full factorial design with fewer test runs. The design is highly randomized, orthogonal, robust, and resolution IV design. In resolution IV design, one can distinctly determine main effects (linear effects) of the factors on the response variables, but two-factor interactions are confounded with other two factor interactions. Confounding in general means that two different effects are blended and it is impossible to determine the distinct effect of a term with its confounded terms. On the other hand, screening design is highly randomized, orthogonal design with the fewest total experimental runs. The design is suitable to determine main effects (linear effects) of the factors on the response variables [31, 32].

6.2 Experimental Plan and Procedures

Initially, a fractional factorial design with 16 experimental test runs was planned for the kiln tests. Due to various operational issues, the problem in hotdisc operation, the mechanical problem in the rawmill motor and delay in the waste oil delivery, tests were postponed indefinitely after completion of just 5 out of 16 planned tests. According to this plan, a new stockpile in the quarry with low sulphur would be prepared, and the effect of low sulphur stockpile would be observed in the kiln feed within a week after the 1st test. These problems have posed a need for a new experimental plan with a fewer number of test runs so that the tests conditions are as identical as possible. Thus, instead of continuing with an old experimental plan (fractional factorial design (resolution IV design) with 16 runs), experiments were performed based on a modified design, a screening design with 8 test runs. The screening design is suitable to determine main effects (linear effects) of the factors on the response variables with fewer experimental runs and it is sufficient to pinpoint the relative impact of kiln parameters on the variation in SO_X emissions from the plant [31, 32].

A complete description of the experimental plan together with experimental design matrix is in Appendix H. The kiln tests were performed according to the orthogonal experimental design matrix (Table 6.1). The design is a screening design with 8 test runs (1, 3, 4, 6, 7, 8, 10, 12, and 13) formulated using **R** (statistical software). It consists of 7 independent factors, namely kiln feed, RDF feeding, tyre feeding, coal feeding in the kiln, bypass water supply rate and energy input rate per ton of clinker from the rotary kiln fuels. All factors are set at two levels, a high level and a low level. In addition to these tests, test run number 2, 5, 9, and 11 performed according to previous plan (fractional factorial design) was also used for further analysis. Spot samples of clinker, kiln feed, hotmeal, bypass dust flowing out of the cyclone, bypass dust flowing out of the bypass filter and CKD flowing out of the fabric filter was taken for all 12 tests and used for further experimental analysis. The plan of in-situ analysis of the preheater exhaust gas flowing out of the rawmill and out of the fabric filter was aborted as portable gas analyser could not be used during the test period.

Table 6.1: Orthogonal design matrix implemented in the kiln tests.

Test runs	Date	Timeframe	Kiln feed	Rawmill feed	Coal feed	RDF feed	Tyre feed	Bypass water	Waste oil
			t/h	t/h	t/h	kg/h	kg/h	m3/h	kg/h
1	20/04	14:00-18:00	101	110	3.2	0	0	4.5	0
2	20/04	18:00-22:00	101	110	2.5	2000	0	3	700
3	26/04	10:00-14:00	101	140	2.9	0	1500	3	0
4	26/04	18:00-22:00	101	110	2.4	2000	1500	3.0	450
5	21/04	02:00-06:00	101	140	2.5	0	0	4.5	600
6	25/04	14:00-18:00	95	140	2.85	2000	0	3	0

7	25/04	18:00-22:00	95	110	2.7	2000	1500	4.5	0
8	25/04	22:00-02:00	95	110	2.5	0	0	3	150
9	24/04	22:00-02:00	95	140	3.15	0	0	3	0
10	26/04	22:00-00:30	95	140	2.4	0	1500	4.5	300
11	24/04	18:00-22:00	95	110	3.0	2000	0	4.5	0
12	26/04	14:00-18:00	101	140	2.4	2000	0	3	300

6.3 Description of the Measurement Systems

This section presents a description of measurement systems installed in Norcem cement plant in Kjøpsvik to measure SO_2 level in the stack gas and bypass gas.

6.3.1 Gas Analyzer in the Stack

The plant has installed GasMet CEMs II supplied by M/S Yter Avansert Gass Analyse (YAGA) based on Online-Fourier Transform Infrared Spectroscopy (FTIR) for continuous in-situ gas monitoring in the stack gas. FTIR technology is based on the principle that absorption of a broad spectrum of infrared light by particular gas is a function of chemical bonds between atoms in the gas molecule. As each gas is completely different with respect to atomic bonds, the light intensity of specific wavelength absorbed by particular gas is different from other gases. The light intensity is then calibrated to determine the composition of the gas.

In the plant, GasMet CEMs II measures flow rate, dust content, the composition of different gases (O_2, H_2O, CO_2, NO_X, SO_X, HCL, HF, CO, NH_3) and total organic carbon (TOC). In case of SO_2 measurement in the stack gas, the precision of the system is about $\pm 1.7\%$. As per operation manual, it must be calibrated every week (automatic calibration) and a comprehensive manual calibration by suppliers once a year. So far, the equipment has been calibrated as mentioned in the manual without any operational difficulties. Beside calibration, it is cleaned every week to remove deposition of unwanted chemicals (mainly acid deposition). Figure 5.2 shows a schematic diagram of GasMet CEMs II.
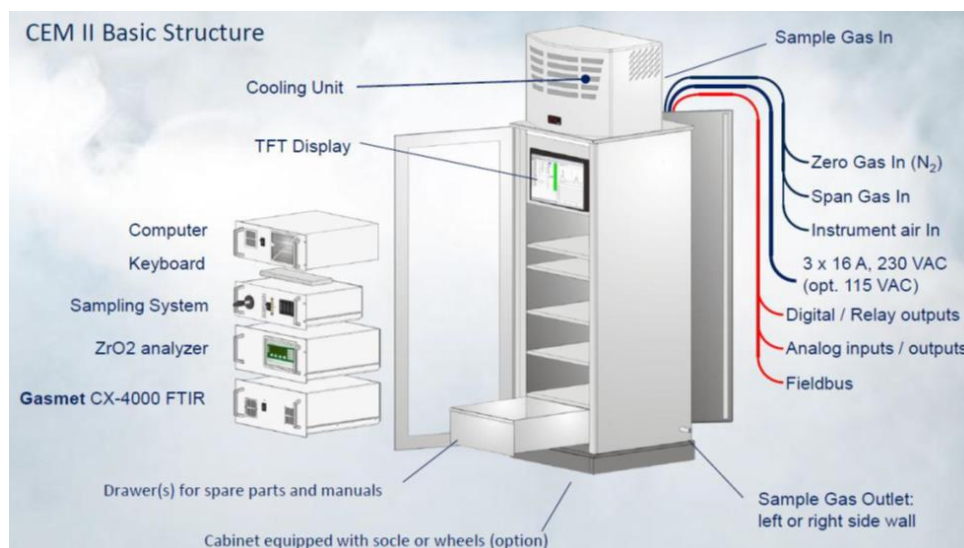

Figure 6.2: Schematic view of GasMet CEMs II measurement system (Source: **YAGA**).

GasMet CEMs II is also used to measure continuous gas flow rate in the stack gas. A speedometer measures the velocity of the gas in the stack gas and volume flow rate is calculated using Equation 7.1. The system calculates normalised dry gas flow rate by considering temperature and moisture level in the stack gas. The uncertainty in actual gas flow

measurement is about ±0.5%, but considering uncertainty in the measurement of moisture level and temperature, the uncertainty in normalised gas flow measurement is expected to be about ±1.34%,

$$\dot{V}_{stack,actual} = A_{stack} \cdot v_{stack,measured} \tag{6.1}$$

Where,

$\dot{V}_{stack}$ Volume flow rate of gas in the stack pipe

A_{stack} Cross-sectional area of the stack pipe

$v_{stack,measured}$ Measured velocity of the gas in the stack pipe

6.3.2 SO₂ Measurement System in the Bypass

The plant has installed NEOM LaserGas^{TM} Q-ICL Edition (an optical instrument) supplied by M/S NEO Monitor AS based on infrared single-line spectroscopy for continuous in-situ gas monitoring in the bypass gas. The main difference in the working principle between FTIR and infrared single-line absorption spectroscopy is, FTIR uses a broad spectrum of infrared light to measure the composition of diverse types of gases, but single-line spectroscopy uses a narrow band corresponding to an absorption line of the particular gas to measure the composition of that particular gas. The precision of this system is about ±1% of the typical measured value. As mentioned in the supplier's technical document, it should be calibrated at least one to 4 times in a year to maintain the desired accuracy. However, like GasMet CEMs II analyser for the stack gas, it is calibrated (manual calibration) every week, and it is cleaned physically to remove deposition of unwanted chemicals (mainly acid deposition). Figure 5.3 shows a schematic diagram of NEOM LaserGas^{TM} Q-ICL Edition.

1. Receiver electronics and housing

2. Transmitter electronics and housing   with LCD

3. Alignment and purging unit

4. Window unit
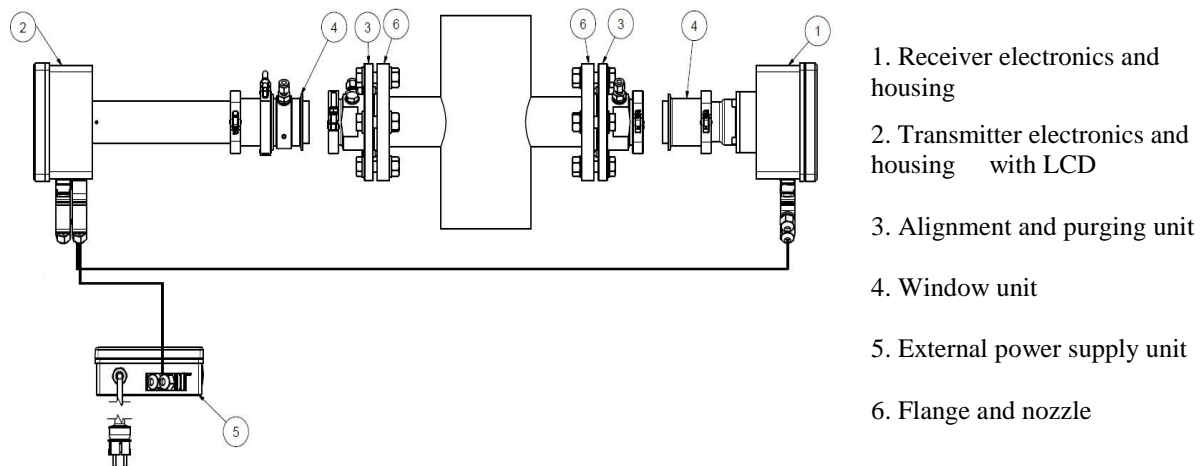
5. External power supply unit

6. Flange and nozzle

Figure 6.3: LaserGas Q monitor units and their main components (Source: **User reference- Neo Monitor AS**).

7 Results and Discussions

In this chapter, results of kiln tests focusing on sulphur flow calculations and regression model formulation are discussed. Sulphur flow calculations in all the tests are performed based on the model formulated in Chapter 3. Furthermore, impacts of the critical parameters on SO_2 emissions in the stack gas and underlying principles behind their effects on SO_2 emissions are discussed.

7.1 Experimental Results

This section presents a summary of the experimental results: quality of fuels, analysis of spot samples of different solid material streams and a summary of experimental parameters along with SO_2 emissions in the stack gas.

7.1.1 Quality of Fuels

The quality data of fuels used during the test period is summarised in Table 7.1. It shows coal quality at 40°C and as the received quality of waste oil (suppliers document). Tyre and animal meal quality data are from the prior tests. In the case of RDF-pellets, it shows the quality data of a spot sample of RDF-pellets which was taken before the first test. All the data in Table 7.1 corresponds to the quality at the feeding temperature of respective fuels in the kiln.

Table 7.1: Quality data of fuels used in the test period.

Fuels	Lower heating value [MJ/kg]	S content [% w/w]	Cl content	Moisture content [% w/w]
Coal	29.2	0.33	0.0% w/w	1.0
Waste oil	37.8	0.29	80 mg/kg	10.3
Tyre	22.9	1.28	0.1 % w/w	-----
RDF-pellets	22.9	0.20	1.2% w/w	7.17
Animal meal	16.0	0.5	---	---

7.1.2 XRF Analysis of the Spot Samples

The experimental plan (Appendix H) included analysis of preheater exhaust gas, gas flowing out of the rawmill, and gas flowing out of the fabric filter using the portable gas analyser. Since available analyser could not be used for spot analysis due to instrument problems, the plan of analysing gas samples was abandoned. Spot samples of the bypass dust flowing out of the cyclone, CKD flowing out of the fabric filter, bypass dust flowing out of the bypass filter, hotmeal, kiln feed and clinker were taken and analysed using X-Ray fluorescence analysis (XRF) in the Lab. The analysis was performed by laboratory staff in Norcem cement plant in Kjøpsvik. SO_3 content in the clinker, bypass dust out of the bypass filter, hotmeal as well as free lime in the clinker are shown in Table 7.2.

Table 7.2: SO_3 content ([% w/w]) in various solid streams.

Test run	Bypass dust out of the cyclone	Bypass dust out of the filter	CKD out of the fabric filter	Hotmeal	Clinker	Kiln feed
1	6.8	18.7	0.83	3.35	1.38	0.91
2	16.5	18.6	0.83	5.90	0.75	0.92
3	20.0	17.0	0.75	6.58	0.49	0.88

4	20.2	17.3	0.73	7.17	0.85	0.89
5	12.9	14.0	0.78	3.55	1.22	0.91
6	22.3	20.9	0.76	6.88	0.5	0.90
7	17.4	20.1	0.77	8.36	0.56	0.89
8	13.6	22.0	0.75	4.22	0.66	0.88
9	21.9	22.9	0.75	5.15	1.06	0.90
10	14.2	22.1	0.74	3.53	1.64	0.88
11	17.1	19.7	0.82	5.15	1.02	0.91
12	14.9	23.2	0.76	4.92	1.36	0.88

Bypass dust contribution from the cyclone was negligible in comparison to the bypass filter, so sulphur content in the cyclone is not used for further analysis. Other quality analysis data are used for sulphur flow calculations and subsequent representation of sulphur flow in Sankey diagram. Figure 7.1 shows an overview of the SO_3 content in the clinker and hotmeal in 12 tests. In Test 3, 4, 6, and 7, SO_3 content in the clinker was substantially high, but sulphur flow in the clinker was extremely low indicating that significant amount of sulphates in the hotmeal was burnt off in the kiln instead of leaving with the clinker. This effect can also be seen in SO_3 content in the bypass dust. In all but test 5, SO_3 content in the bypass dust was almost uniform. In Test 5, SO_3 content in the bypass dust out of the filter was substantially low which coincided with low SO_3 content in the hotmeal and at the same time high SO_3 content in the clinker. In case of clinker quality, only two tests, Test 1 and Test 12, had free lime more than 2% and other tests had acceptable clinker quality.
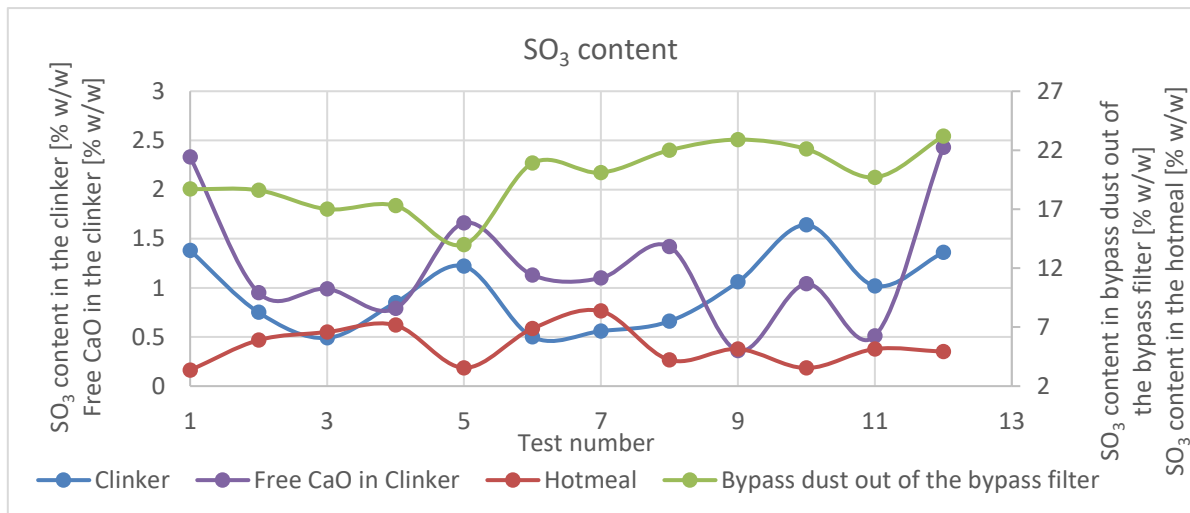

Figure 7.1: SO_3 content in the hotmeal and bypass dust out of the fabric filter.

7.1.3 Summary of the Test Results

As discussed in section 6.1, several operational difficulties during the tests led to a delay in test schedule and, subsequently forced to reduce the total number of test runs. In total, 12 test runs were performed; 4 of the tests were based on the prior design (fractional factorial design with 16 test runs), and 8 of the tests were based on the modified screening design. Figure 7.2, Figure 7.3, and Figure 7.4 12 figures showing the SO_2 level in the stack gas during 12 tests. Y-axis values in all the figures are scaled to a maximum value of 2000 dry @ 10% O_2 which facilitate direct comparison of emissions in different tests. Among 12 tests, Test 1, 5, 8, 10, and 12 correspond to low SO_2 emissions (Figure 7.2), Test 2, 6, 9, and 11 correspond to the medium SO_2 emissions (Figure 7.4), and Test 3, 4 and 7 correspond to high SO_2 emissions in the stack

gas (Figure 7.3). The tests with high emission (Test 4, 7 and 3) correspond to the test with the hotdisc operation with both RDF and tyre (Test 4 and Test 7), and only tyres (Test 3) at higher kiln feed (101 t/h). It indicates that unstable hotdisc operation during those tests has caused very high emission in the stack gas. The tests with medium SO_2 emissions correspond to either RDF feeding only (Test 2, 6, and 11), or very high energy input per unit ton of clinker from rotary kiln fuels (Test 9). Other tests with low sulphur emissions correspond to either RDF feeding or tyre feeding at low kiln feed or no fuel in the hotdisc.
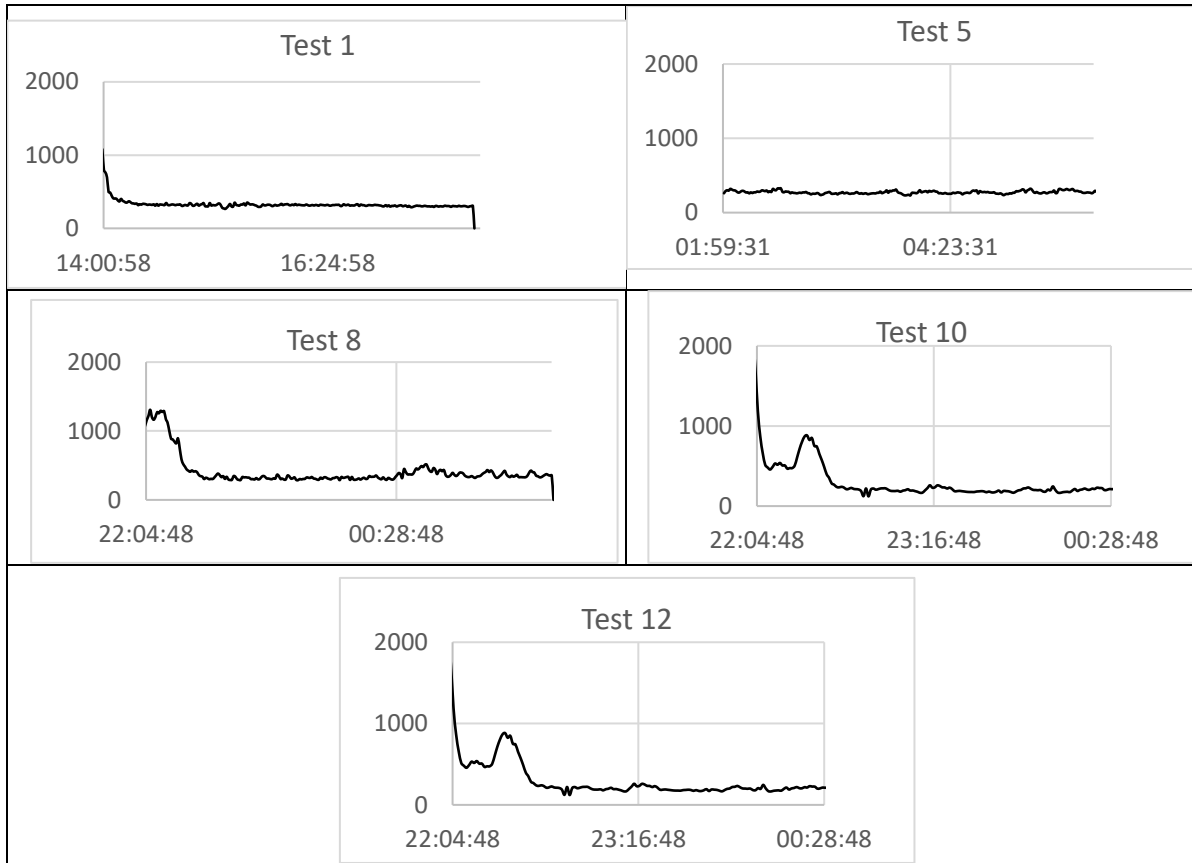
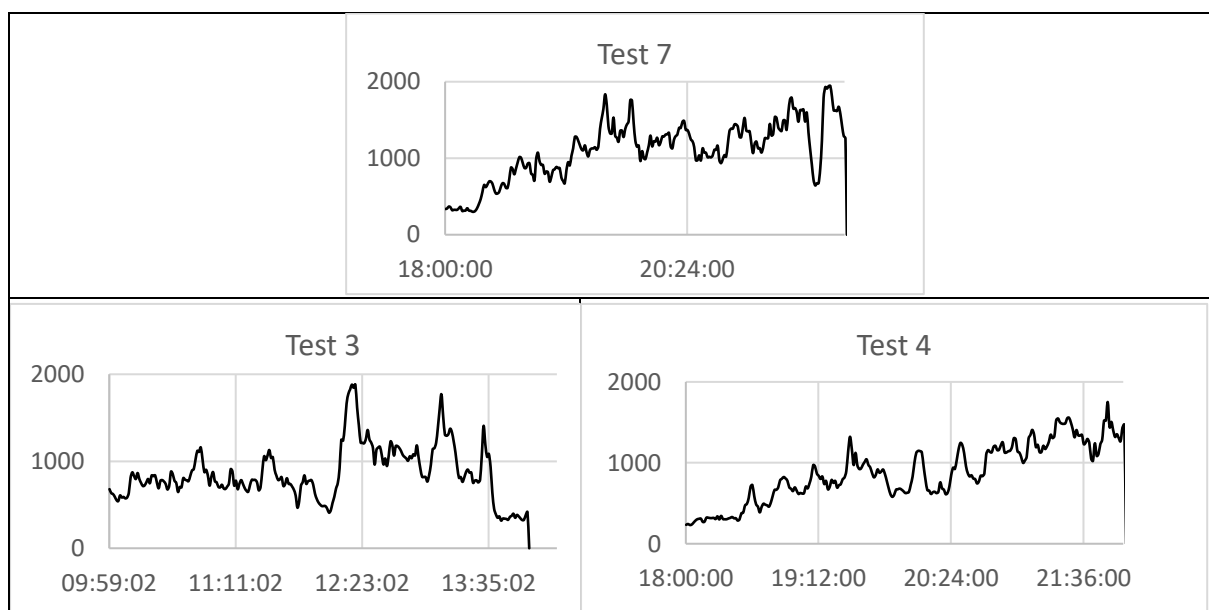Figure 7.2: Tests with low SO_2 level in the stack gas [mg/Nm^3 dry @10% O_2].

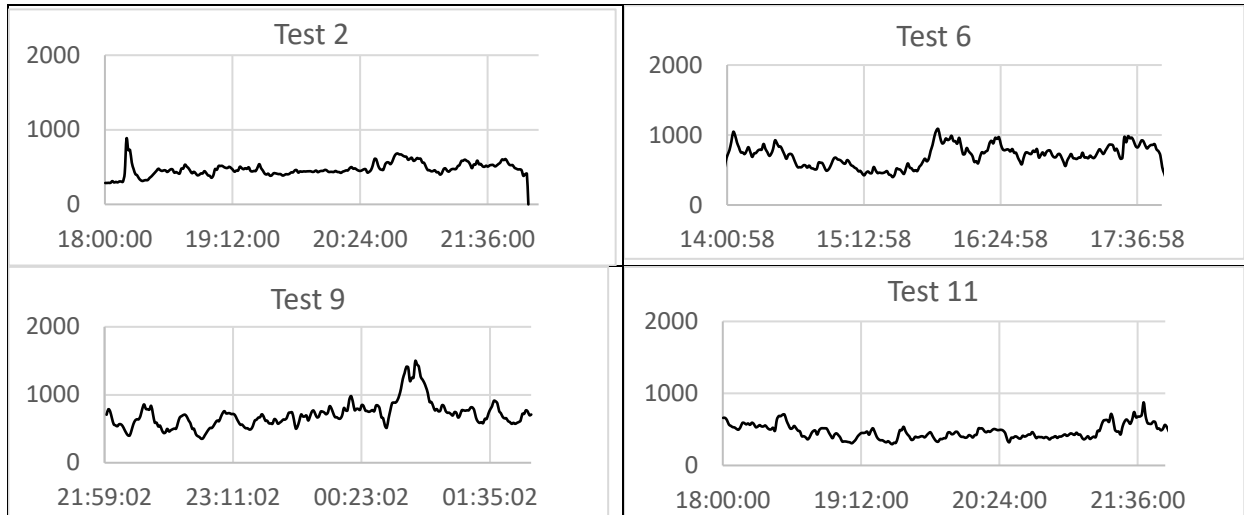Figure 7.3: Test with high SO_2 emission in the stack gas [mg/Nm^3 dry @10% O_2].

Figure 7.4: Test with medium SO_2 level in the stack gas [mg/Nm^3 dry @10% O_2].

As seen in Figure 7.2, Figure 7.3, Figure 7.4, change in the kiln parameters resulted in instability in the kiln process and SO_2 emissions in the stack gas instantly after the change in kiln parameters. For this reason, timeframe with most stable operation during 4-hour tests is used for further analysis. The number of raw timestamps data and timeframe considered for further analysis and the total number of discarded raw timestamps data in the 4-hour test period are summarised in Table 7.3.

Table 7.3: Total number of data points considered for further analysis in each test runs.

Test runs	Date	Timeframe of the test	Timeframe of the data used for analysis	Total number of data points used for analysis	Total number of discarded data points
1	20/04	14:00-18:00	16:00-17:59	120	120
2	20/04	18:00-22:00	20:00-21:54	115	125
3	26/04	10:00-14:00	12:31-13:30	60	180
4	26/04	18:00-22:00	20:00-20:59	60	180
5	21/04	02:00-06:00	04:00-05:57	118	122
6	25/04	14:00-18:00	16:30-17:29	60	181
7	25/04	18:00-22:00	20:00-21:29	91	150
8	25/04	22:00-02:00	23:00-23:59	60	180
9	24/04	22:00-02:00	23:00-23:59	60	180
10	26/04	22:00-00:30	23:00-23:59	60	180
11	24/04	18:00-22:00	19:00-20:59	120	120
12	26/04	14:00-18:00	15:31-17:30	120	120

The minimum, maximum and mean value of the model parameters (experimental factors) in the selected period for each test are shown in Table 7.4. Among the tabulated data, average data are used for sulphur calculations and model formulation, and the maximum and minimum values are used to transform actual values (average values in the selected period) to coded form (variable range [0,1]) which is subsequently used for model formulation and analyse the impact of individual parameters. The upcoming section in this chapter presents sulphur flows calculations and representation of sulphur flow in Sankey Diagrams, regression model formulation and assessment of the impact of significant parameters on SO_2 emissions.

Table 7.4: Summary of experimental test data in the selected period for each test.

Model parameters		1	2	3	4	5	6	7	8	9	10	11	12
Kiln feed (t/h)	Min	101.4	101.6	101.1	100.8	101.4	94.6	94.6	94.9	94.7	94.8	94.7	100.7
	Max	101.8	102.6	102.1	101.1	102.1	95.2	95.1	95.2	95.2	95.1	95.4	101.3
	Mean	101.4	101.9	101.4	100.9	101.7	94.9	94.9	95.0	94.9	94.9	95.1	100.9
Rawmill feed (t/h)	Min	109.4	109.5	139.4	109.6	139.3	83.4	109.7	109.4	139.3	139.3	109.5	139.4
	Max	110.4	110.0	140.5	110.6	140.4	140.3	110.5	110.5	140.2	140.3	110.3	140.5
	Mean	101.4	110.0	139.9	110.0	139.8	138.9	110.1	110.0	139.8	139.8	110.0	139.8
Coal feed in the kiln (t/h)	Min	3.2	2.5	2.8	2.4	2.5	2.68	2.7	2.5	3.15	2.4	3.0	2.4
	Max	3.2	2.5	2.9	2.4	2.5	2.95	2.7	2.5	3.15	2.4	3.0	2.4
	Mean	3.2	2.5	2.9	2.4	2.5	2.84	2.7	2.5	3.15	2.4	3.0	2.4
Tyre Feeding (kg/h)	Min	0.0	0.0	1410.0	1449.8	0.0	0.0	1467.5	0.0	0.0	1467.0	0.0	0.0
	Max	0.0	0.0	1529.0	1524.1	0.0	0.0	1531.0	0.0	0.0	1526.0	0.0	0.0
	Mean	0.0	0.0	1476.0	1481.5	0.0	0.0	1499.0	0.0	0.0	1490.0	0.0	0.0
RDF feeding (kg/h)	Min	0.0	1966.3	0.0	1873.1	0.0	1978.2	1879.8	0.0	0.0	0.0	1546.7	2061.3
	Max	0.0	2128.2	0.0	2097.5	0.0	2120.2	2107.6	0.0	0.0	0.0	1984.5	2211.8
	Mean	0.0	2027.6	0.0	1999.3	0.0	2045.1	2003.7	0.0	0.0	0.0	1855.8	2114.0
Waste oil feeding (kg/h)	Min	0.0	0	0.0	442.9	580.8	0.0	0.0	148.6	0.0	292.1	0.0	296.1
	Max	0.0	710.7	0.0	456.1	618.1	0.0	0.0	151.9	0.0	304.7	0.0	305.2
	Mean	0.0	687.8	0.0	449.9	599.9	0.0	0.0	149.9	0.0	299.7	0.0	300.0
Bypass water supply (m³/h)	Min	3.9	2.5	2.9	3.0	4.1	2.7	4.4	2.9	2.8	4.5	4.0	4.5
	Max	5.0	2.9	4.3	3.4	4.9	3.0	4.7	3.1	3.6	5.0	4.9	5.2
	Mean	4.4	3.5	3.1	3.2	4.5	2.8	4.5	3.0	3.0	4.7	4.4	4.7
Energy per ton of clinker from kiln fuels (MJ/ton of clinker)	Min	1429.6	1303.9	1258.3	1337.7	1456.2	1385.3	1290.7	1287.5	1505.1	1330.1	1429.8	1251.2
	Max	1436.1	1529.6	1304.0	1349.4	1477.4	1393.6	1298.0	1292.0	1509.4	1341.1	1440.5	1260.5
	Mean	1432.4	1517.7	1288.6	1344.2	1465.7	1389.7	1294.6	1289.7	1513.5	1336.3	1434.7	1256.4
SO_2 level in the stack gas (mg/Nm^3 wet)	Min	178.7	245.4	464.1	357.3	137.8	327.7	554.4	166.0	290.3	90.1	178.6	116.6
	Max	206.5	447.1	1106.3	782.8	203.5	508.9	1082.0	205.6	460.5	154.1	318.0	197.8
	Mean	190.4	324.3	671.3	575.8	170.7	431.3	767.0	185.9	384.5	110.2	242.2	149.8
SO_2 level in the stack gas (mg/Nm^3 dry @10% O_2)	Min	305.0	399.5	753.6	611.6	234.4	556.3	934.9	285.8	488.9	165.9	294.4	212.1
	Max	331.4	682.8	1770.9	1303.9	323.1	863.2	1791.2	366.3	768.9	259.8	705.7	320.5
	Mean	316.8	514.7	1057.2	940.1	276.6	721.0	1269.5	315.3	645.3	196.7	460.4	247.6

7.2 Sulphur Flow Calculations and Sankey Diagrams

Sulphur flow in different flow streams for 12 tests are calculated and presented in Sankey Diagrams. The mean process data used for sulphur flow calculations is presented in Table 7.4, and Appendix I and quality data of fuels and solid material streams are presented in Table 7.1 and 7.2 respectively. The procedures for reference sulphur flow calculations in Period-1[12] is in Appendix F, and Sankey Diagram representation of sulphur flow in all tests are in Appendix J.

All the diagrams represent approximate sulphur flow during the selected period in each test. The calculations are based on few ill-defined approximations. Kiln feed to hotmeal ratio is approximated using similar ratio estimation as used for kiln feed to hotmeal ratio estimation. However, due to huge recirculation between preheater-calciner-kiln, hotmeal flow approximated using this ratio can be substantially different from the actual flow. Bypass gas flow is calculated using gas flow data from process audit data from 2017. In the case of CKD, CKD contribution from the raw material is predicted using process data provided by technical support from Heidelberg Technical Centre (HTC), and it is assumed that CKD contribution depends linearly on gas flow in the stack gas, and kiln feed (refer section 3.4.2). Due to these ill-defined approximations, sulphur flow in CKD, gas flowing out of preheater exhaust gas, gas flowing out of the rawmill, bypass gas, hotmeal, and rotary kiln gases can be substantially different from the actual flow, but, these diagrams can still be used as reference (not in decision making) for further discussions about sulphur behaviour in the kiln process.

Figure 7.5, Figure 7.6, and Figure 7.7 are Sankey Diagram representations of sulphur flows in 3 tests (Test 9, 7 and 10) out of 12 tests. Test 9 corresponds to a medium sulphur emission period, Test 7 corresponds to the highest sulphur emission period, and Test 10 corresponds to the lowest sulphur emission in the stack gas. In Test 9 (test with the highest energy input per ton of the clinker from the rotary kiln fuels), sulphur emission is primarily influenced by sulphur flow in the bypass gas. The average sulphur flow in Test 9 via bypass gas is 25.0 kg/h which is 48.6% of the total flow in the stack gas (highest percentage in 12 tests). However, in Test 7, sulphur flow in the bypass gas is 36.2 kg/h (35.1% of the total flow in the stack gas), and in Test 10, sulphur flow in the bypass gas is 1.2 kg/h (7.9% of the total flow in the stack gas). It is also clear from the diagrams that the sulphur flow in the bypass gas is primarily influenced by huge recirculation of sulphur between preheater-calciner-kiln. In Test 7, the recirculation[13] is 1963.9 kg/h (sulphur flow in the hotmeal), which is 5.8 times the sulphur flow in the kiln feed (337.8 kg/h), but in Test 10, the recirculation[12] is 491.8 kg/h (1.5 times kiln feed sulphur flow), and in Test 9, the recirculation[12] is 1035.4 kg/h (3 times kiln feed sulphur flow).

In all three tests, sulphur input from the fuels (mainly tyre and RDF) are negligible in comparison to sulphur flow in the kiln feed, clinker and in the stack gas. Despite insignificant sulphur flow, sulphur flow in the stack gas and recirculation between preheater-calciner-kiln have increased with the use of tyre and RDF (Test 7 and Test 4 (refer Table I.4 in Appendix J)). It indicates that the use of these fuels has caused adverse operational impact in the kiln process. In addition, sulphur flow in the clinker is significantly lower with the use of tyre and RDF in the hotdisc; The sulphur flow in a clinker in Test 7 is (136.3 kg/h) while it is 257.9 kg/h in Test 9 and 399.1 kg/h in Test 10. In the case of CKD, sulphur flow is highest in Test 10, but the differences in sulphur flow in CKD between the tests are negligible.

---

[12] Refer Section 5.4.2 for a description of Period-1.

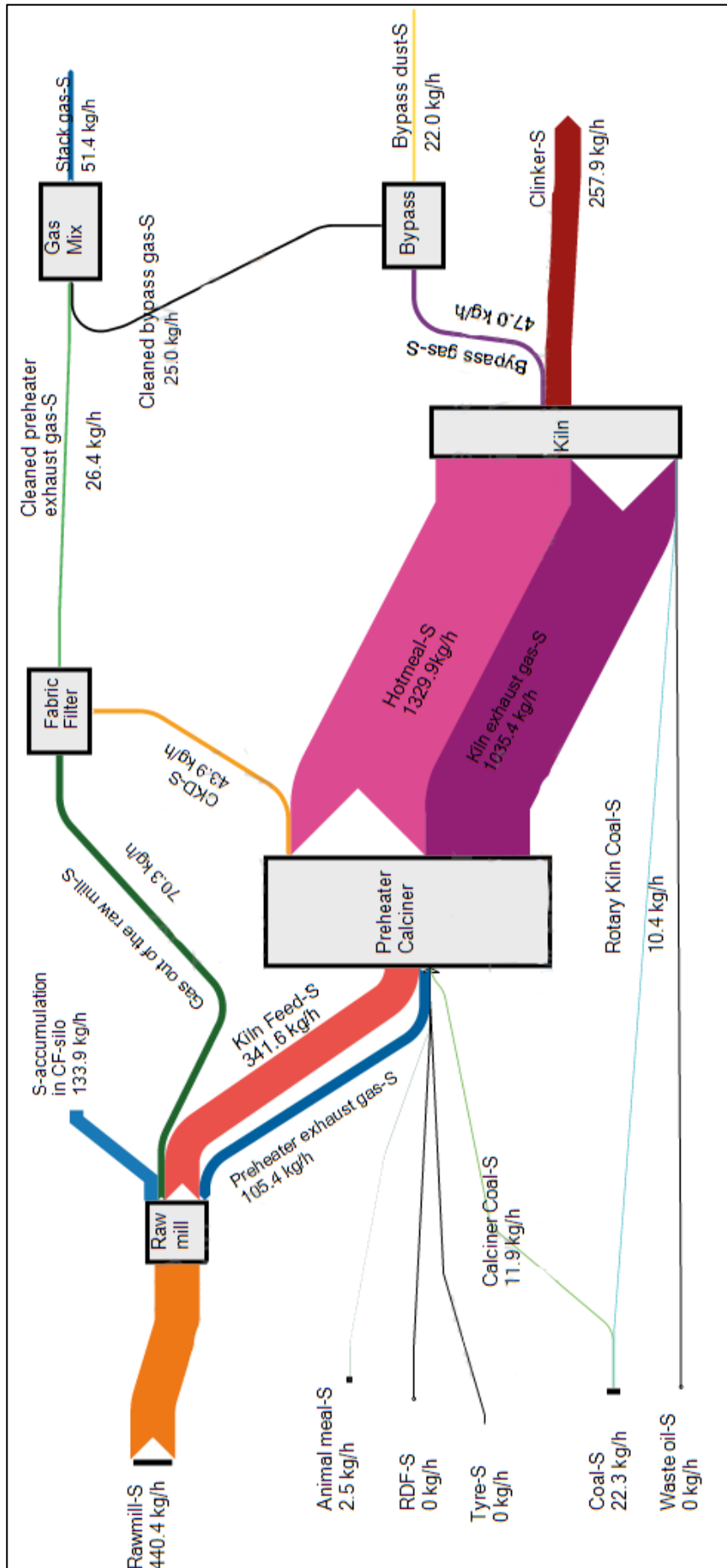[13] Sulphur flow in the rotary kiln exhaust gas.

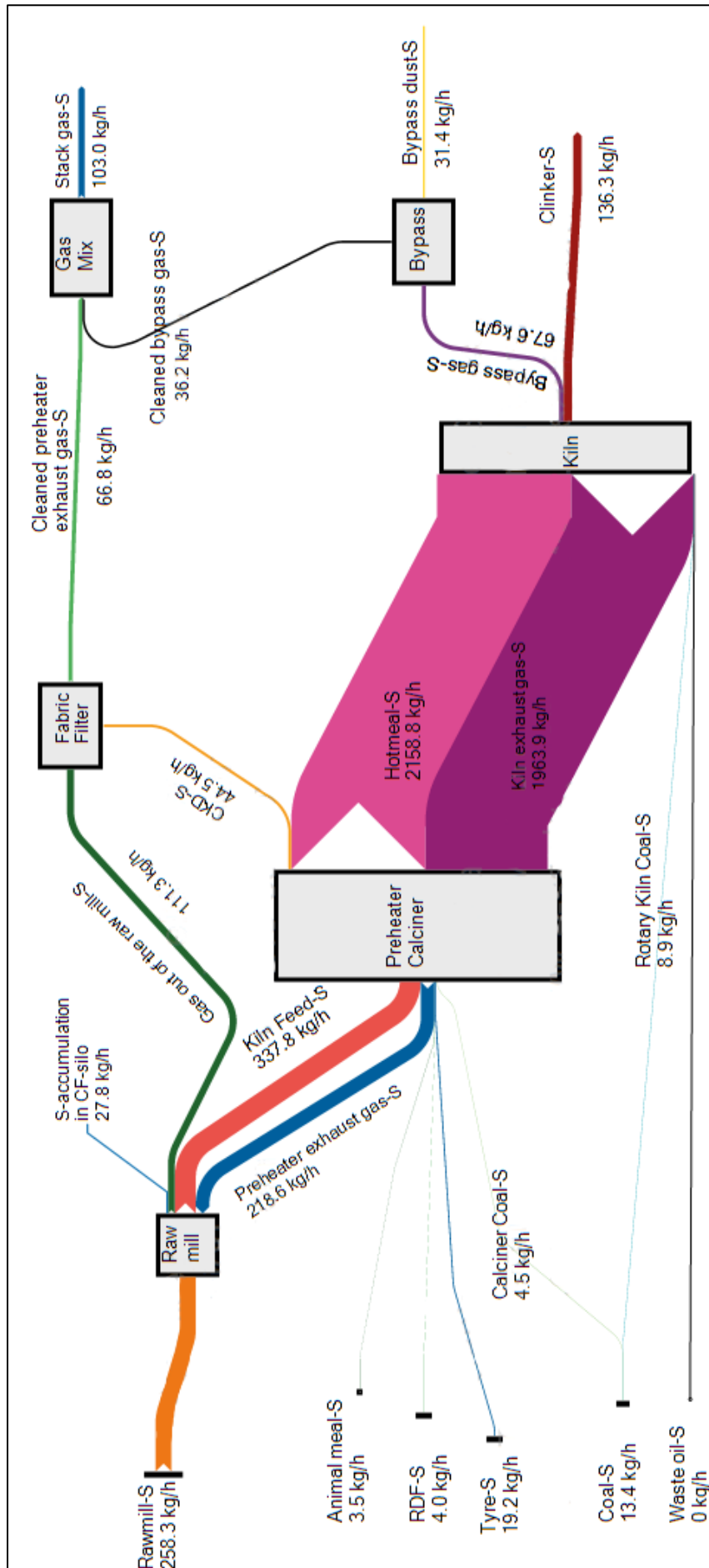Figure 7.5: Sankey diagram representing sulphur flows in Test 9.

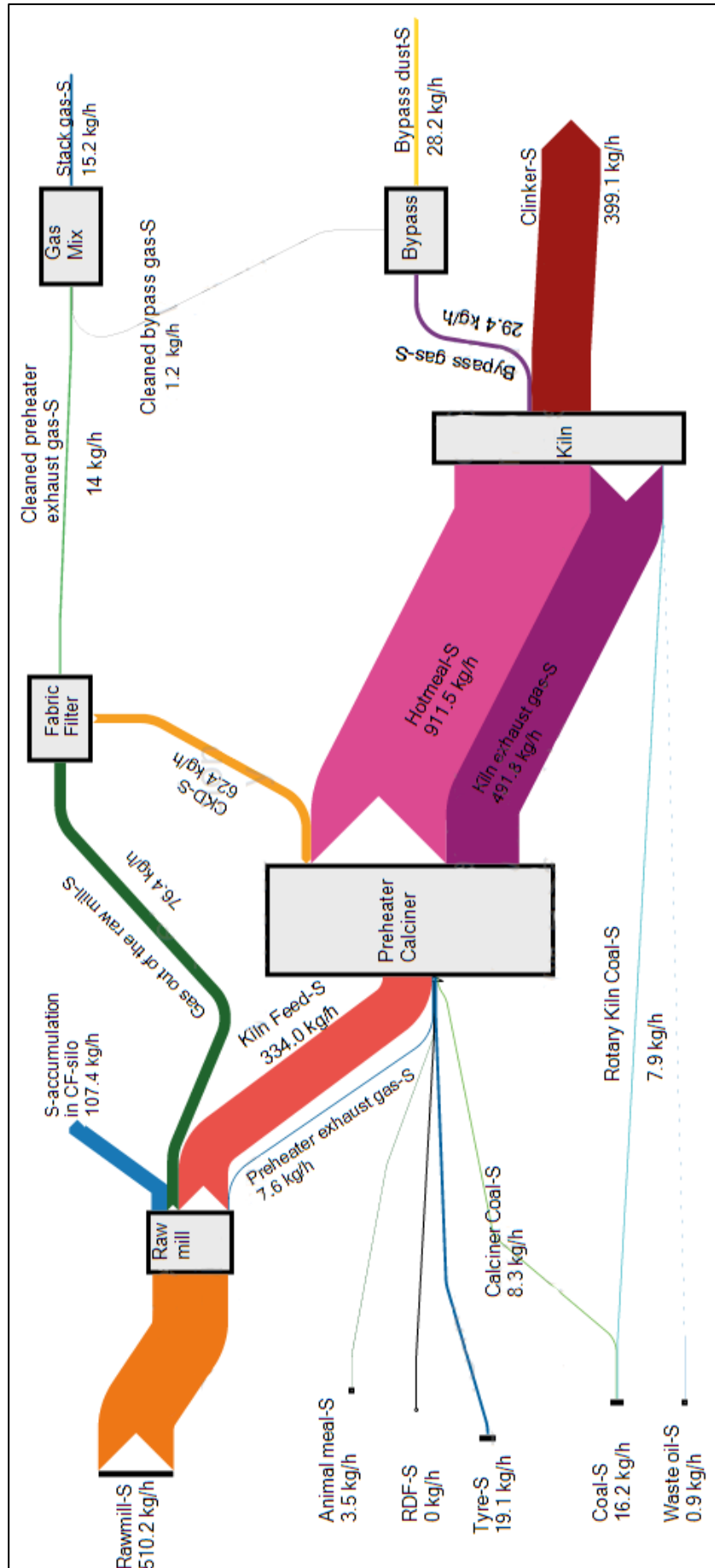Figure 7.6: Sankey diagram representing sulphur flows in Test 7.

Figure 7.7: Sankey diagram representing sulphur flows in Test 10.

7.3 Multivariate Regression Analysis

Equation 7.1 is a regression model (Model-2) of SO_2 emission in the stack gas (mg/Nm^3 dry @10% O_2) formulated using normalised (coded) parameter values. The parameter values were standardised (coded) using maximum and minimum values in the selected period of each test (Table 7.4). The goodness of fit R^2_{M2} of the regression model is significantly high (89%) which shows that the model parameters are the primary cause of the variation in sulphur emissions. It is also evident in Figure 7.8, which shows measured and predicted SO_2 level in 12 tests. The curves are overlapping to a certain degree, which emphasises that the model parameters are the primary cause of variation in sulphur emissions.

$$C_{\mathrm{SO_2},g,stack} = 230.2 - 279.5\dot{V}_{W,BP,in} - 63.9\dot{E}_{F,RK.in} - 0.7\dot{m}_{RaM,RM,in}$$
$$+ 43.1\dot{m}_{KF,PT,in} + 455.9\dot{m}_{C,RK,in} - 302.2\dot{m}_{RDF,Calc,in} + 537.4\dot{m}_{T,Calc,in} \tag{7.1}$$

$$R^2_{M2} = 0.89 \tag{7.2}$$
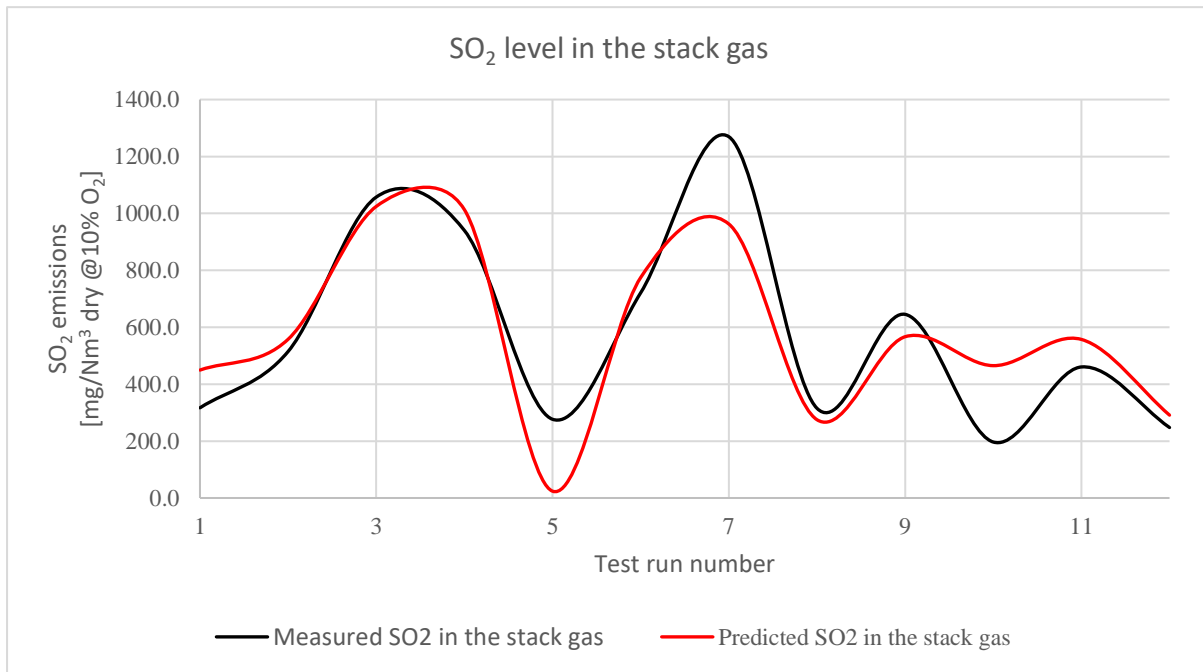
Figure 7.8: Measured and predicted SO_2 level in the stack gas ([mg/Nm^3 @10% O_2]) in 12 tests.

Figure 7.9 shows coefficients of Model-2 which are sorted in descending order of coefficient values. Tyre feeding (m_T_Calc_in), RDF feeding (m_RDF_Calc_in), and coal feeding in the kiln (m_C_RK_in) have the most significant positive[14] impact on the sulphur emissions in the stack gas. On the other hand, bypass water supply (V_W_BP_in) has a significant negative[15] effect on the SO_2 emissions. Other parameters, kiln feed (m_KF_PT_in), rawmill feed (m_RMF_RM_in), and energy input from rotary kiln fuels (E_F_UTC_RK_in) have a negligible impact on the SO_2 emissions in the stack gas.

---

[14] Positive effect means an increase in a parameter results in an increase in output variable or vice versa.

[15] Negative effect means an increase in a parameter results in a decrease in output variable or vice versa.
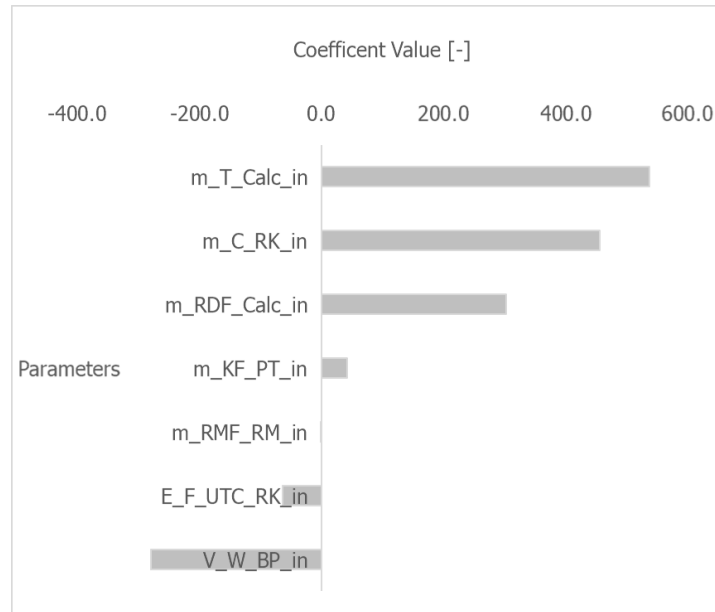
Figure 7.9: Coefficients of the regression model.

7.4 Discussions on Impacts of Model Parameters on SO$_2$ Emissions

In this section, the effect of significant parameters and possible reasons behind their impacts on SO$_2$ emissions are discussed.

7.4.1 Tyre and RDF feeding

Figure 7.10 shows average SO$_2$ emission in the stack gas vs tyre feeding during the test period. Tyre feeding is presented in coded form (0-low level and 1-high level). Out of the four tests with tyre feeding at a high-level, SO$_2$ emission was lowest in Test 10. In that test, only tyre was fed into the hotdisc and kiln feed was at a low level (95 t/h). In other tests, there were considerably high SO$_2$ emissions when tyre feeding was at a high-level (Test 3, 7, 4), but either medium or low emissions when tyre feeding was at a low level (other tests).
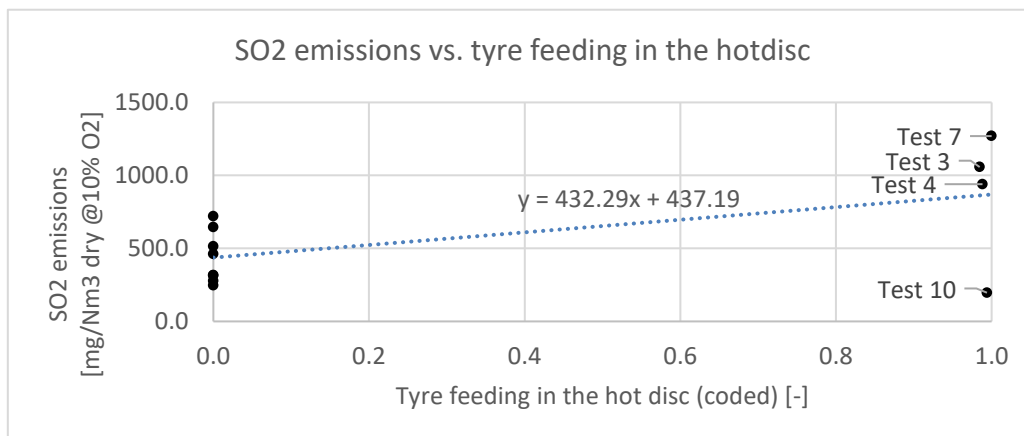
Figure 7.10: Average SO$_2$ emissions in stack gas ([mg/Nm^3 dry @10% O$_2$]) vs. average tyre feeding (coded [-]).

Figure 7.11 shows average SO$_2$ emission in the stack gas vs RDF feeding in 12 tests. In both cases with RDF feeding at a low level and high-level, SO$_2$ emissions were primarily at medium or low level. However, in Test 4 and Test 7, SO$_2$ emissions were at high levels.
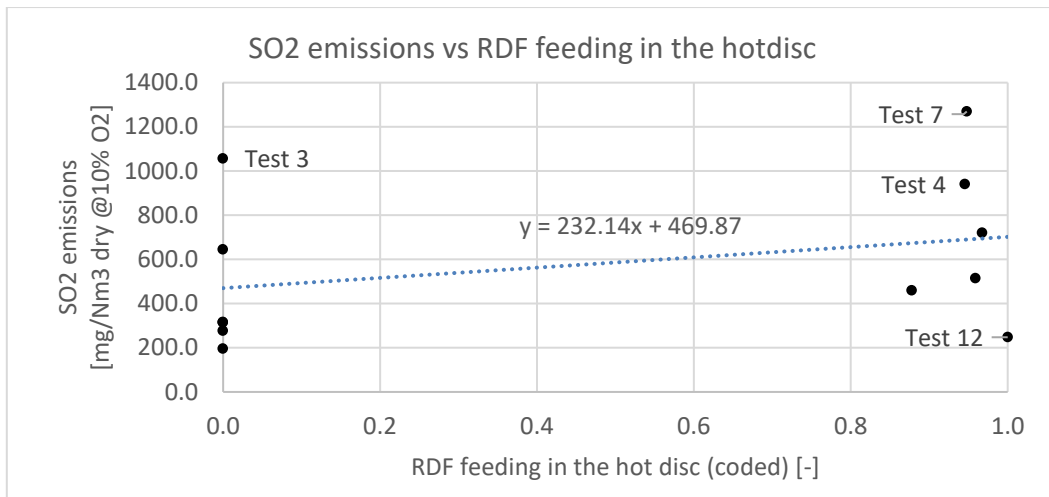
Figure 7.11: Average SO_2 emissions in the stack gas ([mg/Nm^3 dry @10% O_2]) vs average RDF feeding (coded [-]) in the hotdisc.

As seen in Figure 7.10 and Figure 7.11, the emission is usually higher when both tyre and RDF were at high-level. To illustrate the combined effect of both tyre and RDF feeding, trends of emission in the stack gas, total fuel in the hotdisc (tyre and RDF) and CO in the kiln inlet in different tests are shown in Figure 7.12. It indicates that CO level in the kiln inlet was highest (Test 4 and Test 7) when both RDF and tyre were fed into the hotdisc. The increase in CO level caused reducing environment in the kiln inlet and lower stages of preheater tower. As a result, SO_2 emissions in the stack gas in Test 4 and Test 7 were substantially higher than in Test 10 (only tyre) and Test 12 (just RDF).
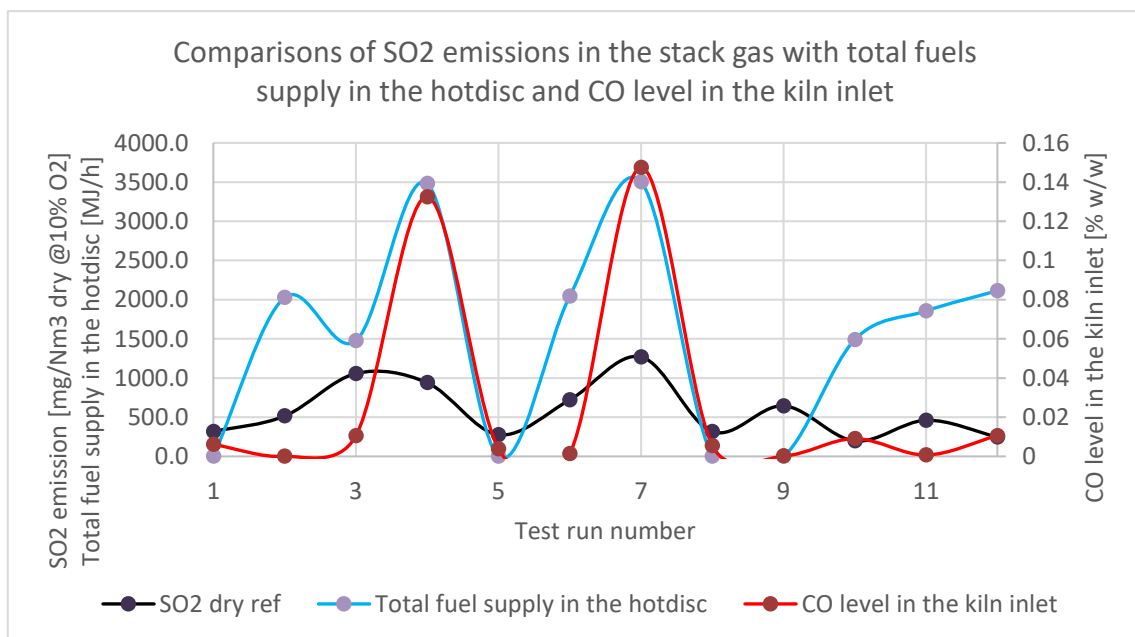
Figure 7.12: A plot of average SO2 emissions in the stack gas ([mg/Nm^3 dry @10% O_2]), average total fuel supply ([kg/h]) in the hotdisc, and average CO level in the kiln inlet ([% w/w]) in all 12 tests.

The variation in CO in the kiln inlet and subsequently higher SO_2 emissions in the stack gas could be directly linked with the faulty hotdisc operation: considerable fluctuation of temperature in the hotdisc and hotmeal dividing gate. Figure 7.13, Figure 7.14, and Figure 7.15 shows CO level in the kiln inlet, temperature fluctuations in the hotdisc and hotmeal dividing gate opening in Test 4, Test 10 and Test 12 respectively in the selected period. For

straightforward comparison, Y-axis values in all the figures are scaled to the same maximum limit.

As seen in Figure 7.13, there was a drastic fluctuation and abrupt changes in temperature and hotmeal dividing gate opening in Test 4. During Test 4, the maximum limit of automatic control of the dividing gate opening was set to 36%. During the test period, the temperature in the hotdisc often crossed maximum setpoint (1180°C), but the automatic control was not able to lower the temperature by adjusting dividing gate opening. For this reason, operators (manually) frequently changed the dividing gate opening from 36% to 45% causing an abrupt change in hotdisc operation. These abrupt changes destabilised the temperature in the kiln inlet, calciner and preheater tower, as well as increased CO level in the kiln inlet. In Test 10 (only tyre) and Test 12 (just RDF), the hotdisc operation was well within automatic control zone as the total fuel supply in the hotdisc was lower than in Test 4. Due to the automatic control of gate opening in the entire test period, the hotdisc operation was relatively smoother which resulted in lower CO level and substantially lower SO$_2$ emissions in the stack gas. Test 3 was an exception with only tyre feeding. The potential reason behind higher emissions in Test 3 is linked with the difference in kiln feed and discussed in section 7.4.3.
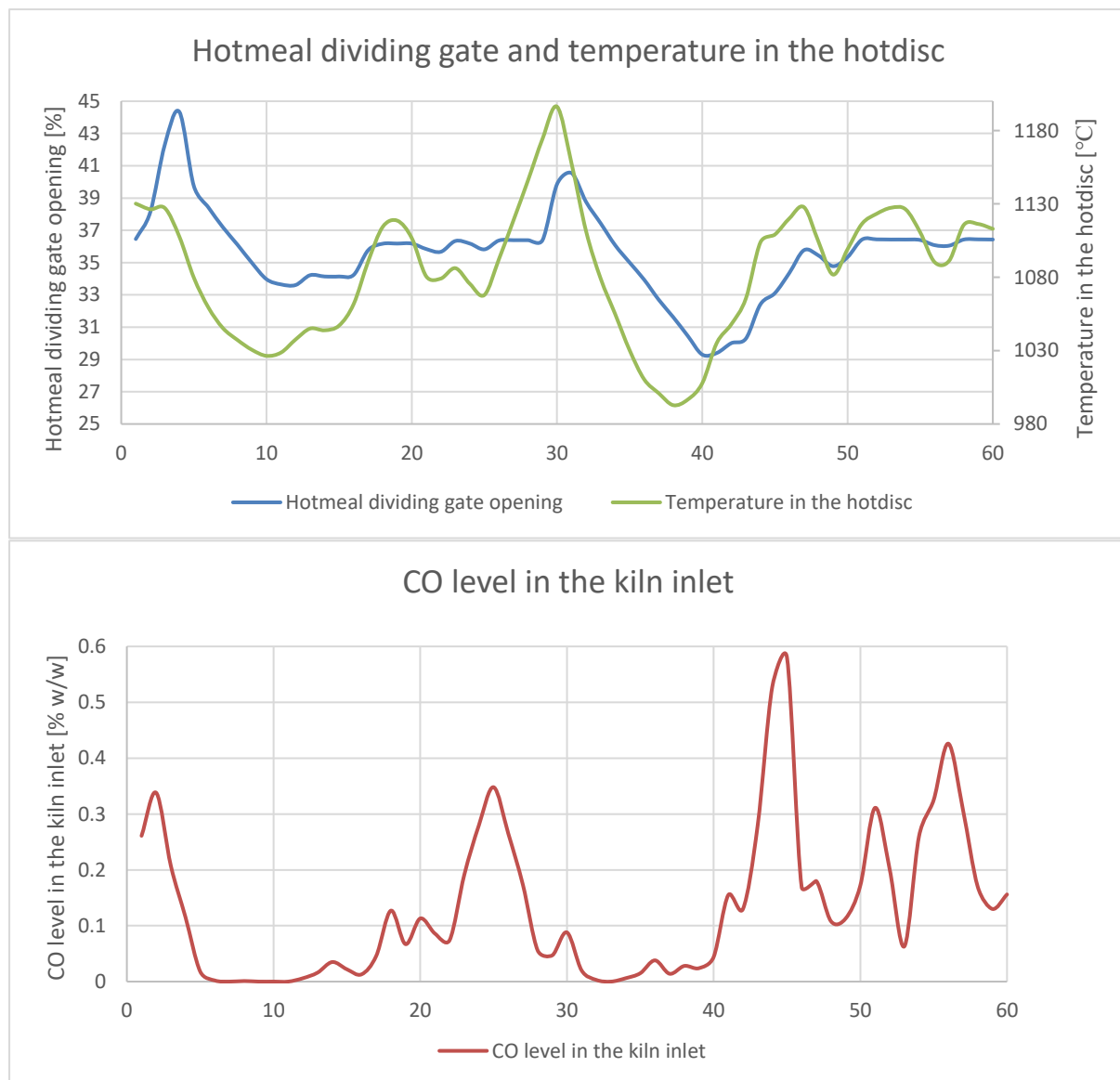

Figure 7.13: Trends of CO level in the kiln inlet [% w/w], the temperature in the hotdisc [°C] and hotmeal dividing gate opening [%] in Test 4.
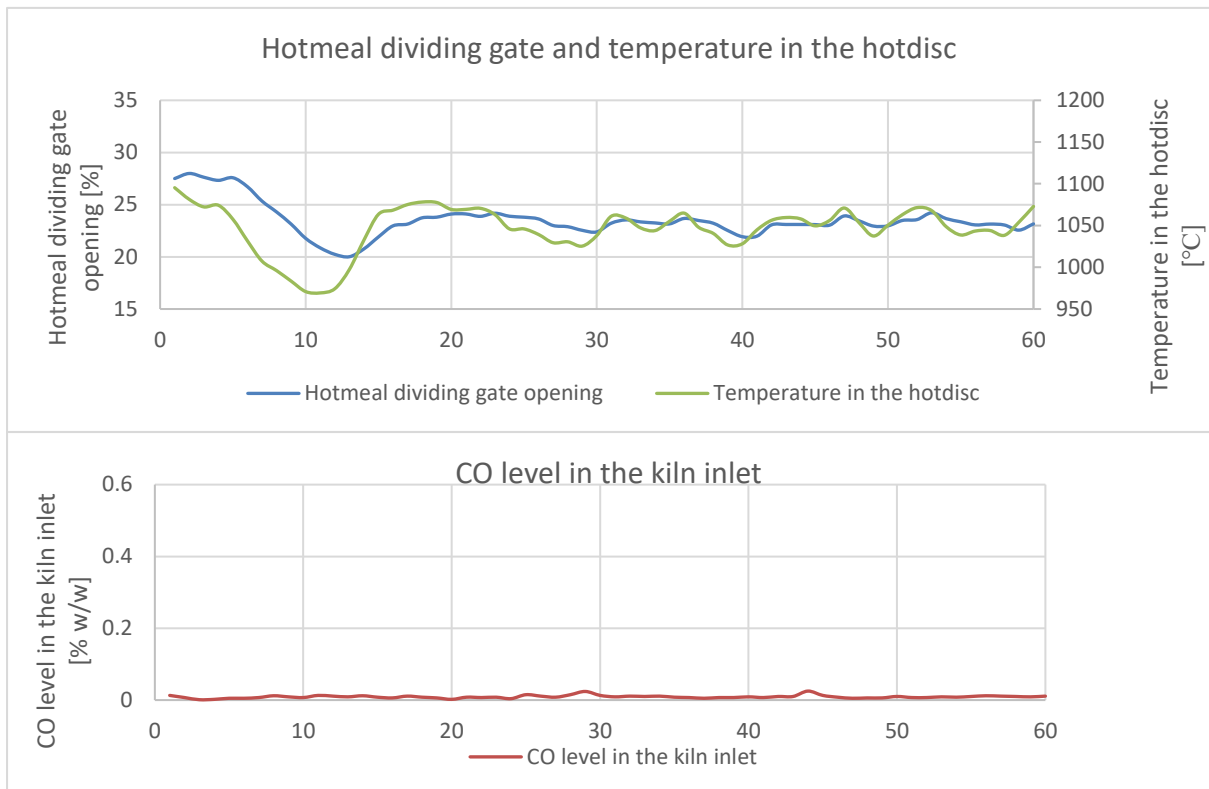
Figure 7.14: Trends of CO level in the kiln inlet [% w/w], the temperature in the hotdisc [°C] and hotdisc dividing gate opening [%] in Test 10.
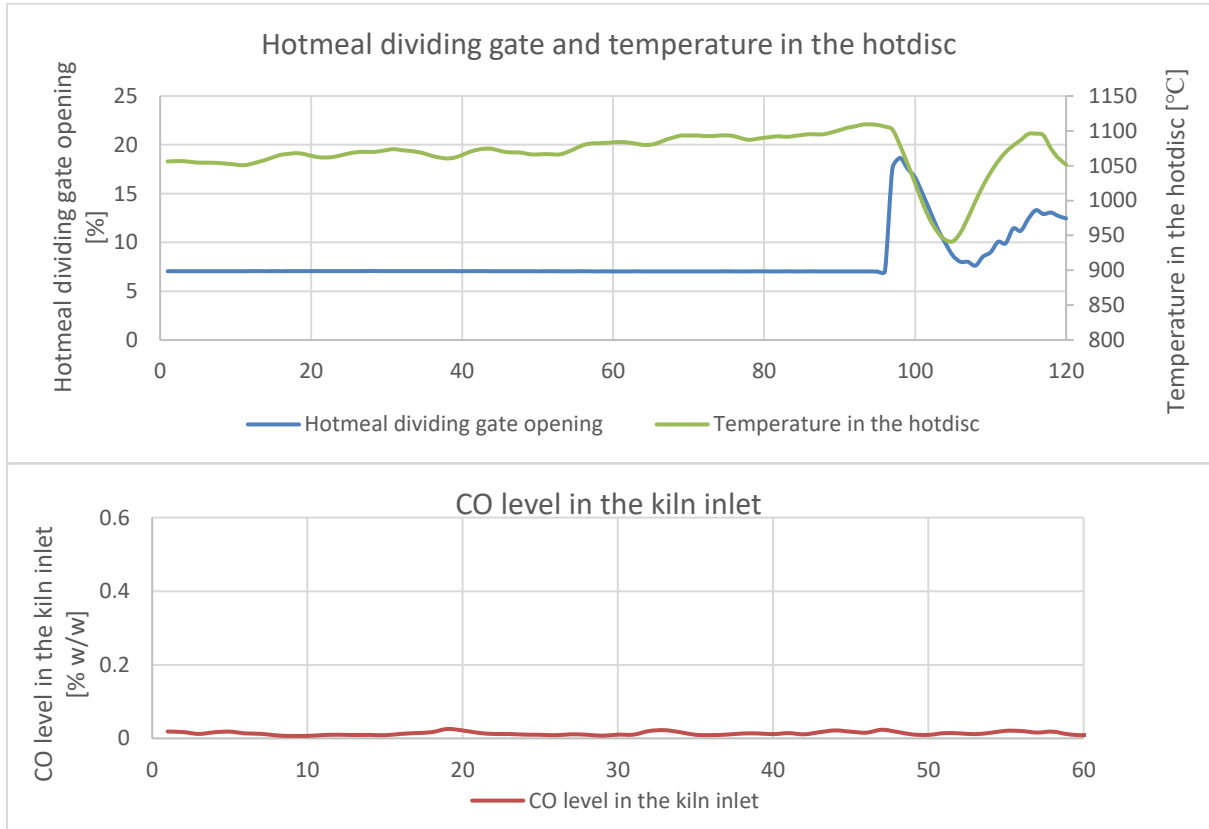

Figure 7.15: Trends of CO level in the kiln inlet [% w/w], the temperature in the hotdisc [°C] and hotdisc dividing gate opening [%] in Test 12.

Effect of Tyre Piece size on Hotdisc Operation and SO₂ Emissions

Beside faulty hotdisc operation, tyre piece sizes were suspected as the potential reason behind higher CO level in the kiln inlet. Big chunks of tyres are usually difficult to burn, and as a result, unburnt tyre pieces mix with the hotmeal and fall into the calciner and subsequently to the kiln inlet. The tyre pieces potentially create reducing environment in the kiln inlet and consequently higher emissions in the stack gas. In order to illustrate the effect of tyre sizes on CO level and emissions, hotdisc process data (averaged timestamp data at an interval of 1 minutes) from 16:14 to 19:33 on 18th January 2017 (Period-3) and from 07:55 to 11:13 on 18th January 2017 (Period-4) was plotted in Figure 7.16 and Figure 7.17 respectively. Period-3 corresponds to the timeframe in which test was performed with small tyre pieces[16], and Period-4 corresponds to the hotdisc operation with mixed tyre pieces.

In both periods, the hotdisc operation was relatively smoother with automatic control in comparison to hotdisc operations in Test 7. Correspondingly, SO₂ emissions in the stack gas in both periods were substantially lower in comparison to the emissions in Test 7. The difference in emissions in Test 7 and Period-3 or Period-4 was mainly due to faulty operation in the hotdisc. Although the hotdisc operation was normal in both periods, there are significant variations in hotdisc dividing gate opening and temperature in Period-4 in comparison to Period-3. Now, it is impossible to conclude that tyre sizes were the only reason behind the fluctuations of temperature, CO level and the emissions in Period-4, but the fluctuations can be definitely related to the tyre piece sizes. Thus, it can be stated that large tyre pieces are one of the reason behind higher CO level in the kiln inlet, fluctuations in hotdisc temperature and higher SO₂ emissions in the stack gas. A possible solution to tackle this problem is to use only small tyre pieces or increase the fuel residence time in the hotdisc. The residence time in the hotdisc could be increased by separate feeding of RDF and tyre and operating just tyres at lower hotdisc rotation speed and just RDF at higher rotation speed.
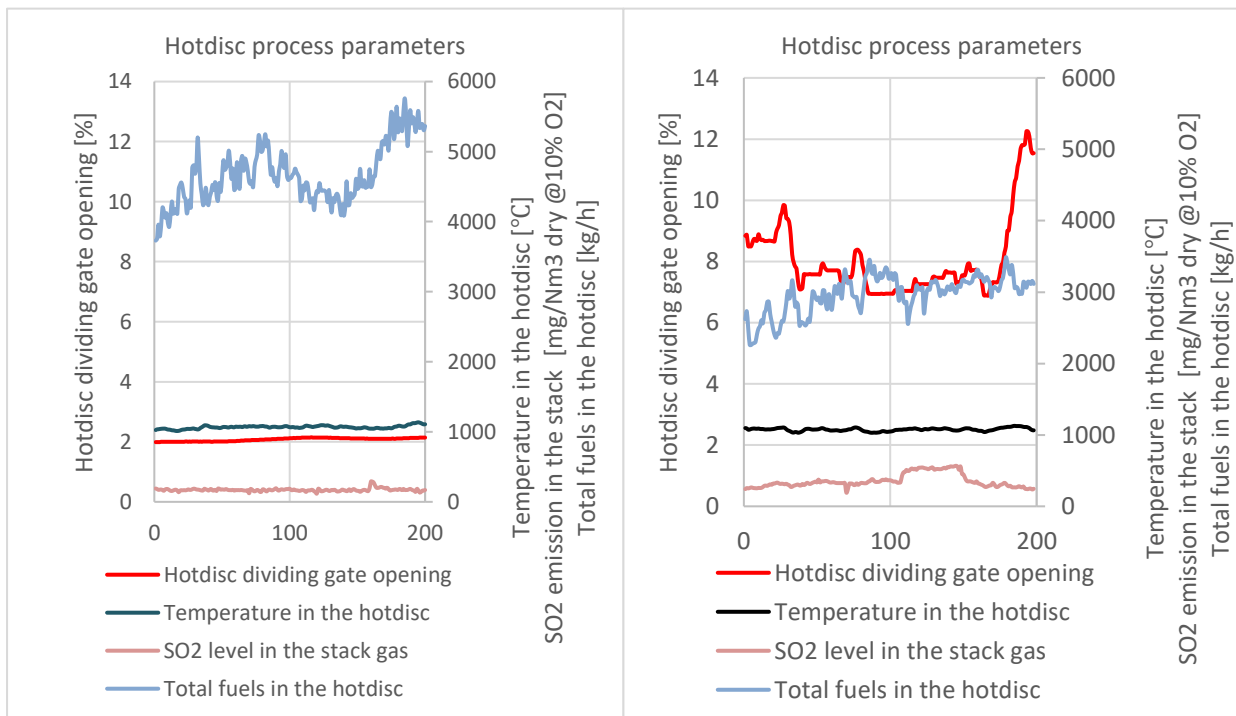

Figure 7.16: Hotdisc process parameters with feeding of small tyre pieces.

Figure 7.17: Hotdisc process parameters with feeding of mixed tyre pieces.

---

[16] The test with feeding of small tyre pieces were performed by plant management in Jan 2017.

7.4.2 Bypass Water Supply

Figure 7.18 shows average SO_2 emissions at the different coded level of the bypass water supply. The trendline shows that SO_2 level decreased with an increase in bypass water supply. To confirm that bypass water supply had a negative impact on the SO_2 emissions, the main test (Test 10) was performed between 22:30 on 26th April 2018 to 00:30 on 27th April 2018. In the later part (01:45-02:00 on 27th April 2018), all the parameters were kept constant, and only bypass water supply was changed from 4.5 m³/h to 3 m³/h. The trends of SO_2 emissions with varying bypass water supply is shown in Figure 7.19.

The first 60 data points in the curve are from the main test between 23:00 to 23:59 on 26th April 2018. Last 15 data points are from the later part of the tests (01:45 to 02:00 on 27th April 2018). It shows that bypass water supply has a negligible impact on the SO_2 emissions in the stack gas. Instead, additional operational problems such as the frequent rise of temperature in the bypass gas flowing out of the GSA above the maximum limit occurred when bypass water supply was set to high level. In addition, more kiln gas is expected to leave via bypass duct, resulting in an increase in the total energy consumption. Hence, it can be concluded that bypass water supply should be set to 3 m³/h to have a smooth operation in bypass system as increasing bypass water supply is undesirable due to increase in energy consumption, and frequent operational problem in the bypass system.
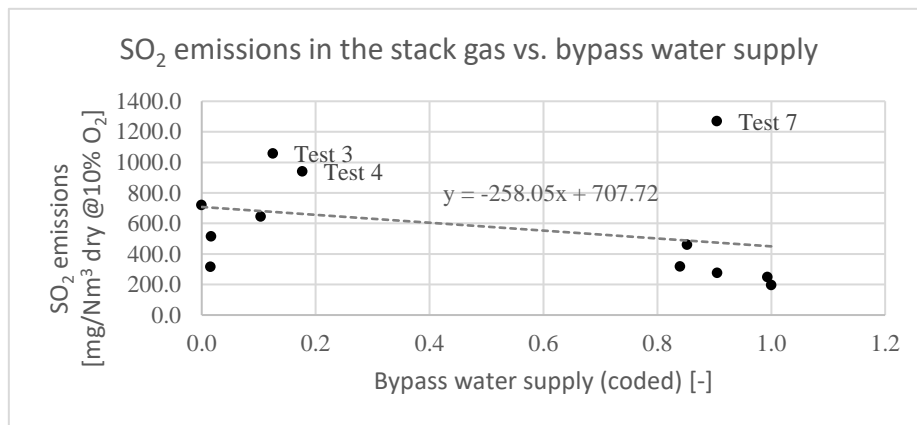

Figure 7.18: Average SO_2 emissions in the stack gas ([mg/Nm³ @10% O_2]) vs bypass water supply (coded [-]).
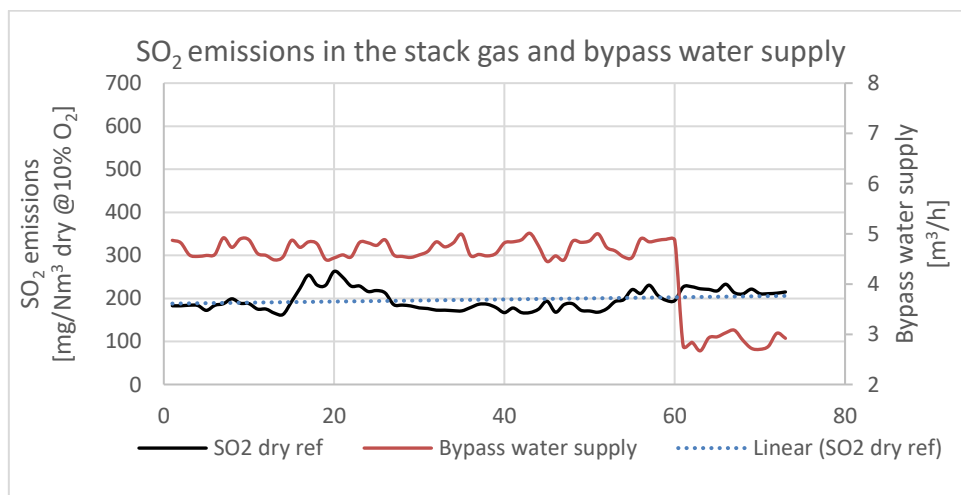

Figure 7.19: Trends of average SO2 emissions in the stack gas ([mg/Nm³ @10% O_2]) and average bypass water supply ([m³/h]).

7.4.3 Kiln Feed

Figure 7.20 shows SO_2 emissions in the stack gas at the different coded level of kiln feed. It shows that kiln feed has an insignificant negative impact on the SO_2 emissions in the stack gas. These results are partially impacted by the tyre and RDF feeding in the hotdisc (specifically Test 7). In general, it is observed that O_2 level in the kiln inlet was usually lower when kiln feed was at higher level and O_2 level in the kiln inlet was below 4% w/w (sometimes even below 3% w/w). Although Figure 7.20 indicates a negative impact of kiln feed on the SO_2 emissions, the positive effect of kiln feed can be seen between Test 3 and Test 10.

Test 10 and Test 3 differ in two aspects; kiln feed (high level- Test 3, Low level- Test 10) and coal feeding (high level- Test 3, low level- Test 10). In both cases, RDF feeding, approximate energy input per unit ton of clinker were at low levels, and tyre feeding was at high level. However, there was a substantial difference in emissions between these tests (average emissions of 1057.2 mg/Nm^3 dry @10% O_2 in Test 3 and 196.7 mg/Nm^3 dry @10% O_2 Test 10 respectively). The abnormal emission difference between these tests can be related to unstable kiln operation at higher kiln feed. As seen in Figure 7.21, O_2 level in the kiln inlet was usually 4% w/w or lower (minimum setpoint value) in Test 3. This effect was primarily enhanced by the use of tyre in the hotdisc (also RDF in Test 2) since a large fraction of kiln air passes through a tertiary air duct to the hotdisc. It has potentially caused deficit of O_2 level at higher kiln feed, as, higher kiln feed requires higher air flow via rotary kiln. It is impossible to conclude with absolute certainty that there are interaction effects between kiln feed and hotdisc operation in the emissions based on this experimental design (screening design), so, further investigations are essential to determine the effect of hotdisc operation at higher kiln feed.
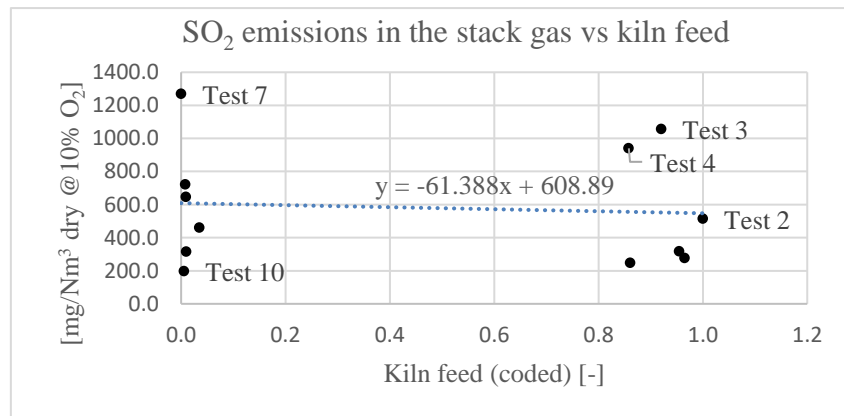

Figure 7.20: Average SO_2 emissions in the stack gas ([mg/Nm^3 @10% O_2]) vs average kiln feed (coded [-]).
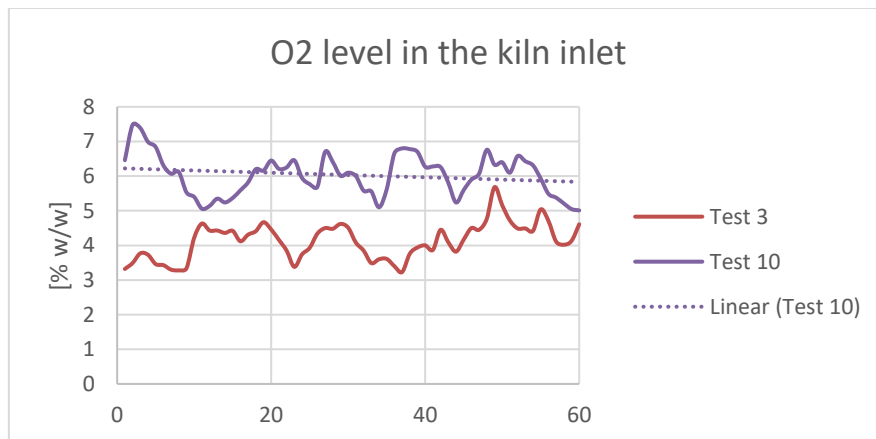

Figure 7.21: Trends in O_2 level in the kiln inlet in Test 3 and Test 10.

7.4.4 Coal Feeding in the kiln

As seen in Figure 7.22 and coal feeding in the kiln ($\dot{m}_{C,RK,in}$) in Model-2, coal feeding has a significant positive impact on the SO$_2$ emissions in the stack gas. Due to lower LSF value of kiln feed, high-level of coal feeding in the experimental plan was changed from 3.2 t/h in Test 1 to 2.9 t/h in Test 3 (@101 t/h kiln feed) and 3.0 t/h in Test 11 to 2.7 t/h in Test 6 (@ 95 t/h kiln feed). As a result, the experimental design matrix lacks perfect orthogonality, and actual impact of coal feeding on the emissions cannot be stated with absolute certainty. However, it can be stated that emission increases with increasing coal feeding in the kiln or lower waste oil feeding. The negative impact of waste oil can be seen between Test 5 (waste oil feeding-600 kg/h, coal feeding-2.5 t/h) and Test 1 (waste oil feeding- 0 kg/h, coal feeding-3.2 t/h). Both tests have identical parameters in terms of tyre feeding (0 kg/h), RDF feeding (0 kg/h) and kiln feed (101 kg/h), almost identical energy input rate (1423 MJ/ton of clinker-Test 1 and 1467 MJ/ton of clinker- Test 5), and different parameter values in terms of bypass water supply (4.5 m^3/h-Test 1 and 3 m^3/h-Test 5) and rawmill feed (110 t/h-Test 1 and 140-t/h-Test 2). As discussed in earlier sections, the impact of rawmill feed and bypass water supply were negligible. Hence, the difference between these tests can be related to a variation in coal or waste oil feeding.
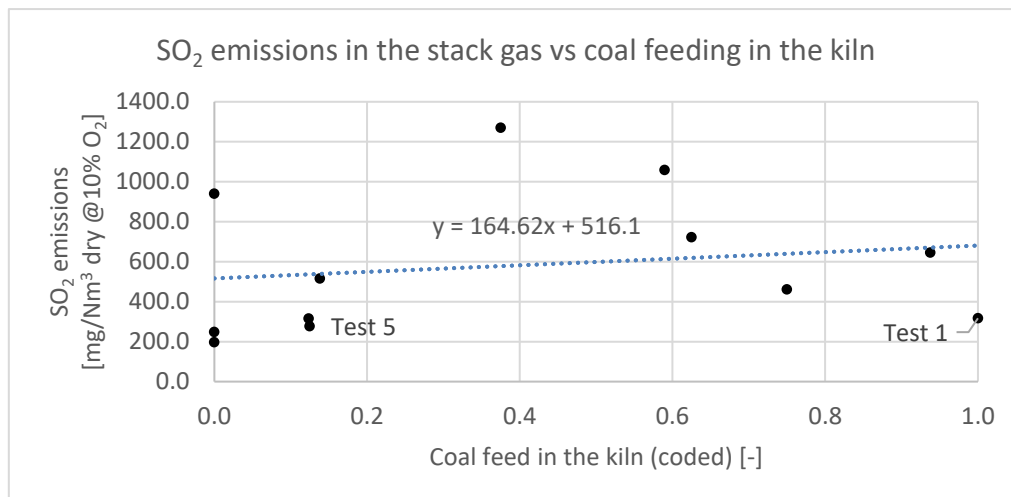

Figure 7.22: Average SO$_2$ emissions in the stack gas ([mg/Nm^3 @10% O$_2$]) vs average kiln feed (coded [-]).

Based on discussions above, it can be concluded that waste oil feeding does not increase the emissions from the plants. Instead, the emissions are higher at higher coal feeding (or lower waste oil feeding). It can be explained based on combustion theory of solid and liquid fuels. Liquid fuels generally atomise easily and burn efficiently, while solid fuel like coal yields combustible vapour and takes relatively longer time for complete combustion. As a result, the probability of contact between unburnt fuel radicals and solid materials in the kiln is higher with coal fuels than in the case of waste oil resulting in reducing environment in the kiln outlet and subsequently, decomposition of sulphates to SO$_2$ via Reaction 3.11 and 3.12.

7.4.5 Energy Input per Unit Ton of Clinker from Rotary Kiln Fuels

As mentioned in section 7.4.4, energy input per unit ton of clinker from rotary kiln fuels lacks orthogonality due to a continuous change in the coal feeding during the kiln tests. As a result, the energy input rate is uniformly distributed between the low level (0) and high-level (1) instead of tests at only high and low-level (Figure 7.23). It was expected prior to the test that energy input rate has a positive impact on the SO$_2$ emissions, but Model-2 and Figure 7.23

show a negative effect on the variation in the emissions. The unexpected negative impact was due to the fact that energy rate in the kiln in most of the test was significantly lower and varied between 1200 to 1550 MJ/ton of clinker. In the test with significantly higher energy input rate (above 1500 MJ/ton of clinker in Test 2, and Test 9) emissions were at medium level. It indicates that the emissions are relatively higher than in normal operation with increasing energy input rate from rotary kiln fuels. The increased emission in the case of higher energy input rate could be related to increased dissociation of calcium sulphates at the higher temperature. Although control of energy input rate in the kiln is usually dictated by Alite content in the clinker, optimising energy input rate from rotary kiln fuels considering clinker quality and SO_2 emissions is recommended for future operations.
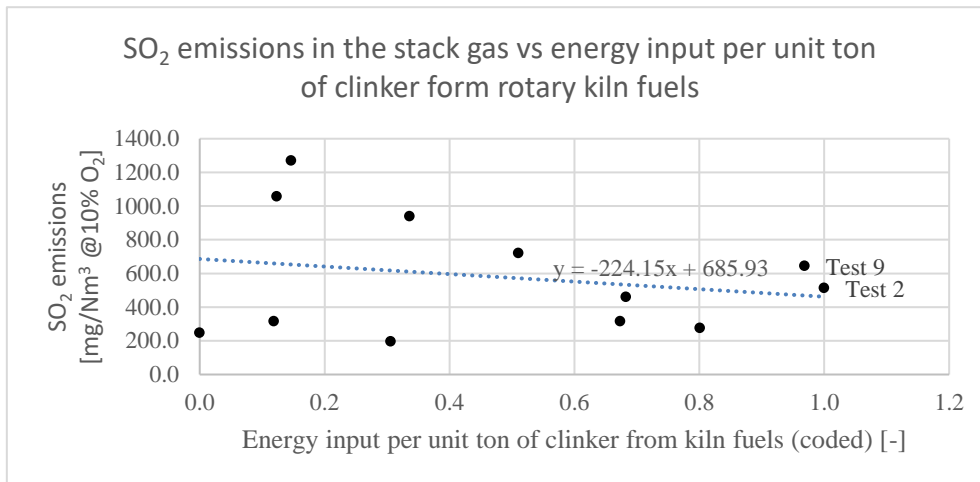

Figure 7.23: Average SO_2 emissions in the stack gas ([mg/Nm^3 @10% O_2]) vs average kiln feed (coded [-]).

8 Conclusions and Recommendation for Future Work

Analysis of historical SO_2 emissions in Week-1 and Week-2 shows that the variations in SO_2 emissions were primarily influenced by variations in SO_3 content in the kiln feed and rawmill feed. Kiln tests varying other parameters, kiln feed, RDF feeding, tyre feeding, bypass water supply, coal feeding in the kiln, energy input per unit of clinker from rotary kiln fuels and rawmill feed were performed to determine the impact of these parameters on the emissions.

Despite limitations to perform kiln test according to the orthogonal design matrix and at the same time faulty hotdisc operation, it can be concluded based on the kiln test results that tyre and RDF feeding are the most significant parameters that have positive impacts on the SO_2 emissions in the stack gas. The abrupt changes in hotmeal feeding into the hotdisc with the tyre and RDF feeding increases CO level in the kiln inlet which subsequently results in increased SO_2 emissions in the stack gas. Moreover, sulphur flow in the hotmeal and kiln exhaust gas increases with tyre and RDF feeding in the hotdisc. The higher emission problem when hotdisc in operation can be addressed by automatic control of hotdisc dividing gate. Moreover, operating hotdisc with either only tyre at lower rotation speed or only RDF at higher rotation speed could be an alternative solution to this problem.

In the case of other factors, it cannot be stated with absolute certainty that these parameters have a significant impact on the emissions. However, coal feeding, kiln feed and energy input per unit ton of clinker show a positive effect on the emissions while assessing individual test results. With almost identical energy input rate from rotary kiln fuels, increasing coal feeding by lowering waste oil feeding in the kiln increases the emissions from the plant. Although further investigations are necessary to establish exact impact and reasons behind the effects of coal feeding, relatively slower combustion of coal can be one of the reasons behind the positive effects of coal in the emissions. Moreover, increasing total energy input rate from rotary kiln fuels (by either increasing coal or waste oil feeding) increases dissociation of sulphates in the kiln and subsequently increases emissions from the plant. In the case of kiln feed, maintaining the O_2 level in the kiln inlet during hotdisc operation is essential to keep in check SO_2 emission at higher kiln feed. Based on the test results, it can be stated that bypass water supply and rawmill feed have a negligible impact on the emissions.

The proposed SWFGD installation addresses the emission problem in Kjøpsvik plant without any additional consequences with respect to process/operational and energy and environmental aspects. However, the results of kiln tests indicate that emissions can be relatively higher than the design value in compound mode (RM-ON mode). If the same tests were performed in direct mode (RM-OFF mode), emission could have been substantially higher than in compound mode. Hence, it is deemed essential for the plant to take appropriate action by operating plant with optimal kiln feed, smooth hotdisc operation, and optimal energy input to the kiln from rotary kiln fuels.

Recommendations for Future Work

During the kiln tests, the mechanical problem in hotmeal dividing gate control, maintenance of rawmill motor, delay in delivery of waste oil forced a delay in the test schedule and reduce the total number of test runs. In addition, coal feeding and energy input rate from rotary kiln fuels were altered during the tests violating principle of systematic orthogonal variations. Moreover, the experimental design implemented in this study does not include variations of SO_3 content in the kiln feed and RDF types. Thus, this study suggests performing more experimental tests

with varying RDF type, SO_3 level in the kiln feed and rawmill operation mode along with spot analysis of preheater exhaust gas, gas flowing out of the rawmill and gas flowing out of the fabric filter. These tests will enable to determine more accurate sulphur flow calculations and sulphur behaviour in the kiln with the variation in kiln parameters.

References

[1]   F. Schorcht, I. Kourti, B. Scalet, S. Roudier, and L. D. Sancho, "Best Available Techniques (BAT) Reference Document for the Production of Cement, Lime and Magnesium Oxide," in "European Commission Joint Research Centre Institute for Prospective Technological Studies," 2013, pp. 66.

[2]   European Commission for Standardization, "European Standard," in *EN 197-1*, Central Secretariat: rue de Stassart, 36 B-1050 Brussels, 2000, pp. 7.

[3]   Portland Cement Association. (2017, 30.01.2018). *How Cement is Made*. Available: http://www.cement.org/cement-concrete-applications/how-cement-is-made

[4]   N. B. Winter. (2018, 31.01.2018). *Portland cement clinker - overview*. Available: https://www.understanding-cement.com/clinker.html

[5]   CEMBUREAU, "Best Available Techniques for the Cement Industry," Rue d'Arlon 55-B-1040 Brussels, 1999.

[6]   L.-A. Tokheim, "The impact of staged combustion on the operation of a precalciner cement kiln," PHD Thesis, Deparment of Technology, Telemark College, Porsgrunn, 1999.

[7]   K. E. Peray and J. J. Waddell, *The rotary cement kiln*. Edward Arnold, 1986.

[8]   S. W. Miller and J. P. Hansen, "Methods for reducing SO_2 emissions," in *IEEE-IAS/PCA 2004 Cement Industry Technical Conference (IEEE Cat. No04CH37518)*, 2004, pp. 79-92.

[9]   C. Maarup and K. Hjuler, "Gas-Solid Heat Exchanger for Cement Production," Technical University of Denmark, Department of Chemical and Biochemical Engineering, 2013.

[10]   FLSmidth, "Preheater calciner systems,"Brochure, 2011. Available: http://www.flsmidth.com/~/media/Brochures/Brochures%20for%20kilns%20and%20firing/PreheatercalcinersystemsV2.pdf

[11]   Sintef Energy AS, "Design and performance of CEMCAP cement plant with MEA post combustion capture," Report, Trondheim, 2015. Available: https://www.sintef.no/globalassets/sintef-energi/cemcap/d4.2-design-and-performance-of-cemcap-cement-plant-with-mea-post-combustion-capture_rev1~1.pdf

[12]   J. Thomas and H. Jennings. (2018, 05.02.2018). Available: http://iti.northwestern.edu/cement/index.html

[13]   R. Favalli, L. F. Fabiani, and L. F. D. Pinho, "Enhancing the Performance of Kiln Burners," *World cement,* 2015, pp. 111-114

[14]   A. Steien, "Innflytelse av råmelparametre og prosessforhold på reaktivitet/brenninggsgrad av Portlandklinker," Master Thesis, Inst. for materialteknologi og elektrokjemi, Norges teknisk-naturvitenskapelige universitet, Trondheim, 2000.

[15]   A. Philip, C. Hung, A. L. Chin-Fatt, A. J. Jackura, M. I. McCabe, and T. Herman, *The cement plant operations Handbook*. Surrey: Tradeship Publications, 2005.

[16] J. O. Haugom, A. O. Kvitvik, K. P. Christensen, and FLSmidth, "Hotdisc Installation at Norcem A.S, Kjøpsvik: Project Realization and Operational Experience," *World cement,* 2002, pp. 348-551.

[17] B. P. Keefe and R. E. Shenk, "The best total value for pyro technology," in *2007 IEEE Cement Industry Technical Conference Record*, 2007, pp. 81-89.

[18] J. S. Salmento and R. E. Shenk, "Accurately predicting cement plant emissions," in *IEEE-IAS/PCA 2004 Cement Industry Technical Conference (IEEE Cat. No04CH37518)*, 2004, pp. 333-343.

[19] E. Jons, S. Hundebol, and K. Clausen, "New Reasons for Installing a Chloride By-Pass. Interaction Between Chloride and Sulphur," ed, 2008, pp. 195-209.

[20] W. M. Swift, A. Panek, G. W. Smith, G. J. Vogel, and A. A. Jonke, "Decomposition of Calcium Sulfate : a Review of the Literature ; ANL (Series) ; Argonne National Laboratory Report ANL-76-122 ; Argonne National Laboratory Reports," ed: Argonne National Laboratory, 1976.

[21] R. Zevenhoven and P. Kilpinen, *Control of pollutants in flue gases and fuel gases*. Helsinki University of Technology Espoo, Finland, 2001.

[22] G. Caiazzo, G. Langella, F. Miccio, and F. Scala, "Seawater SO 2 Scrubbing in a Spray Tower for Marine Application," in *35th Meeting of the Italian Section of the Combustion Institute, Milano, Italy*, 2012, pp. 10-12.

[23] B. Lange, T. Markus, and L. P. Helfst, "Impacts of Scrubbers on the environmental situation in ports and coastal waters," Report, University of Bremen, Bremen, Germany2015.

[24] T. Bakke, E. Yakushev, M. Schaanning, and S. Brooks, "Evaluation of the environmental impact from flue gas seawater scrubbing at the Qatalum aluminium smelter in Qatar," 2010.

[25] K. Rose, D. Kelly, C. Kemker, K. Fitch, and A. Card. (2016, 24.04.2018). *Fundamentals of Environmental Measurements*. Available: www.fondriest.com/environmental-measurements/parameters/water-quality/ph/

[26] G. N. Mhatre and S. B. Chaphekar, "The effect of mercury on some aquatic plants," *Environmental Pollution Series A, Ecological and Biological,* vol. 39, no. 3, pp. 207-216, 1985.

[27] Division of Science, Research and Environmental Health. (2018, 29/04/2018). *Chapter 6-Ecological Effects of Mercury*. Available: http://www.state.nj.us/dep/dsr/vol2-Chapter6.pdf

[28] V. Valentini, "Effects of Dioxins on Fish," European Parliament, 2001. Available: http://www.europarl.europa.eu/stoa/webdav/shared/4_publications/briefings/11_en.pdf

[29] P. Papsai, "Measurement of mercury speciation emitted in the main stack," in "Measurement campaign at Norcem Kjopsvik cement plant,"Report, General Electric, 2017.

[30] Oxford English Dictionary, "Oxford english dictionary," *Simpson, JA & Weiner, ESC,* 1989.

[31]   J. P. Davim, J. P. Davim, and SpringerLink, *Design of Experiments in Production Engineering*, 1st ed. 2016. ed. (Management and Industrial Engineering). Springer International Publishing : Imprint: Springer, 2016.

[32]   D. C. Montgomery, *Design and analysis of experiments*, 5th ed. New York: Wiley, 2001.

Appendices

Appendix A FMH606 Master's thesis description

University College of Southeast Norway

HSN

Faculty of Technology, Natural Sciences and Maritime Sciences, Campus Porsgrunn

FMH606 Master's Thesis

Title: Reduction in sulphur emissions from the Norcem cement plant in Kjøpsvik

USN supervisor: Prof. Lars-André Tokheim

External partner: Norcem Kjøpsvik (Annika Steien, Manager of Process and Environment)

Task background:

Norcem is part of HeidelbergCement Group, which is one the leading manufacturers of cement and concrete in the world, with 60 000 employees in 60 countries. The Norcem plan in Kjøpsvik (County of Nordland) is the world's northernmost cement plant. It has 115 employees and produces 500 000 tons of cement per year.

NORCEM
HEIDELBERGCEMENT Group

In a cement kiln system (see Figure 1), fuels are combusted to provide thermal energy for the calcination in the precalciner and the clinker formation in the rotary kiln (see Figure 1). The exhaust gas is a mixture of combustion products (mainly N_2, CO_2, O_2 and H_2O) and CO_2 from the decarbonation of the calcium carbonate in the limestone ($CaCO_3(s) \rightarrow CaO(s) + CO_2$). In addition, there are minor exhaust gas components like SO_2, NOx, HCl and VOC. The SO_2 emissions are thought to be due mainly to oxidation of solid sulphur components in the raw materials (the limestone-rich raw meal), but may also be impacted by the process conditions in the kiln system and the fuel mixture.
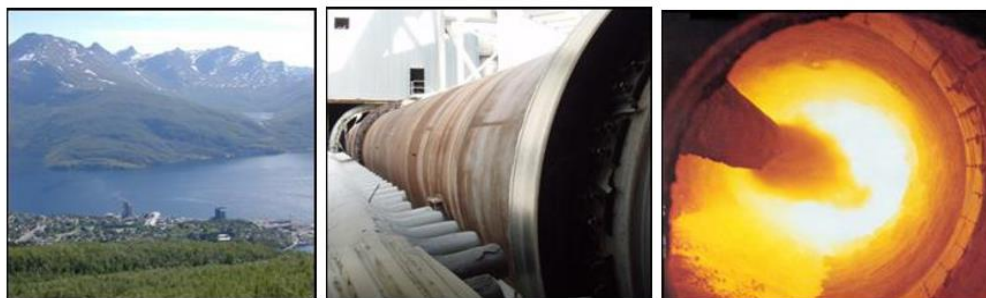

Figure 1: The Kjøpsvik cement plant (left), the rotary kiln (middle) and the kiln burner (right).

The SO_2 concentration in the exhaust gas released to the surroundings typically varies in the range 250 – 700 mg/Nm³ (dry gas @ 10 % O_2). In 2017, the average concentration was 402 mg/Nm³, but the emission limit of 500 mg/Nm³ (dry gas @ 10 % O_2, daily average) was exceeded 53 times, which is not an environmentally sustainable situation. Hence, to solve the SO_2 emission problem, a new SO_2 reduction system, based on seawater scrubbing, will be installed at the plant during 2018 and 2019, and started up after the plant maintenance shutdown in February 2019.

The setpoints of the SO_2 scrubber may depend on the SO_2 concentration in the uncleaned gas, and this concentration in turn depends on the kiln operation, as described above. To optimize the operation of the future scrubber, it will be useful to have a better

Address: Kjølnes ring 56, NO-3918 Porsgrunn, Norway. **Phone:** 35 57 50 00. **Fax:** 35 55 75 47.

understanding of the different factors that impact the SO_2 level in the uncleaned exhaust gas (i.e. upstream of the scrubber).

It would be of interest to know how the SO_2 level in the kiln bypass exit gas is impacted by the fuel mix in the rotary kiln burner, the sulphur level in the limestone (and possibly other raw materials) and the level of sulphur circulation between the rotary kiln and the calciner.

Task description:

The task could include the following sub-tasks:

- Problem description and definition of task objectives
- Kiln system description (before SO_2 scrubber installation)
- Discussion of factors affecting sulphur behaviour in the kiln system and the resulting SO_2 emissions
- Analysis and interpretation of (historical and/or current) plant SO_2 emissions data
- Sulphur material balance of the kiln system, focusing on factors impacting the SO_2 level in the bypass gas
- SO_2 scrubber system description, including a short description of expected consequences (environmental factors, energy considerations and process operational aspects) of the SO_2 scrubber installation
- Identification of factors (for example, the fuel mix in the rotary kiln burner) that may impact the SO_2 concentration in the bypass gas and/or the exhaust gas, including analysis and interpretation of process, emissions and quality data
- Planning and execution of kiln tests to further investigate the identified factors impacting the SO_2 emissions
- Identification of possible reasons for high SO_2 concentrations and suggestion of measures to minimize them

Student category: Process Technology (PT) or Energy and Environmental Technology (EET)

Practical arrangements:

The student will live and work in Kjøpsvik during the thesis work. Norcem Kjøpsvik will cover accommodation, and a budget for travelling expenses will be made available.

Subsequent employment as a project engineer on the scrubber installation project during the second half of 2018 and the first half of 2019 could also be considered.

Signatures:

Supervisor (date and signature): 29/01/2018 *Lars Andre Tokheim*

Student (date and signature): 29|01|2018

Appendix B Process flow diagram of the cement production process in Norcem Kjøpsvik

Process flow diagram, Norcem Cement Plant, Kjøpsvik
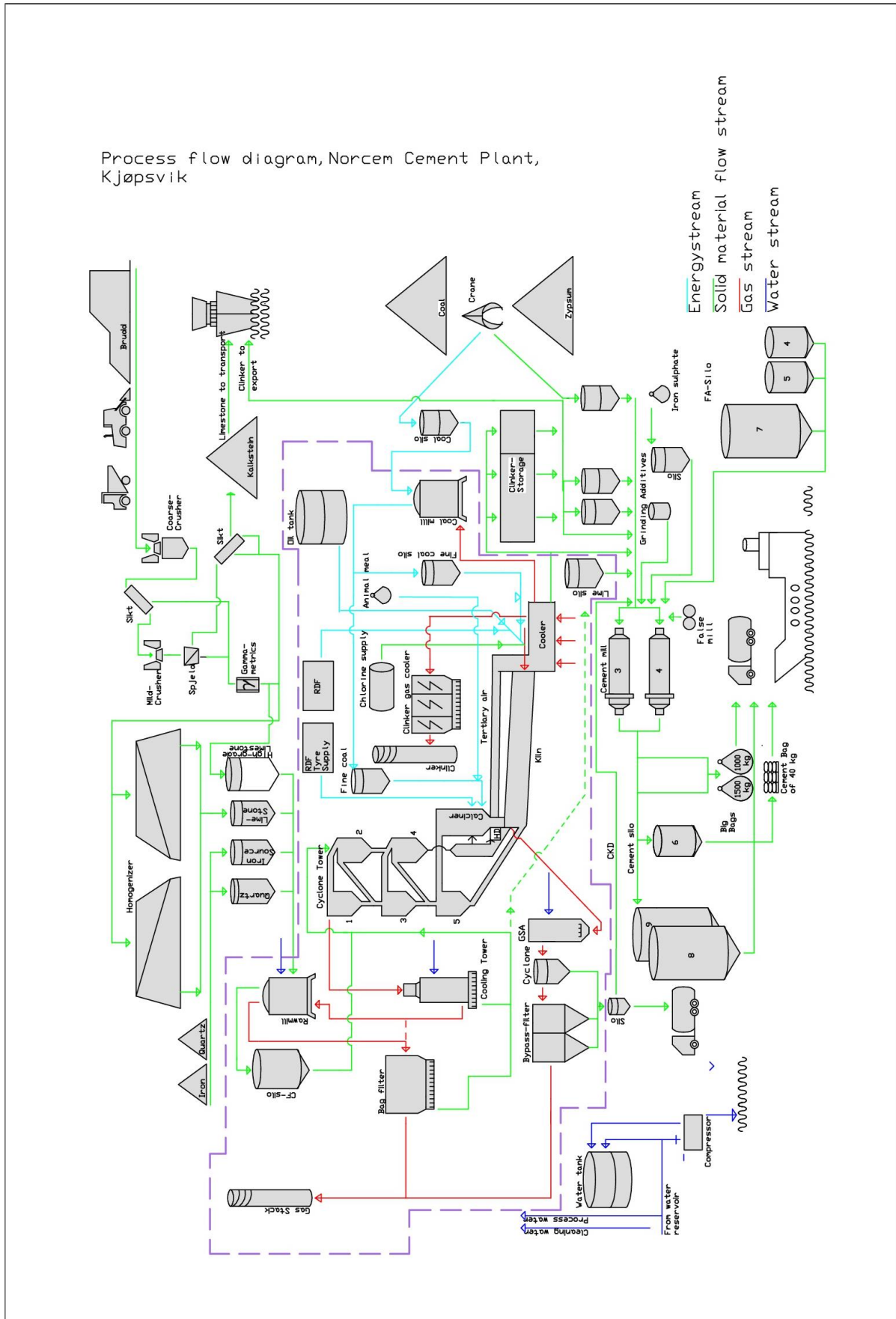
Appendix C Process audit results of gas flows and compositions

Actual operational data based on process audit						
Kiln gases incl. Bypass			**Kiln Bypass**	**Cooler Vent Air**		
Time of Audit: CW49 / 2017 Production: 1.544 t/d	Direct mode	Compound mode	Independent from Direct or Compound mode	Coal Mill On 80% of kiln operation time	Coal Mill Off 20% of kiln operation time	Max
Gasflow — Nm3/h wet	229.890	257.396	22.126	55.021	87.836	120.000
Nm3/h dry	199.315	223.051	18.995			
T °C	143	113	147	195	225	280
O2 % wet	12,03%	11,18%	17,07%			
CO2 % wet	12,39%	11,35%	3,71%			
H2O % wet	13,30%	13,34%	14,15%			
O2 % dry	13,87%	12,90%	19,88%	21,00%	21,00%	21,00%
CO2 % dry	14,29%	13,10%	4,32%	0,00%	0,00%	0,00%
H2O % dry	0,00%	0,00%	0,00%	0,00%	0,00%	0,00%
Future operational data based on process audit and reached by process optimization						
Kiln gases incl. Bypass			**Kiln Bypass**	**Cooler Vent Air**		
Optimized operation*	Direct mode	Compound mode	Independent from Direct or Compound mode	Coal Mill On 80% of kiln operation time	Coal Mill Off 20% of kiln operation time	Max
Gasflow — Nm3/h wet	181.982	220.413	22.126	80.000	100.000	120.000
Nm3/h dry	144.835	182.630	18.995			
T °C	143	113	147	195	225	280
O2 % wet	9,60%	8,46%	17,07%			
CO2 % wet	17,32%	14,55%	3,71%			
H2O % wet	20,41%	17,14%	14,15%			
O2 % dry	12,06%	10,20%	19,88%	21,00%	21,00%	21,00%
CO2 % dry	21,76%	17,56%	4,32%	0,00%	0,00%	0,00%
H2O % dry	0,00%	0,00%	0,00%	0,00%	0,00%	0,00%

*Considered process optimizations are as follows:
- Increased production up to 1.700 t/d
- Targeted O2 after PHT 4,5%, false air reduction and optimized split between Secondary- and Tertiary air
- Max water to GCT in Direct Mode, closed Fresh Air Damper!
- False air reduction downstream Preheater up to Main filter fan
  Direct mode from 21,7% to 10% realted to outlet flow
  Compound mode from 37,2% to 18,5% related to outlet flow
- Increased cooler intake air for better quenching of the clinker

Colour code: Worst case for Scrubber
Best case for Scrubber

Appendix D Calculation of kiln feed to hot meal ratio

The ratio of kiln feed to hot meal is approximate ratio estimation. The ratio can vary with t and quality of the kiln feed. However, the ratio can be used in approximation flow of hot meal

1) **Calculation of solid after a loss on ignition**
- Average kiln feed per hour in the specified period (Period-1 in Week-1)

$$\dot{m}_{KF,PT,in} = 95 \text{ t/h}$$

- Average LOI of the hot meal

$$LOI_{HM} = 4.3\%$$

- Average LOI of the kiln feed

$$LOI_{HM} = 35.5\%$$

- Assuming raw material dominates in the hot meal as well as kiln feed, Equation D.1 represents the material balance based on LOI calculation.

(D.1)

$$\dot{m}_{KF,PT,in} \cdot (1 - LOI_{KF}) = \dot{m}_{HM\_KF,PT,in}(1 - LOI_{HM})$$

$$\dot{m}_{HM\_KF,PT,in} = \frac{\dot{m}_{KF,PT,in} \cdot (1 - LOI_{KF})}{(1 - LOI_{HM})}$$

$$\dot{m}_{HM\_KF,PT,in} = 63.96 \text{ t/h}$$

2. **Dust loss calculation**
- The concentration of dust in the stack gas

- Average gas flow rate in the stack gas

$$\dot{V}_{stack} = 200000 \text{ Nm}^3/\text{h}$$

- Dust emitted to the atmosphere in an hour

$$\dot{m}_{D,stack} = \dot{V}_{stack} \cdot C_{D,stack}$$

3. **Ash input from the coal and alternative fuels (tyre and RDF in the calciner)**
- Ash contribution of coal fed into the calciner

    Average ash composition in the coal fed in the calciner

$$w_{Ash,C,Calc,in} = 15\% \text{ wt/wt}$$

    Average coal input into the calciner

$$\dot{m}_{C,Calc,in} = 2 \text{ t/h}$$

Ash contribution from the coal fed into the calciner

$$\dot{m}_{Ash,C,Calc,in} = \dot{m}_{C,Calc,in} \cdot w_{Ash,C,Calc,in}$$

$$\dot{m}_{Ash,C,Calc,in} = 0.3 \text{ t/h}$$

- Ash contribution from the RDF fed into the calciner
  Average ash composition in the RDF fed in the calciner

$$w_{Ash,RDF,Calc,in} = 12\% \text{ wt/wt}$$

Average RDF input into the calciner

$$\dot{m}_{RDF,Calc,in} = 1 \text{ t/h}$$

Ash contribution from the coal fed into the calciner

$$\dot{m}_{Ash,RDF,Calc,in} = \dot{m}_{RDF,Calc,in} \cdot w_{Ash,RDF,Calc,in}$$

$$\dot{m}_{Ash,RDF,Calc,in} = 0.1 \text{ t/h}$$

- Ash contribution from the tyre fed into the calciner
  Average ash composition in the RDF fed in the calciner

$$w_{Ash,T,Calc,in} = 15\% \text{ wt/wt}$$

Average tyre input into the calciner

$$\dot{m}_{T,Calc,in} = 1700 \text{ t/h}$$

Ash contribution from the tyre fed into the calciner

$$\dot{m}_{Ash,T,Calc,in} = \dot{m}_{T,Calc,in} \cdot w_{Ash,T,Calc,in}$$

$$\dot{m}_{Ash,T,Calc,in} = 0.26 \text{ t/h}$$

4. The total mass flow rate of the hot meal

$$\dot{m}_{HM,RK,in} = \dot{m}_{HM\_KF,RK,in} + \dot{m}_{Ash,C,Calc,in} + \dot{m}_{Ash,RDF,Calc,in} + \dot{m}$$

$$\dot{m}_{HM,RK,in} = 64.6 \text{ t/h}$$

5. Hot meal to kiln feed ratio

$$R_{KF\_2\_HM} = \frac{\dot{m}_{KF,PT,in}}{\dot{m}_{HM,RK,in}}$$

$$R_{KF\_2\_HM} = 1.47$$

Appendix E Reference cement kiln dust flow in compound mode (RM-ON mode).

Table E.1: Cement kiln dust flow in reference condition.

Description	Value
CKD flow back into the preheater tower	20.8 t/h
Kiln Feed	110 t/h
Raw mill contribution in the cement kiln dust	12 t/h
Raw material feeding rate	150 t/h
Dry gas flow in the stack	17500 Nm^3/h

Appendix F Reference procedure for sulphur flow calculation

Reference calculation period: Period-1 (17th December 2017, 3:00 PM to 11:00 PM)

1) **Sulphur contribution from the calciner fuels**
   - Sulphur in the coal flowing into the calciner is computed using Equation 3.25.

$$\dot{m}_{S,C,Calc,in} = \dot{m}_{C,Calc,in} \cdot w_{S,C}$$
$$\Rightarrow \dot{m}_{S,C,Calc,in} = 3.4 \cdot 0.0076 \cdot 1000$$
$$\Rightarrow \dot{m}_{S,C,Calc,in} = 25.8 \text{ kg/h}$$

   - Sulphur in the Tyre flowing into the calciner is computed using Equation 3.26. Steel fraction is taken as 15%.

$$\dot{m}_{S,T,Calc,in} = \dot{m}_{T,Calc,in} \cdot w_{S,T} \cdot (1 - \text{steel\_fraction})$$
$$\Rightarrow \dot{m}_{S,T,Calc,in} = 1230 \cdot 1.5 \cdot 0.85$$

   - Sulphur in the RDF flowing into the calciner is computed using Equation 3.27.

$$\dot{m}_{S,RDF,Calc,in} = \dot{m}_{RDF,Calc,in} \cdot w_{S,RDF}$$
$$\Rightarrow \dot{m}_{S,RDF,Calc,in} = 435 \cdot 0.0021$$
$$\Rightarrow \dot{m}_{S,RDF,Calc,in} = 0.9 \text{ kg/h}$$

   - Sulphur in the animal meal flowing into the calciner is computed using Equation 3.28.

$$\dot{m}_{S,AM,Calc,in} = \dot{m}_{AM,Calc,in} \cdot w_{S,T}$$
$$\Rightarrow \dot{m}_{S,AM,Calc,in} = 47 \cdot 0.005$$
$$\Rightarrow \dot{m}_{S,AM,Calc,in} = 0.2 \text{ kg/h}$$

   - Total sulphur input from the calciner fuels into the system is computed using Equation 3.24.

$$\dot{m}_{S,F,PT,in} = \dot{m}_{S,C,Calc,in} + \dot{m}_{S,T,Calc,in} + \dot{m}_{S,RDF,Calc,in} + \dot{m}_{S,AM,Calc,in}$$
$$\Rightarrow \dot{m}_{S,F,PT,in} = 25.8 + 15.7 + 0.9 + 0.2$$
$$\Rightarrow \dot{m}_{S,F,PT,in} = 42.7 \text{ kg/h}$$

2) **Sulphur contribution from the rotary kiln fuels**
   - Sulphur in the coal flowing into the rotary kiln is computed using Equation 3.36.

$$\dot{m}_{S,C,RK,in} = \dot{m}_{C,RK,in} \cdot w_{S,C}$$
$$\Rightarrow \dot{m}_{S,C,RK,in} = 3.3 \cdot 0.0076 \cdot 1000$$
$$\Rightarrow \dot{m}_{S,C,RK,in} = 25.1 \text{ kg/h}$$

- Sulphur in the waste oil flowing into the calciner is computed using Equation 3.37.

$$\dot{m}_{S,WO,RK,in} = \dot{m}_{C,WO,in} \cdot w_{S,WO}$$

$$\Rightarrow \dot{m}_{S,WO,RK,in} = 0 \cdot 0.0034$$

$$\Rightarrow \dot{m}_{S,WO,RK,in} = 0 \text{ kg/h}$$

- Total sulphur contribution from the rotary kiln fuels into kiln is computed using Equation 3.35.

$$\dot{m}_{S,F,RK,in} = \dot{m}_{S,C,RK,in} + \dot{m}_{S,WO,RK,in}$$

$$\Rightarrow \dot{m}_{S,F,RK,in} = 25.1 + 0$$

$$\Rightarrow \dot{m}_{S,F,RK,in} = 25.1 \text{ kg/h}$$

3) Sulphur outflow from the clinker

- Sulphur in terms of SO_3 in the clinker is computed using Equation 3.39.

$$\dot{m}_{SO_3,CL,RK,out} = \dot{m}_{CL,RK,out} \cdot w_{SO_3,CL,RK,out}$$

$$\Rightarrow \dot{m}_{SO_3,CL,RK,out} = 63.5 \cdot 0.012 \cdot 1000$$

$$\Rightarrow \dot{m}_{SO_3,CL,RK,out} = 762.0 \text{ kg/h}$$

- Sulphur flow in the clinker is computed using Equation 3.40.

$$\dot{m}_{S,CL,RK,out} = \dot{m}_{SO_3,CL,RK,out} \cdot \frac{Mw_S}{Mw_{SO_3}}$$

$$\Rightarrow \dot{m}_{S,CL,RK,out} = 762.0 \cdot \frac{32}{80}$$

$$\Rightarrow \dot{m}_{S,CL,RK,out} = 304.8 \text{ kg/h}$$

4) Sulphur in the kiln feed

- Sulphur flow in terms of SO_3 in the kiln feed is computed using Equation 3.21.

$$\dot{m}_{SO_3,KF,PT,in} = \dot{m}_{KF,PT,in} \cdot w_{SO_3,KF,PT,in}$$
$$\Rightarrow \dot{m}_{SO_3,KF,PT,in} = 99.0 \cdot 0.01$$
$$\Rightarrow \dot{m}_{SO_3,KF,PT,in} = 990 \text{ kg/h}$$

- Sulphur flow in the kiln feed is computed using Equation 3.22.

$$\dot{m}_{S,KF,PT,in} = \dot{m}_{SO_3,KF,PT,in} \cdot \frac{Mw_S}{Mw_{SO_3}}$$

$$\Rightarrow \dot{m}_{S,KF,PT,in} = 990.0 \cdot \frac{32}{80}$$
$$\Rightarrow \dot{m}_{S,KF,PT,in} = 396.0 \text{ kg/h}$$

5) Sulphur in the hot meal

- Hot meal flow is computed using Equation 3.15.

$$\dot{m}_{HM,RK,in} = \dot{m}_{KF,PT,in} \cdot \frac{1}{R_{KF\_2\_HM}}$$

$$\Rightarrow \dot{m}_{HM,RK,in} = 99.0 \cdot \frac{1}{1.47}$$

$$\Rightarrow \dot{m}_{HM,RK,in} = 67.3 \text{ t/h}$$

- Sulphur flow in terms of SO_3 in the hot meal is computed using Equation 3.30.

$$\dot{m}_{SO_3,HM,RK,in} = \dot{m}_{HM,RK,in} \cdot w_{SO_3,HM,RK,in}$$

$$\Rightarrow \dot{m}_{SO_3,HM,RK,in} = 67.4 \cdot 0.0435$$

$$\Rightarrow \dot{m}_{SO_3,HM,RK,in} = 2929.6 \text{ kg/h}$$

- Sulphur flow in the hot meal is computed using Equation 3.31.

$$\dot{m}_{S,HM,RK,in} = \dot{m}_{SO_3,HM,RK,in} \cdot \frac{Mw_S}{Mw_{SO_3}}$$

$$\Rightarrow \dot{m}_{S,HM,RK,in} = 2929.0 \cdot \frac{32}{80}$$

$$\Rightarrow \dot{m}_{S,HM,RK,in} = 1171.8 \text{ kg/h}$$

6) Calculation of total sulphur outflow in the stack gas

- SO_2 outflow in the stack gas is computed using Equation 3.69.

$$\dot{m}_{SO_2,G,Stack} = \dot{V}_{G,Stack} \cdot C_{SO_2,G,Stack}$$

$$\Rightarrow \dot{m}_{SO_2,G,Stack} = 170000 \cdot 464 \cdot 10^{-6}$$

$$\Rightarrow \dot{m}_{SO_2,G,Stack} = 78.9 \text{ kg/h}$$

- Sulphur outflow in the stack gas is computed using Equation 3.70.

$$\dot{m}_{S,G,Stack} = \dot{m}_{SO_2,G,Stack} \cdot \frac{Mw_S}{Mw_{SO_2}}$$

$$\Rightarrow \dot{m}_{S,G,Stack} = 78.9 \cdot \frac{32}{64}$$

$$\Rightarrow \dot{m}_{S,G,Stack} = 39.4 \text{ kg/h}$$

7) Calculation of sulphur in the bypass dust

- Sulphur flow in terms of SO_3 in the bypass dust is computed using Equation 3.63.

$$\dot{m}_{SO_3,D,BP,out} = \dot{m}_{D,BP,out} \cdot w_{SO_3,D,BP,out}$$

$$\Rightarrow \dot{m}_{SO_3,D,BP,out} = 0.24 \cdot 0.088$$

$$\Rightarrow \dot{m}_{SO_3,D,BP,out} = 21.1 \text{ kg/h}$$

- Sulphur flow in the bypass dust is computed using Equation 3.64.

$$\dot{m}_{S,D,BP,out} = \dot{m}_{SO_3,D,BP,out} \cdot \frac{Mw_S}{Mw_{SO_3}}$$

$$\Rightarrow \dot{m}_{S,D,BP,out} = 21.1 \cdot \frac{32}{80}$$

$$\Rightarrow \dot{m}_{S,D,BP,out} = 8.4 \text{ kg/h}$$

8) Calculation of sulphur flow in the bypass gas

- There is a lack of gas measurement system in the bypass gas. But based on past measurements available, a linear interpolation method is used to estimate gas flow in the bypass. Table F.1 lists the measured gas flow in the reference condition. Appendix C consists of complete process audit results of gas measurements performed in 2017.

Table F.1: Gas flows measurements and gas compositions when raw mill is in operation (compound mode).

Gas		Flow rate Nm³/h
Bypass gas	Wet	22126
	Dry	18995
Stack gas	Wet	257396
	Dry	223051

Total dry gas flow in the stack in the calculation period, $\dot{V}_{G,Stack} = 17000 \ \mathrm{Nm^3/h}$

Total wet gas flow in the bypass gas is computed based on linear approximation (Equation 3.14) with reference measurement data in Table F.1.

$$\dot{V}_{G,BP,out,wet} = \frac{\dot{V}_{G,stack,dry}}{\dot{V}_{G,stack,dry,ref}} \cdot \dot{V}_{G,BP,out,wet,ref}$$

$$\dot{V}_{G,BP,out,wet} = \frac{170000}{223051} \cdot 22126$$

$$\dot{V}_{G,BP,out,wet} = 16863 \ \mathrm{Nm^3/h}$$

The gas flow at actual temperature is computed as,

$$\dot{V}_{G,BP,out,wet} = \dot{V}_{G,BP,out,wet} \cdot \frac{T_{BP,out}}{T_{Normal}}$$

$$\dot{V}_{G,BP,out,wet} = 16863 \cdot \frac{142.6 + 273.15}{273.15}$$

$$\dot{V}_{G,BP,out,wet} = 25667 \ \mathrm{m^3}$$

Then, SO₂ flow out of the bypass gas is computed using Equation 3.62.

$$\dot{m}_{SO_2,G,BP,out} = \dot{V}_{G,BP,out} \cdot C_{SO_2,G,BP,out}$$

$$\Rightarrow \dot{m}_{SO_2,G,BP,out} = 25667 \cdot 170 \cdot 10^{-6}$$

$$\Rightarrow \dot{m}_{SO_2,G,BP,out} = 11.9 \ \mathrm{kg/h}$$

- Sulphur flow outflow in the bypass gas is computed using equation 3.63.

$$\dot{m}_{S,G,BP,out} = \dot{m}_{SO_2,G,BP,out} \cdot \frac{Mw_S}{Mw_{SO_2}}$$

$$\dot{m}_{S,G,BP,out} = 11.9 \cdot \frac{32}{64}$$

$$\dot{m}_{S,G,BP,out} = 6.0 \ \mathrm{kg/h}$$

9) Calculation of sulphur flow in the bypass gas flowing out of the kiln

- Sulphur outflow in the bypass dust is computed using sulphur material balance in the bypass Equation 3.60.

$$\dot{m}_{S,G,BP,in} = \dot{m}_{S,BP,out}$$

Sulphur outflow from the bypass is compute using Equation 3.61.

$$\dot{m}_{S,BP,out} = \dot{m}_{S,G,BP,out} + \dot{m}_{S,D,BP,out}$$
$$\Rightarrow \dot{m}_{S,BP,out} = 8.4 + 6$$
$$\Rightarrow \dot{m}_{S,BP,out} = 14.4 \text{ kg/h}$$

Then, sulphur in the bypass gas coming out of the kiln is,

$$\dot{m}_{S,G,BP,in} = \dot{m}_{S,G,BP,out} + \dot{m}_{S,D,BP,out}$$
$$\Rightarrow \dot{m}_{S,G,BP,in} = 14.4 \text{ kg/h}$$

- Sulphur flow in terms of SO_2 in the bypass gas coming out of the kiln is compute using Equation 3.41.

$$\dot{m}_{SO_2,G,BP,in} = \dot{m}_{S,G,BP,in} \cdot \frac{Mw_{SO_2}}{Mw_S}$$

$$\Rightarrow \dot{m}_{SO_2,G,BP,in} = 14.4 \cdot \frac{64}{32}$$

$$\Rightarrow \dot{m}_{SO_2,G,BP,in} = 28.8 \text{ kg/h}$$

10) Calculation of sulphur flow in the preheater exhaust gas coming out of the fabric filter

- Sulphur material balance in the Gas Mix (Equation 3.68) is used to compute sulphur in the gas coming out if the fabric filter.

$$\dot{m}_{S,G,BP,out} + \dot{m}_{S,G,FF,out} = \dot{m}_{S,G,Stack}$$

$$\dot{m}_{S,G,FF,out} = \dot{m}_{S,G,Stack} - \dot{m}_{S,G,BP,out}$$

Then,
$$\Rightarrow \dot{m}_{S,G,FF,out} = 39.4 - 6.0$$
$$\Rightarrow \dot{m}_{S,G,FF,out} = 33.5 \text{ kg/h}$$

- SO_2 flow in the preheater exhaust gas coming out of the fabric filter is computed using Equation 3.59.

$$\dot{m}_{SO_2,G,FF,out} = \dot{m}_{SO_2,G,FF,out} \cdot \frac{Mw_{SO_2}}{Mw_S}$$

$$\Rightarrow \dot{m}_{SO_2,G,FF,out} = 33.5 \cdot \frac{64}{32}$$

$$\Rightarrow \dot{m}_{SO_2,G,FF,out} = 67.0 \text{ kg/h}$$

11) Sulphur accumulation in the CF-silo

- Sulphur accumulation in the CF-silo is computed using Equation 3.49.

$$\Delta \dot{m}_{SO_3,CF,AC} = \Delta \dot{m}_{CF,AC} \cdot w_{SO_3,KF,PT,in}$$
$$\Rightarrow \Delta \dot{m}_{SO_3,CF,AC} = 18.3 \cdot 0.01$$
$$\Rightarrow \Delta \dot{m}_{SO_3,CF,AC} = 183 \text{ kg/h}$$

- Sulphur accumulation in the CF-silo is computed using Equation 3.50.

$$\Delta \dot{m}_{\text{S},CF,AC} = \Delta \dot{m}_{\text{SO}_3,CF,AC} \cdot \frac{Mw_{\text{S}}}{Mw_{\text{SO}_3}}$$

$$\Rightarrow \Delta \dot{m}_{\text{S},CF,AC} = 183 \cdot \frac{32}{80}$$

$$\Rightarrow \Delta \dot{m}_{\text{S},CF,AC} = 73.2 \text{ kg/h}$$

12) Sulphur flow in the cement kiln dust

- Dust contribution from the raw mill is computed using Equation 3.51.

$$\dot{m}_{CKD\_RaM} = \dot{m}_{RaM,RM,in} - \dot{m}_{KF,PT,in} - \Delta \dot{m}_{CF,AC}$$
$$\Rightarrow \dot{m}_{CKD\_RaM} = 129.8 - 100 - 18.3$$
$$\Rightarrow \dot{m}_{CKD\_RaM} = 12.5 \text{ t/h}$$

- Reference data provided by Heidelberg Technical Centre is used to compute cement kiln dust contribution from the preheater exhaust gas. The reference data is in Table E.1 in Appendix E. The reference values are,

Cement kiln dust rate recirculation from the raw mill in a reference case,
$$\dot{m}_{CKD\_G\_PT} = 8.8 \text{ t/h}$$

Kiln feed in a reference case,

$$\dot{m}_{KF,PT,in,ref} = 110 \text{ t/h}$$

Raw material feeding feed in a reference case,

$$\dot{m}_{RaM,RM,in,ref} = 150 \text{ t/h}$$

Gas flow in the stack in a reference condition,

$$\dot{V}_{G,Stack,ref} = 175000 \text{ Nm}^3/\text{h}$$

A linear approximation method is used to compute the flow of cement kiln dust into the preheater tower. Equation 3.16 is used to approximate flow of cement kiln dust into the preheater tower.

$$\dot{m}_{CKD\_G\_PT} = \dot{m}_{CKD,FF,out,ref} \frac{\dot{m}_{KF,PT,in}}{\dot{m}_{KF,PT,in,ref}} \frac{\dot{V}_{G,Stack}}{\dot{V}_{G,Stack,ref}}$$

$$\Rightarrow \dot{m}_{CKD\_G\_PT} = 8.8 \cdot \frac{99}{110} \cdot \frac{170000}{175000}$$

$$\Rightarrow \dot{m}_{CKD\_G\_PT} = 7.7 \text{ t/h}$$

Then, total CKD flow into the preheater tower is computed using Equation 3.52,

$$\dot{m}_{CKD,FF,out} = \dot{m}_{CKD\_G\_PT} + \dot{m}_{CKD\_RaM}$$
$$\Rightarrow \dot{m}_{CKD\_G\_PT} = 12.5 + 7.7$$
$$\Rightarrow \dot{m}_{CKD\_G\_PT} = 20.2 \text{ t/h}$$

Then, sulphur flow in terms of SO_3 in the CKD is computed using Equation 3.57.

$$\dot{m}_{SO_3,CKD,FF,out} = \dot{m}_{CKD,FF,out} w_{SO_3,CKD,FF,out}$$
$$\Rightarrow \dot{m}_{SO_3,CKD,FF,out} = 20.2 \cdot 0.0096$$
$$\Rightarrow \dot{m}_{SO_3,CKD,FF,out} = 193.9 \text{ kg/h}$$

- Sulphur flow in the CKD is computed using equation 3.58

$$\dot{m}_{S,CKD,FF,out} = \dot{m}_{SO_3,CKD,FF,out} \cdot \frac{Mw_S}{Mw_{SO_3}}$$

$$\Rightarrow \dot{m}_{S,CKD,FF,out} = 193.9 \cdot \frac{32}{80}$$
$$\Rightarrow \dot{m}_{S,CKD,FF,out} = 77.5 \text{ kg/h}$$

13) Sulphur material balance in the fabric filter and calculation of sulphur flow into the fabric filter

- Sulphur material balance in the fabric filter (Equation 3.53) is used to compute sulphur flow in the gas coming out of the raw mill (compound mode) into the fabric filter.

$$\dot{m}_{S,FF,in} = \dot{m}_{S,FF,out}$$

Sulphur flow out of the fabric filter is computed using Equation 3.56.

$$\dot{m}_{S,FF,out} = \dot{m}_{S,CKD,FF,out} + \dot{m}_{S,G,FF,out}$$
$$\Rightarrow \dot{m}_{S,FF,out} = 77.5 + 33.5$$
$$\Rightarrow \dot{m}_{S,FF,out} = 111.0 \text{ kg/h}$$

Sulphur flow into the fabric filter is computed using Equation 3.54.

$$\dot{m}_{S,FF,in} = \dot{m}_{S,G,RM,out} + \dot{m}_{S,G,FF,Dir,in}$$

Since, the raw mill is running in compound mode, $\dot{m}_{S,G,FF,Dir,in} = 0$.

Hence, sulphur outflow from the raw mill is computed as,

$$\dot{m}_{S,G,RM,out} = 111.0 \text{ kg/h}$$

- SO_2 flow in the gas coming out of the raw mill is computed using Equation 3.48.

$$\dot{m}_{SO_2,G,RM,out} = \dot{m}_{S,G,RM,out} \cdot \frac{Mw_{SO_2}}{Mw_S}$$

$$\Rightarrow \dot{m}_{SO_2,G,RM,out} = 111.0 \cdot \frac{64}{32}$$
$$\Rightarrow \dot{m}_{SO_2,G,RM,out} = 222.0 \text{ kg/h}$$

14) Sulphur material balance in the rotary kiln and calculation of sulphur flow in the kiln exhaust gas

- Sulphur material balance in the kiln (Equation 3.33) is used to calculate sulphur flow in the kiln exhaust gas.

$$\dot{m}_{S,RK,in} = \dot{m}_{S,RK,out}$$

Sulphur flow into the rotary kiln is computed using Equation 3.34.

$$\dot{m}_{S,RK,in} = \dot{m}_{S,HM,RK,in} + \dot{m}_{S,F,RK,in}$$
$$\Rightarrow \dot{m}_{S,RK,in} = 1171.8 + 25.1$$
$$\Rightarrow \dot{m}_{S,RK,in} = 1196.9 \text{ kg/h}$$

Sulphur outflow from the kiln is computed using Equation 3.38.

$$\dot{m}_{S,RK,out} = \dot{m}_{S,CL,RK,out} + \dot{m}_{S,G,RK,out} + \dot{m}_{S,G,BP,in}$$

From Equation 3.33, 3.34 and 3.38, sulphur flow in the rotary kiln gas is,

$$\dot{m}_{S,G,RK,out} = \dot{m}_{S,RK,in} - \dot{m}_{S,CL,RK,out} - \dot{m}_{S,G,BP,in}$$
$$\Rightarrow \dot{m}_{S,G,RK,out} = 1196.9 - 304.8 - 14.4$$
$$\Rightarrow \dot{m}_{S,G,RK,out} = 877.8 \text{ kg/h}$$

- SO_2 flow in the rotary kiln gas is computed using Equation 3.23.

$$\dot{m}_{SO_2,G,RK,out} = \dot{m}_{S,G,RK,out} \cdot \frac{Mw_{SO_2}}{Mw_S}$$
$$\Rightarrow \dot{m}_{SO_2,G,RK,out} = 877.8 \cdot \frac{64}{32}$$
$$\Rightarrow \dot{m}_{SO_2,G,RK,out} = 1755.6 \text{ kg/h}$$

15) Sulphur material balance in the preheater tower and calculation of sulphur outflow in the preheater exhaust gas
- Sulphur material balance in the preheater tower (Equation 3.17) is used to calculate sulphur outflow in the preheater exhaust gas.

$$\dot{m}_{S,PT,in} = \dot{m}_{S,PT,out}$$

Sulphur inflow into the preheater tower is computed using Equation 3.18.

$$\dot{m}_{S,PT,in} = \dot{m}_{S,CKD,FF,out} + \dot{m}_{S,KF,PT,in} + \dot{m}_{S,F,PT,in} + \dot{m}_{S,G,RK,out}$$
$$\Rightarrow \dot{m}_{S,PT,in} = 77.5 + 396.0 + 42.7 + 877.8$$
$$\Rightarrow \dot{m}_{S,PT,in} = 1394.0 \text{ kg/h}$$

Sulphur outflow from the preheater tower is computed using Equation 3.29.

$$\dot{m}_{S,PT,out} = \dot{m}_{S,HM,RK,in} + \dot{m}_{S,G,PT,out}$$

Combining Equation 3.17, 3.18 and 3.29, sulphur outflow in the preheater gas is,

$$\dot{m}_{S,G,PT,out} = \dot{m}_{S,PT,in} - \dot{m}_{S,HM,RK,in}$$
$$\Rightarrow \dot{m}_{S,G,PT,out} = 1394.0 - 1171.8$$
$$\Rightarrow \dot{m}_{S,G,PT,out} = 222.1 \text{ kg/h}$$

- SO_2 flow in the preheater exhaust gas is computed using Equation 3.32.

$$\dot{m}_{SO_2,G,PT,out} = \dot{m}_{S,G,PT,out} \cdot \frac{Mw_{SO_2}}{Mw_S}$$

$$\Rightarrow \dot{m}_{SO_2,G,PT,out} = 222.1 \cdot \frac{64}{32}$$

$$\Rightarrow \dot{m}_{SO_2,G,PT,out} = 444.2 \text{ kg/h}$$

16) Sulphur material balance in the splitter

- The plant is running in compound mode (rawmill is in operation) so, the split factor (x) is 1. Thus, sulphur flow into the rawmill from the splitter is computed using Equation 3.66.

$$\dot{m}_{S,G,RM,in} = \dot{m}_{S,G,PT,out}$$

$$\Rightarrow \dot{m}_{S,G,RM,in} = 222.1 \text{ kg/h}$$

- SO$_2$ flow in the gas flowing into the rawmill is computed using Equation 3.46

$$\dot{m}_{SO_2,G,RM,in} = \dot{m}_{S,G,RM,in} \cdot \frac{Mw_{SO_2}}{Mw_S}$$

$$\Rightarrow \dot{m}_{SO_2,G,RM,in} = 222.1 \cdot \frac{64}{32}$$

$$\Rightarrow \dot{m}_{SO_2,G,RM,in} = 444.2 \text{ kg/h}$$

17) Sulphur inflow from the rawmill feed

- Sulphur flow in the rawmill feed is computed using overall sulphur balance in the system.

$$\dot{m}_{S,RMF,RM,in} = \dot{m}_{S,CL,RK,out} + \Delta\dot{m}_{S,CF,AC} + \dot{m}_{S,D,BP,out}$$
$$+ \dot{m}_{S,G,stack} - \dot{m}_{F,PT,in} - \dot{m}_{F,RK,out}$$

$$\Rightarrow \dot{m}_{S,RMF,RM,in} = 304.8 + 73.2 + 8.4 + 39.4 - 42.7 - 25.1$$

$$\Rightarrow \dot{m}_{S,RMF,RM,in} = 358.1 \text{ kg/h}$$

Appendix G Summary of sulphur flow calculation in Period-1 and Period-2.

Table G.1: Summary of calculated sulphur flow results on Period-1 in Week-1 (11th December 22:00 t0 12th December 05:00) and Period-2 in Week-2 (24th August 00:00 to 24th August 22:00).

Description	Symbol	Units	Period-1	Period-2
SO_3 in the rawmill feed	$\dot{m}_{SO_3,RMF,RM,in}$	[kg/h]	895.3	923.3
Sulphur in the rawmill feed	$\dot{m}_{S,RMF,RM,in}$	[kg/h]	358.1	369.3
SO_3 accumulation in CF-silo	$\Delta\dot{m}_{SO_3,CF}$	[kg/h]	183.0	189.0
Sulphur accumulation in CF-silo	$\Delta\dot{m}_{S,CF}$	[kg/h]	73.2	75.6
SO_3 flow in the kiln feed	$\dot{m}_{SO_3,KF,PT,in}$	[kg/h]	990.0	859.0
Sulphur flow in the kiln feed	$\dot{m}_{S,KF,PT,in}$	[kg/h]	396.0	343.6
Approximated hotmeal flow	$\dot{m}_{HM,RK,in}$	[t/h]	67.34	70.4
SO_3 flow in the hotmeal	$\dot{m}_{SO_3,HM,RK,in}$	[kg/h]	2929.6	2886.7
Sulphur flow in the hotmeal	$\dot{m}_{S,HM,RK,in}$	[kg/h]	1171.8	1154.7
SO_3 flow in the clinker	$\dot{m}_{SO_3,CL,RK,out}$	[kg/h]	762.0	853.4
Sulphur flow in the clinker	$\dot{m}_{S,CL,RK,out}$	[kg/h]	304.8	341.4
SO_3 flow in the CKD	$\dot{m}_{SO_3,CKD,FF,out}$	[kg/h]	193.9	150.2
Sulphur flow in the CKD	$\dot{m}_{S,CKD,FF,out}$	[kg/h]	77.5	60.1
SO_3 flow in the bypass dust	$\dot{m}_{SO_3,D,BP,out}$	[kg/h]	21.1	45.5
Sulphur flow in the bypass dust	$\dot{m}_{S,D,BP,out}$	[kg/h]	8.4	17.8
Sulphur flow in the coal into the calciner	$\dot{m}_{S,C,Calc,in}$	[kg/h]	25.8	20.4
Sulphur flow in the coal into the calciner	$\dot{m}_{S,C,RK,in}$	[kg/h]	25.1	15.0
Sulphur flow in the waste oil into the kiln	$\dot{m}_{S,WO,RK,in}$	[kg/h]	0	1.5
Sulphur flow in the animal meal into the calciner	$\dot{m}_{S,AM,Calc,in}$	[kg/h]	0.2	0
Sulphur flow in the tyre into the calciner	$\dot{m}_{S,T,Calc,in}$	[kg/h]	15.7	35.6
Sulphur flow in the RDF into the calciner	$\dot{m}_{S,RDF,Calc,in}$	[kg/h]	0.9	0
SO_2 flow in the preheater exhaust gas	$\dot{m}_{SO_2,G,PT,out}$	[kg/h]	444.2	229.8
Sulphur flow in the preheater exhaust gas	$\dot{m}_{S,G,PT,out}$	[kg/h]	222.1	114.9
SO_2 flow in the kiln exhaust gas	$\dot{m}_{SO_2,G,RK,out}$	[kg/h]	1755.4	1617.6
Sulphur flow in the kiln exhaust gas	$\dot{m}_{S,G,RK,out}$	[kg/h]	877.7	808.8
SO_2 flow in the bypass gas flowing out of the kiln	$\dot{m}_{SO_2,G,BP,in}$	[kg/h]	28.8	42.0
Sulphur flow in the bypass gas flowing out of the kiln	$\dot{m}_{S,G,BP,in}$	[kg/h]	14.4	21.0
SO_2 flow in the gas flowing out of the raw mill	$\dot{m}_{SO_2,G,RM,out}$	[kg/h]	222.0	155.6
Sulphur flow in the gas flowing out of the raw mill	$\dot{m}_{S,G,RM,out}$	[kg/h]	111.0	77.8
SO_2 flow in the gas flowing out of the main filter	$\dot{m}_{SO_2,G,FF,out}$	[kg/h]	66.8	35.4

Sulphur flow in the gas flowing out of the main filter	$\dot{m}_{S,G,FF,out}$	[kg/h]	33.4	17.7
Approximated volume flow rate of bypass gas	$\dot{V}_{G,BP,out}$	[m³/h]	25667	25756
SO₂ flow in the gas flowing out of the bypass filter	$\dot{m}_{SO_2,G,BP,out}$	[kg/h]	12.0	6.4
Sulphur flow in the gas flowing out of the bypass filter	$\dot{m}_{S,G,BP,out}$	[kg/h]	6.0	3.2
SO₂ flow in the stack gas	$\dot{m}_{SO_2,G,Stack}$	[kg/h]	78.9	41.8
Sulphur flow in the stack gas	$\dot{m}_{S,G,Stack}$	[kg/h]	39.4	20.9

Appendix H Experimental plan to test the sulphur behaviour in the Norcem cement plant in Kjøpsvik.

<div align="center">

Experimental Plan
of
Testing of the Sulphur Behaviour in Norcem Cement Plant in Kjøpsvik

Prepared By
Umesh Pandey
MS Process Technology

Direct/Indirect participation
Umesh Pandey (Thesis Student), Lars A. Tokheim (USN supervisor), Annika Steien (Norcem Supervisor), Anne Sigrid (Laboratory Chief), Tom Nordal (Production Manager, Norcem Kjøpsvik, Kiln Operators and Lab Staff (Norcem Kjøpsvik)

Planned Date of the experiment
17th April 2018-19th April 2018 and 26th April 2018-28th April 2018

Location of the experiment
Norcem Cement Plant in Kjøpsvik

</div>

1. Introduction

Background

As a part of Master Thesis **"Reduction of Sulphur Emission from the Norcem Cement Plant in Kjøpsvik"**, performing a set of experiments is deemed necessary to discover sulphur behaviour in the kiln. It has been established that there are variations in sulphur emissions from the plant in Kjøpsvik and number of factors has been identified as a possible candidate for these variations. The variation due to these factors is described in Chapter 5 of this report.

Among many relevant parameters, the most critical parameters that have a direct impact on the sulphur emissions and can be controlled without affecting kiln processes and clinker quality are listed below. These parameters will be varied to specific values according to the experimental design.

- SO_3 content in the kiln feed
- Kiln feed (t/h)
- Rawmill feeding (t/h)
- Coal feeding in the kiln (t/h)/ Waste oil feeding in the kiln (kg/h)
- RDF feeding in the Hotdisc (kg/h)
- Tyre Feeding in the Hotdisc (kg/h)
- Bypass water supply (m^3/h)
- Energy Usage Rate in the Kiln (MJ/ton of clinker)

It is impossible to control SO_3 to a distinct level. So, during experimental tests, SO_3 content in the kiln feed is kept to as constant as possible. Other independent parameters, %ID Fan Power to control total flow of kiln gases, the tertiary air damper opening, kiln speed and calciner exhaust gas temperature setpoint, are constraints of this experiments. These parameters are controlled to maintain the quality of clinker (kiln speed, calciner exhaust gas temperature setpoints), and maintain the minimum O_2 level in

the kiln inlet (tertiary air supply and %ID fan power). Thus, these parameters are kept constant unless they do not alter the quality and operability of the kiln process.

Goal of the experiment

The primary goal of the experiment is to verify that variation in the identified parameters can explain most of the variation in the sulphur emissions from the plant. A secondary goal is to use experimental data to formulate a regression model which can be used to predict the sulphur emissions from the plant.

Experimental hypotheses

Aforementioned kiln parameters, as well as sulphur content in the fuels and rawmill feed/kiln feed significantly affect the SO_2 emission in the stack gas.

2. Experimental Design

Design space

Based on the discussion with kiln operators, production manager and Lab chief of the plant, a feasible design space (Table H.1) was drafted. Table H.2 is an overview of the levels of the proposed experimental design. All the parameters have two levels (high and low level) within a design space.

Table H.1: Design space of the experimental test (planned).

Parameters	Units	Min	Max	Typical operating value
Kiln Feeding	t/h	90	115	95
Rawmill Feeding	t/h	0/110	150	130
SO_3 in the Rawmill feed	[-]	High	Low	Low
Coal Feeding in the rotary kiln	t/h	2.4	3.5	3.1
Calciner gas temperature set points	°C	885℃	895	890
Waste oil feeding in the kiln	kg/h	0	1000	200
RDF-pellets	kg/h	0	2500	2000
Tyre feeding	kg/h	0	2500	1500
Bypass Water Supply	m³/h	3.0	4.5	3.0
Energy input from rotary kiln fuels per unit ton of clinker	MJ/t clinker	1200	1600	1490

Table H.2: Design level of the kiln parameters in the tests (planned).

Parameters		Controlling Approach	Operating levels	
			Low Level (0)	High Level (1)
Kiln feeding		Control room	95 t/h	102 t/h
Raw meal feeding		Control room	110 t/h	150 t/h
SO_3 content in the kiln feed		Change of stockpiles	High	Low
Single factor	Coal feeding in the kiln	Control room	2.4 t/h[17] 2.4 t/h[18]	3.4 t/h[1] 3.2 t/h[2]
	Waste oil in the kiln	Control room	Calculated[19]	
RDF	Non-Pellets	Control room	0	1500 kg/h
	Pellets	Control room	0	1500 kg/h
Tyre feeding		Control room	0	1500 kg/h
Bypass water supply		Control room	3.0 m³/h	4.5 m³/h
Energy input per unit ton of clinker from rotary kiln fuels		Control room	1200 MJ/t clinker[9]	1550 MJ/t clinker[10]

---

[17] Low energy input rate from the rotary kiln fuels

[18] High energy input rate from the rotary kiln fuels

[19] Calculated using Equation 4.1

Experimental design matrix

An orthogonal experimental matrix is designed using **R** software for this experimental process. The matrix consists of 8 test runs. Each run has a runtime of 4 hours with a total experimental runtime of 32 hours. Beside varying parameters mentioned in Table H.3, a set of quality data, mentioned in Table H.4, will be measured for further analysis. The frequency of the measurement and expected time of the measurement is listed in Table 3. In Table H.3, test number, 2, 5, 9 and 11 are part of the fractional factorial design which was modified due to the various operational problem. The test run number 1, 6, 7, 8, 3, 4, 12, and 10 is a part of the new design, the screening design.

Table H.4: Experimental Design Matrix.

Test runs	Date	Timeframe	Kiln feed	Rawmill feed	Coal feed	RDF feed	Tyre feed	Bypass water	Waste oil
			t/h	t/h	t/h	kg/h	kg/h	m3/h	kg/h
1	20/04	14:00-18:00	101	110	3.2	0	0	4.5	0
2	20/04	18:00-22:00	101	110	2.5	2000	0	3	700
3	26/04	10:00-14:00	101	140	2.9	0	1500	3	0
4	26/04	18:00-22:00	101	110	2.4	2000	1500	3.0	450
5	21/04	02:00-06:00	101	140	2.5	0	0	4.5	600
6	25/04	14:00-18:00	95	140	2.85	2000	0	3	0
7	25/04	18:00-22:00	95	110	2.7	2000	1500	4.5	0
8	25/04	22:00-02:00	95	110	2.5	0	0	3	150
9	24/04	22:00-02:00	95	140	3.15	0	0	3	0
10	26/04	22:00-00:30	95	140	2.4	0	1500	4.5	300
11	24/04	18:00-22:00	95	110	3.0	2000	0	4.5	0
12	26/04	14:00-18:00	101	140	2.4	2000	0	3	300

Table H.3: Sampling for analysing quality data.

Flow streams	Frequency of sampling	Time
Preheater Exhaust Gas	Single sample per test	3 hours after each test start
Gas flowing out of the raw meal	Single sample per test	3 hours after each test start
Coal Quality	Single sample for all test runs	
Waste Oil quality	Suppliers data	
RDF quality	Single sample for all test runs	
Kiln feed quality	Single sample per test	0-1 hour after each test start
Hotmeal quality	Single sample per test	0-1 hour after each test start
Clinker quality	Every 2nd hour of the regular clock time	
Cement kiln dust quality	Single sample per test	3 hours after each test start
Bypass dust quality	Single sample per test	3 hours after each test start

Appendix I Summary of other parameter values during the kiln tests.

Kiln parameters	Test runs	1	2	3	4	5	6	7	8	9	10	11	12
Animal meal feed [kg/h]	Min	0.0	0.0	660.9	663.1	0.0	672.1	667.5	663.2	487.9	665.1	487.9	658.8
	Max	0.0	0.0	733.0	738.1	0.0	728.0	736.0	720.3	526.3	723.5	516.6	739.5
	Mean	0.0	0.0	694.6	699.1	0.0	700.8	700.4	698.2	500.4	696.0	499.4	697.2
Coal feeding in the calciner [t/h]	Min	5.2	4.0	2.6	0.9	4.9	2.7	1.1	3.4	3.4	2.0	3.0	2.8
	Max	5.5	4.6	3.5	1.7	5.5	2.8	1.6	3.8	3.7	3.0	3.4	3.6
	Mean	5.4	4.2	2.8	1.4	5.2	2.7	1.4	3.6	3.6	2.5	3.2	3.4
CF Silo accumulation rate [t/h]	-	0.0	3.4	27.8	0.0	24.4	33.4	7.8	0.0	37.2	30.5	9.8	26.1
Estimated CKD contribution from the rawmill feed [t/h]	-	8.3	4.6	10.7	9.1	13.7	11.5	7.4	15.0	7.7	14.4	5.1	12.8
SO_2 level in the bypass [mg/m^3]	Min	2.5	595.1	2342.3	1620.4	5.0	1630.5	2335.3	76.8	1260.5	37.8	214.7	5.4
	Max	17.5	1774.9	3000.0	3000.0	266.1	2995.2	3000.0	248.4	2679.4	244.2	956.8	321.8
	Mean	6.5	1108.1	2933.7	2566.4	66.5	2443.3	2911.6	158.2	2078.4	99.8	580.6	93.1
Moisture content in the stack gas [% w/w]	Min	11.8	11.4	12.4	12.3	11.9	11.7	12.4	11.6	11.7	13.1	10.2	13.1
	Max	12.3	12.9	14.8	13.1	12.7	12.4	13.4	12.1	12.4	14.0	14.6	14.1
	Mean	12.1	11.7	13.4	12.7	12.2	12.0	12.8	11.8	12.0	13.5	12.4	13.6
Wet O_2 level in the stack gas [% w/w]	Min	11.2	11.1	10.8	10.9	11.1	11.5	11.1	11.6	11.5	11.4	10.9	11.2
	Max	11.9	11.9	11.6	12.1	11.9	12.1	12.0	12.3	12.1	12.6	12.1	11.9
	Mean	11.6	11.5	11.1	11.5	11.6	11.8	11.6	11.9	11.7	11.9	11.7	11.6
Volume Flow rate in the stack gas [Nm^3 dry @ 10% O_2]	Min	160846	160467	160565	151699	159317	148858	152945	148119	150833	137372	151264	149001
	Max	177892	180506	180760	178689	177649	164031	174363	163560	165751	163879	174667	174556
	Mean	167495	169334	168371	163895	167162	157775	162301	156867	159446	153837	162050	164263

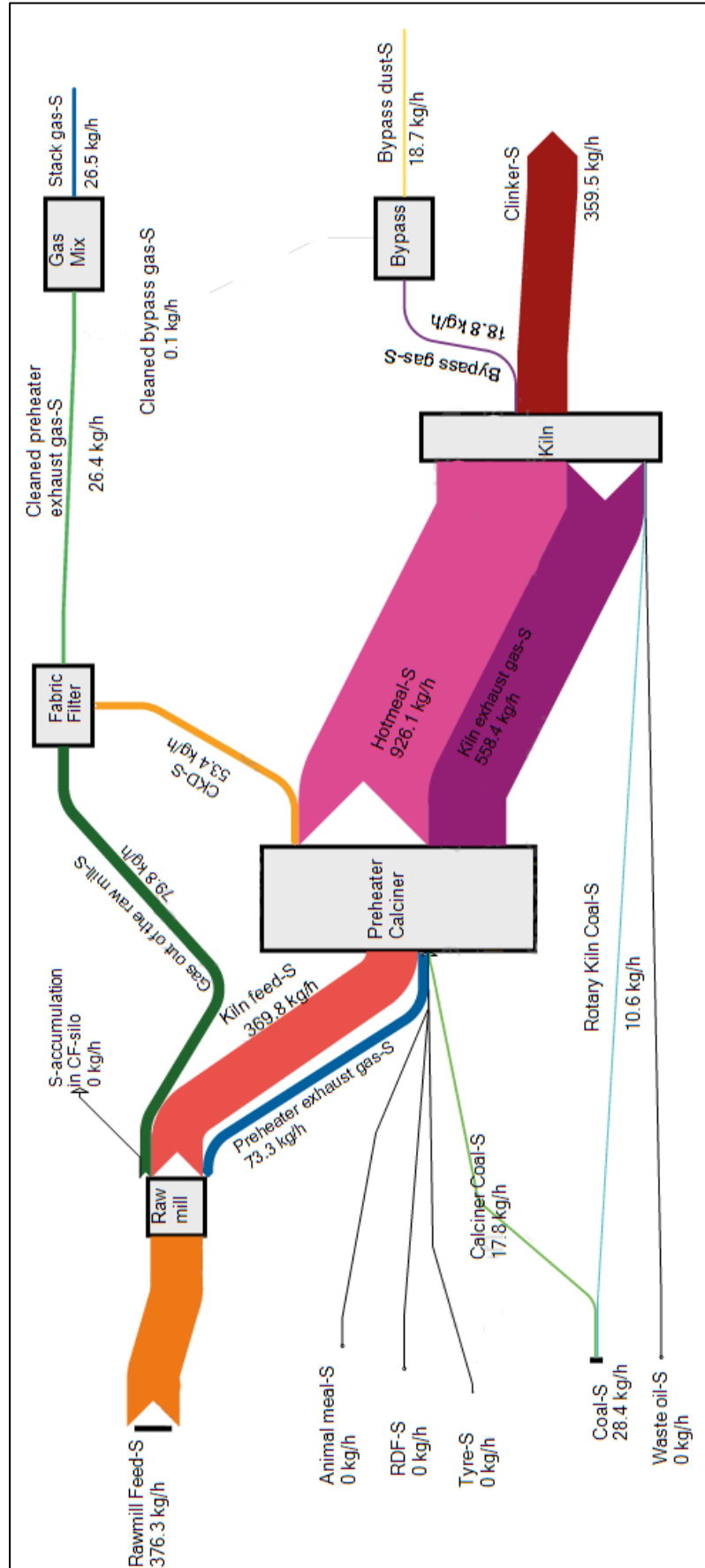**Appendix J Sankey diagrams representing sulphur flow in the kiln tests.**

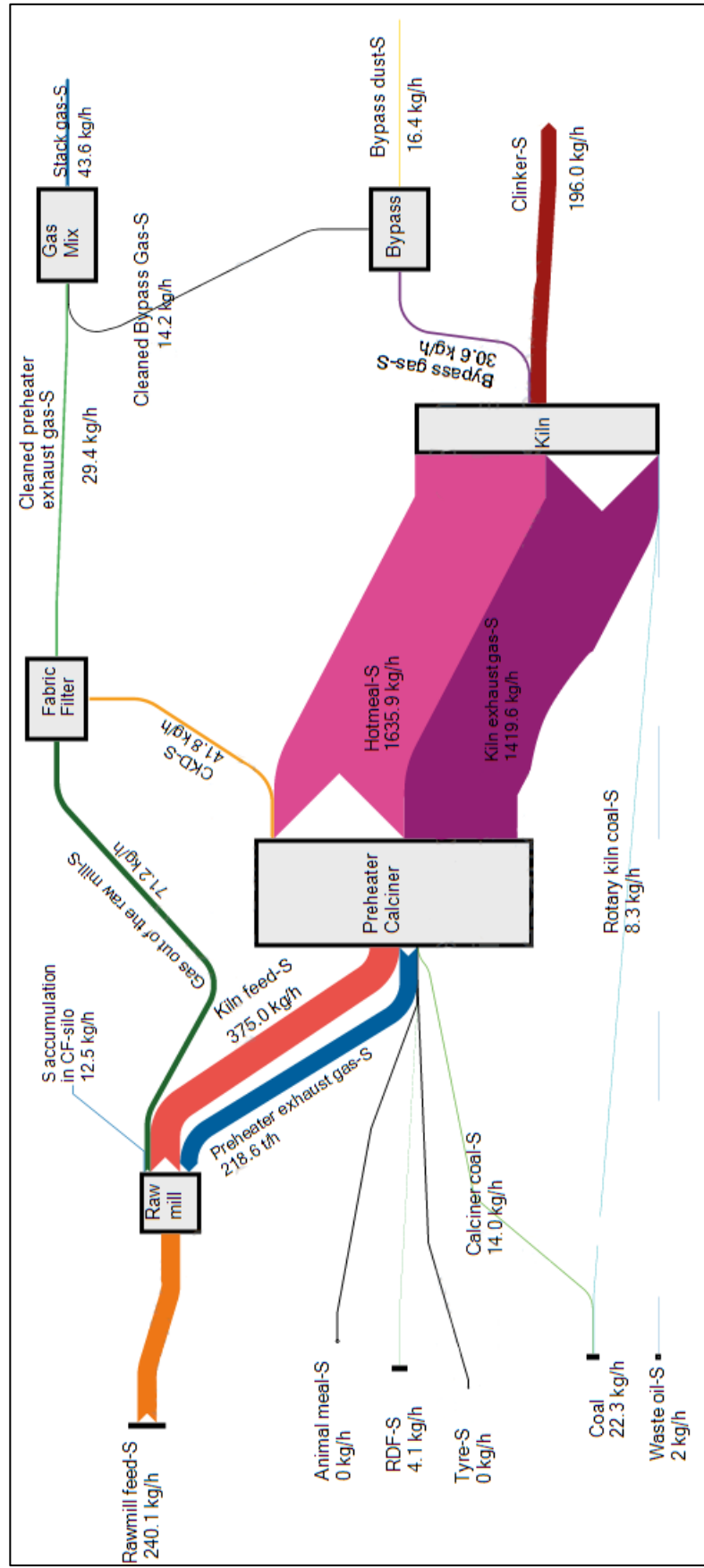Figure J.1: Sankey diagram representing sulphur flow in Test 1.

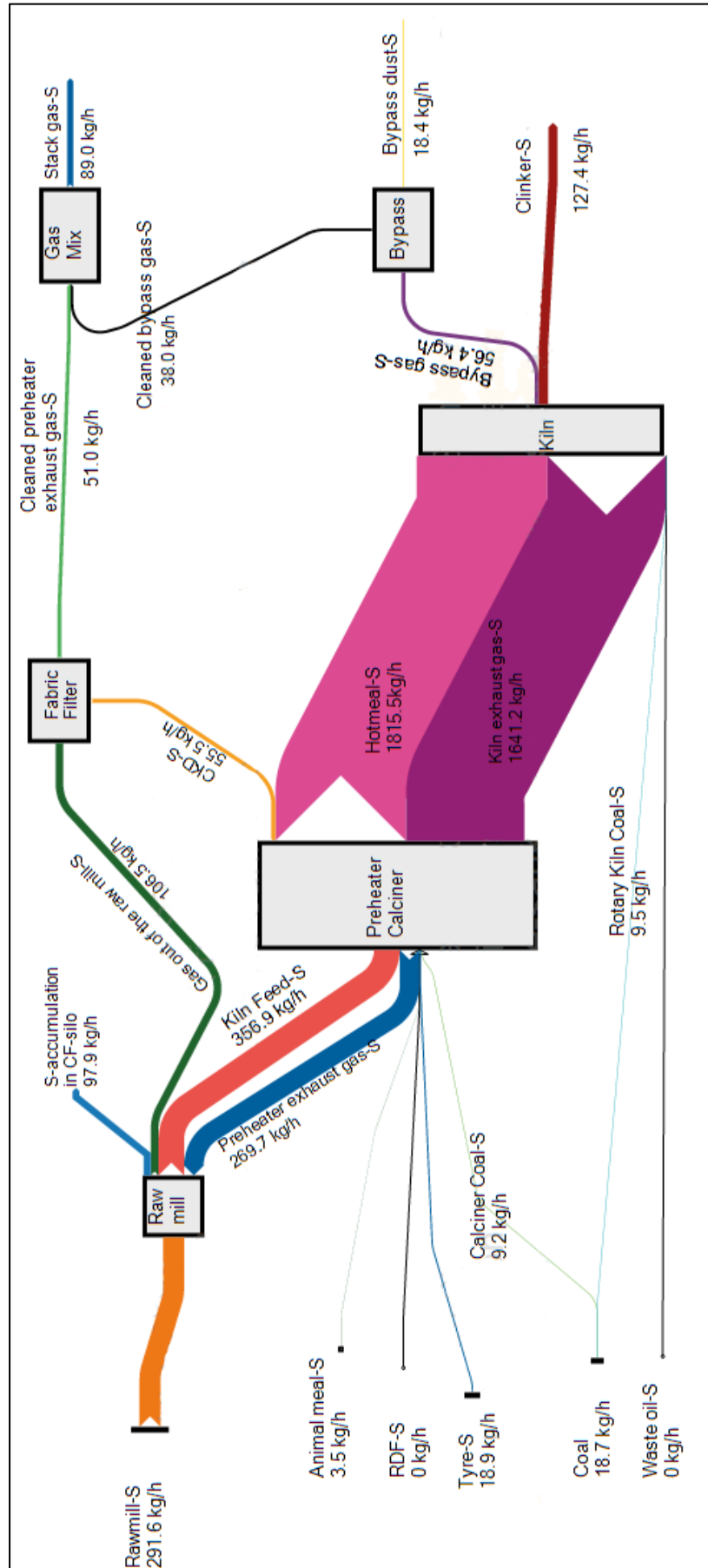Figure J.2: Sankey diagram representing sulphur flows in Test 2.

Figure J.3: Sankey diagram representing sulphur flows in Test 3.
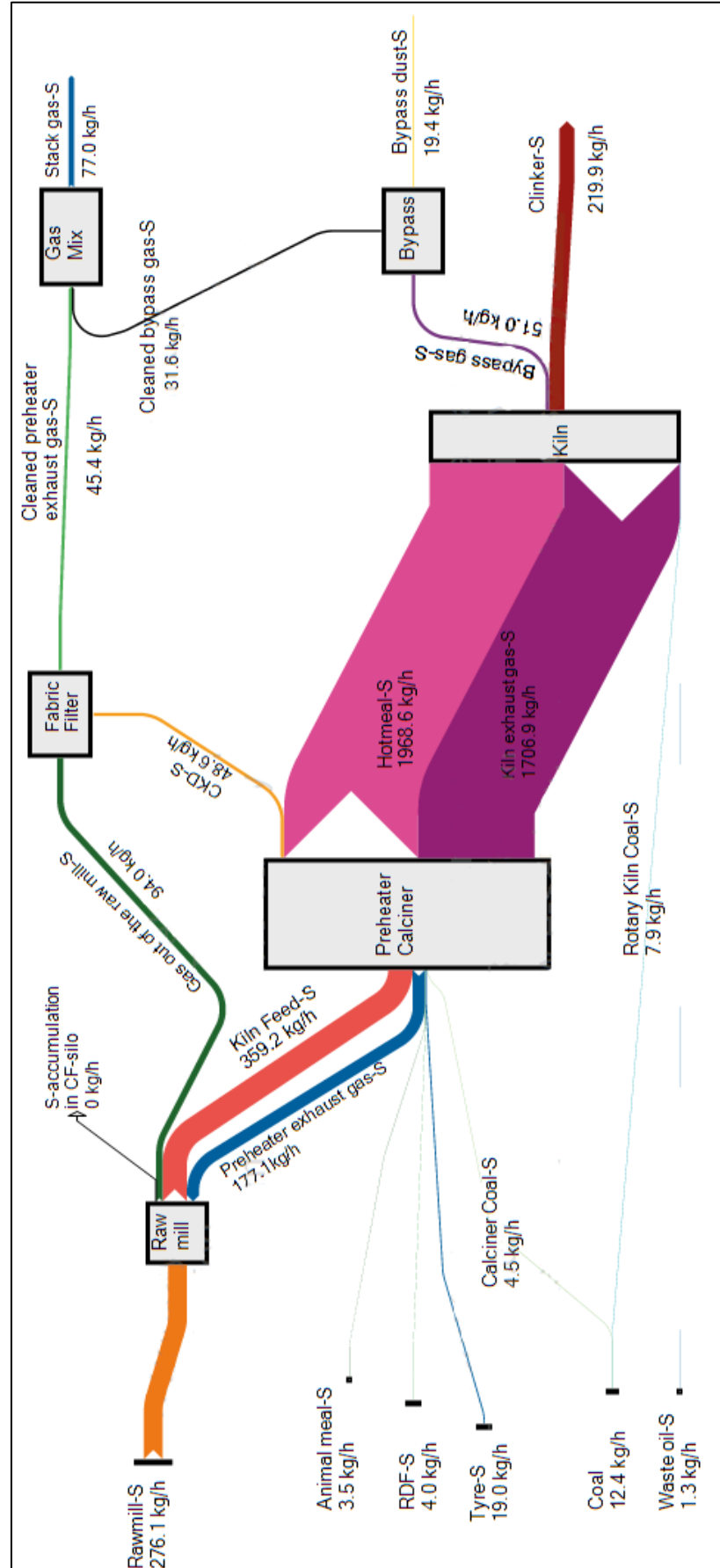
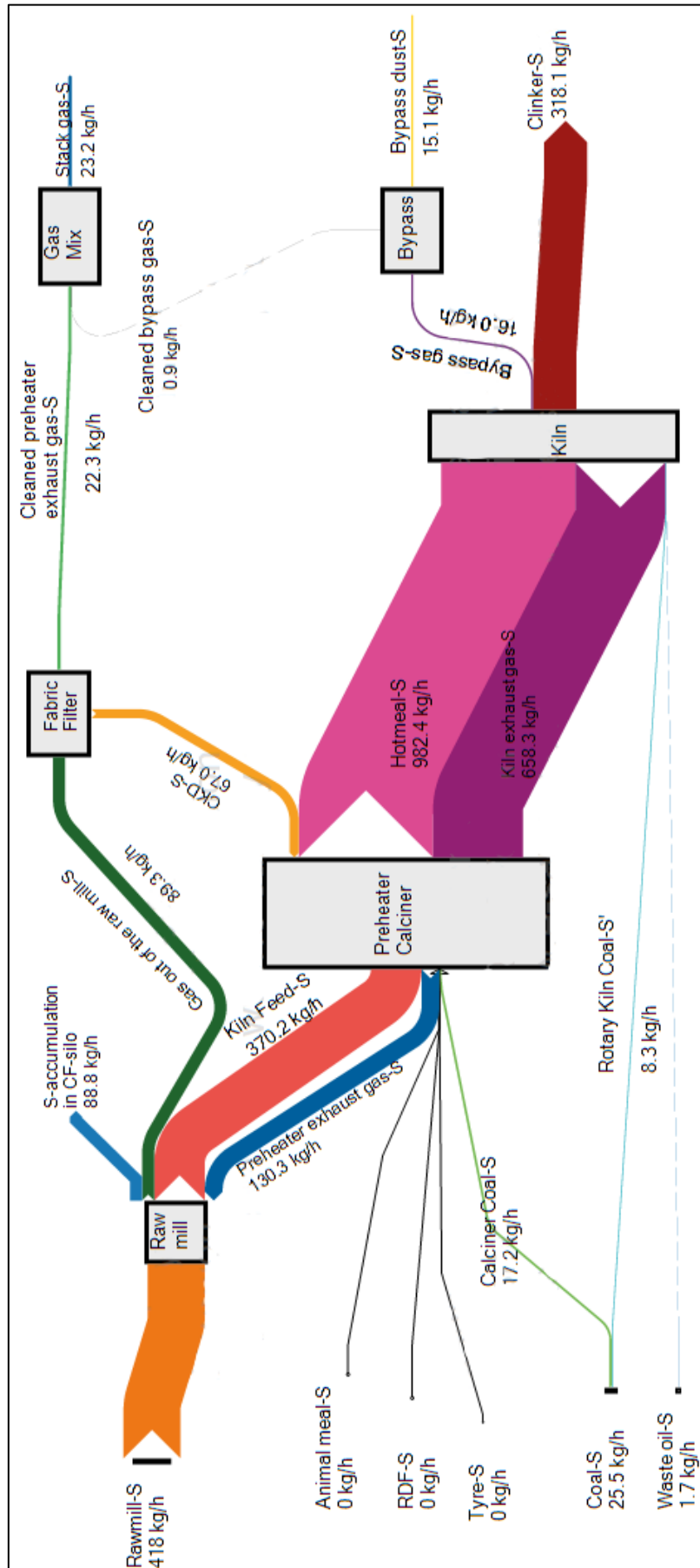Figure J.4: Sankey diagram representing sulphur flows in Test 4.

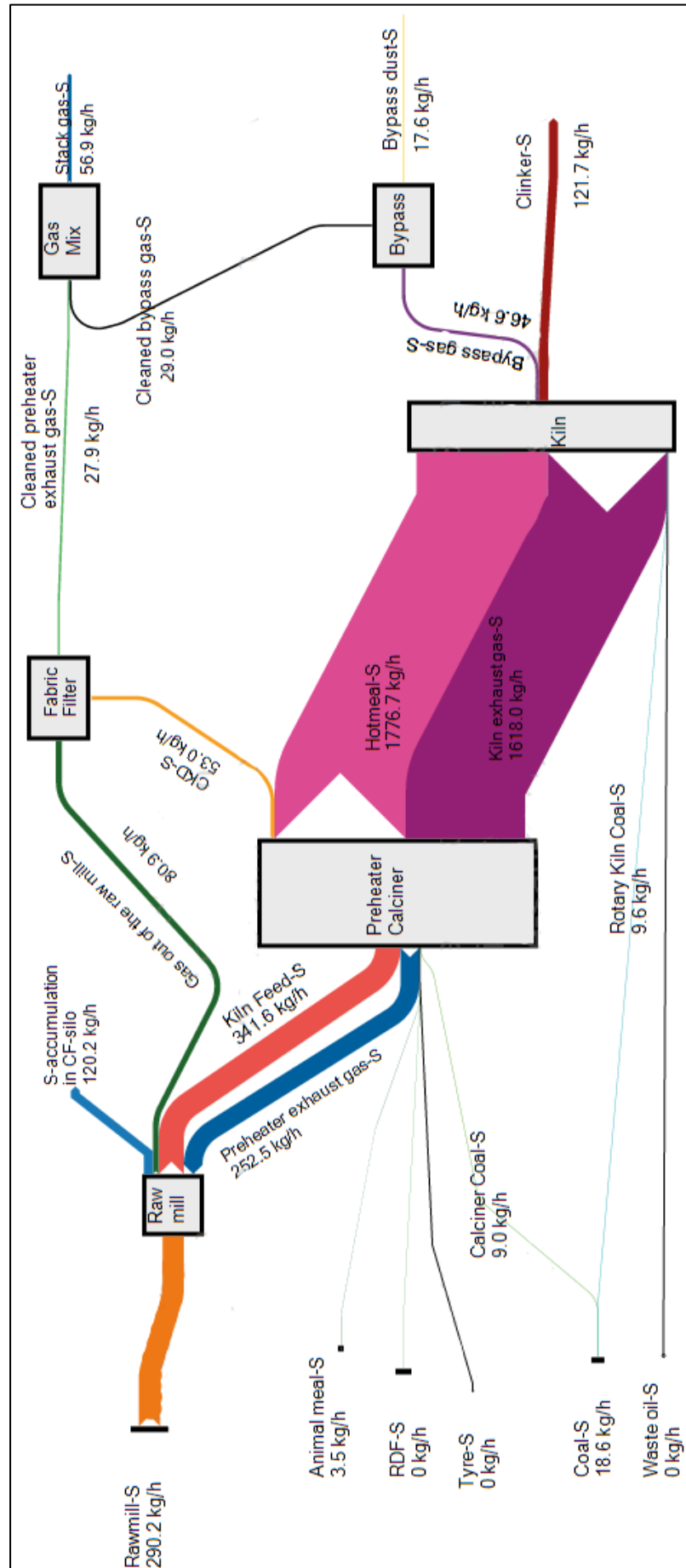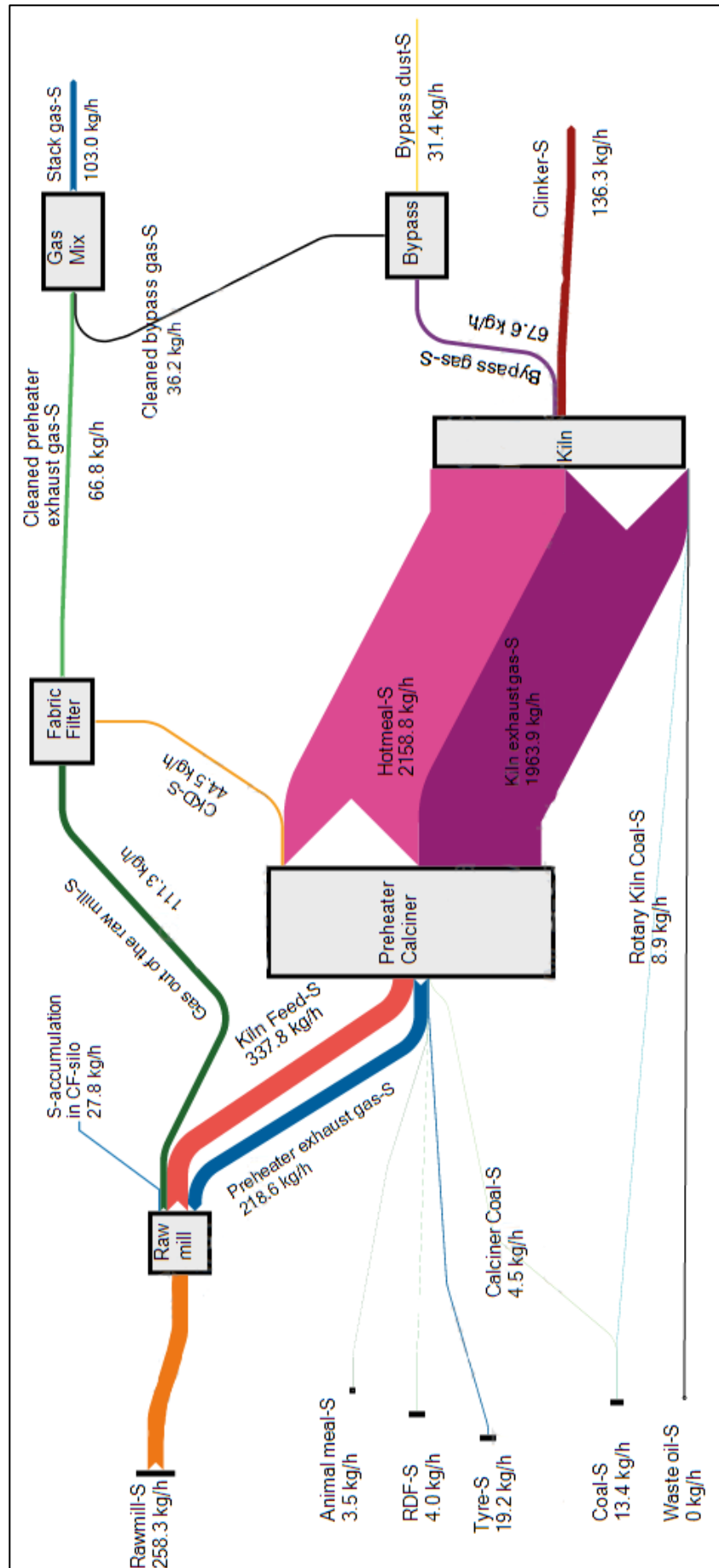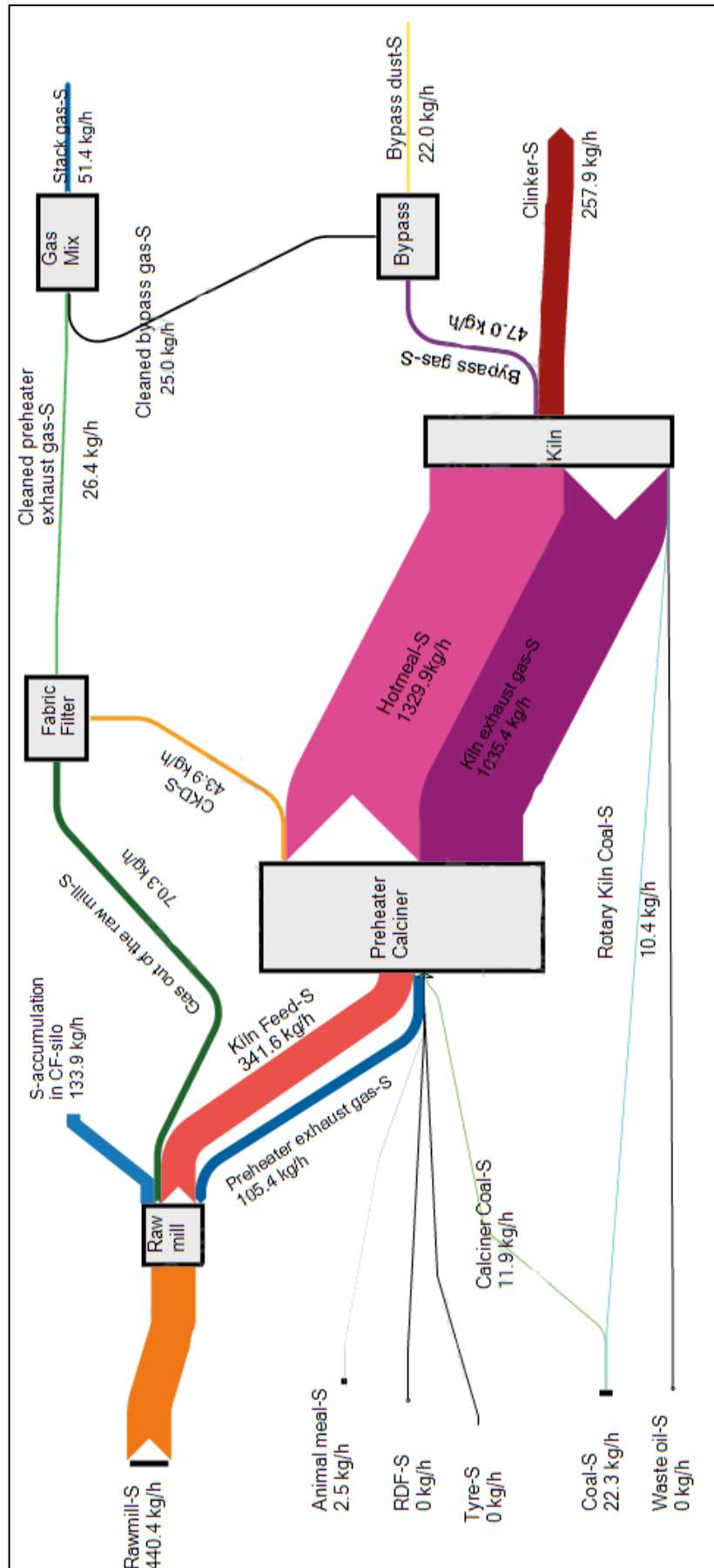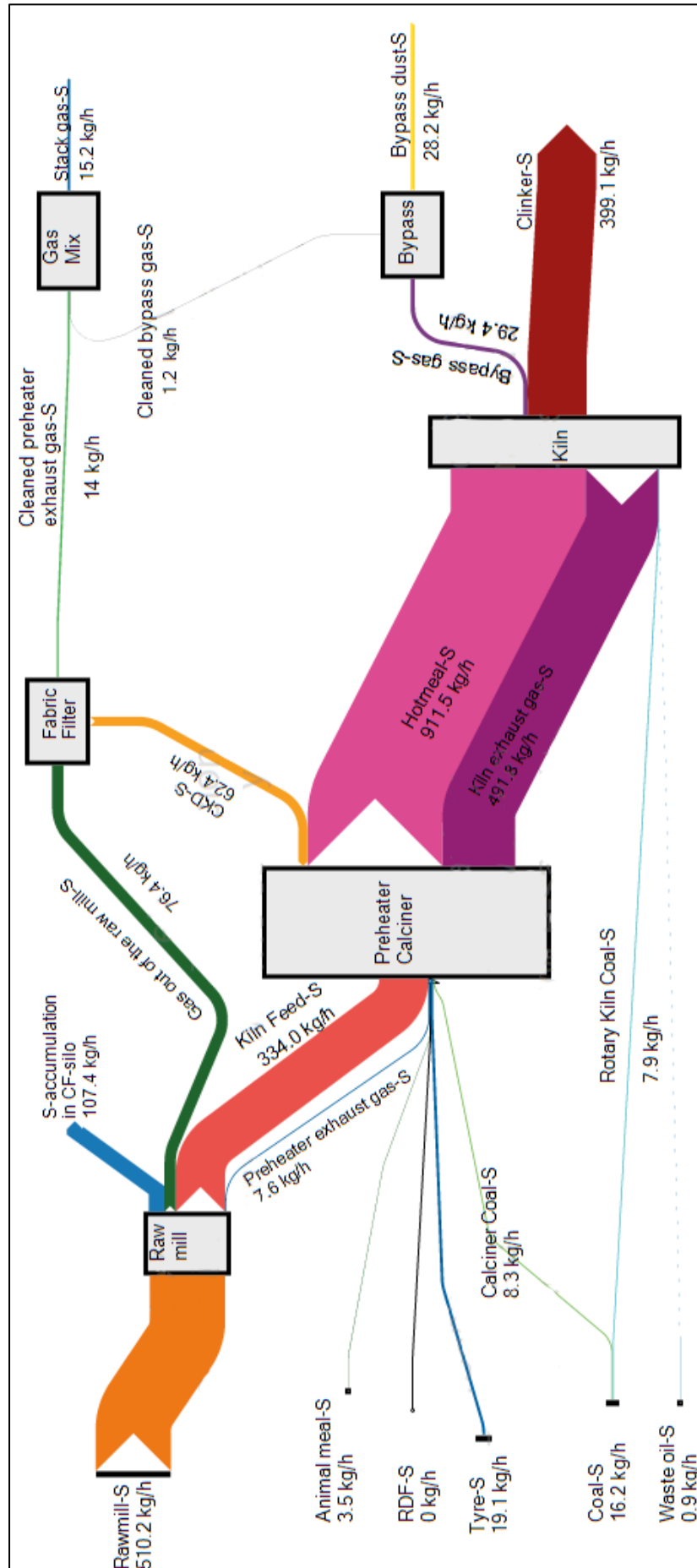Figure J.5: Sankey diagram representing sulphur flows in Test 5.

Figure J.6: Sankey diagram representing sulphur flows in Test 6.

Figure J.7: Sankey diagram representing sulphur flows in Test 7.

Figure J.8: Sankey diagram representing sulphur flows in Test 8.

Figure J.9: Sankey diagram representing sulphur flows in Test 9.

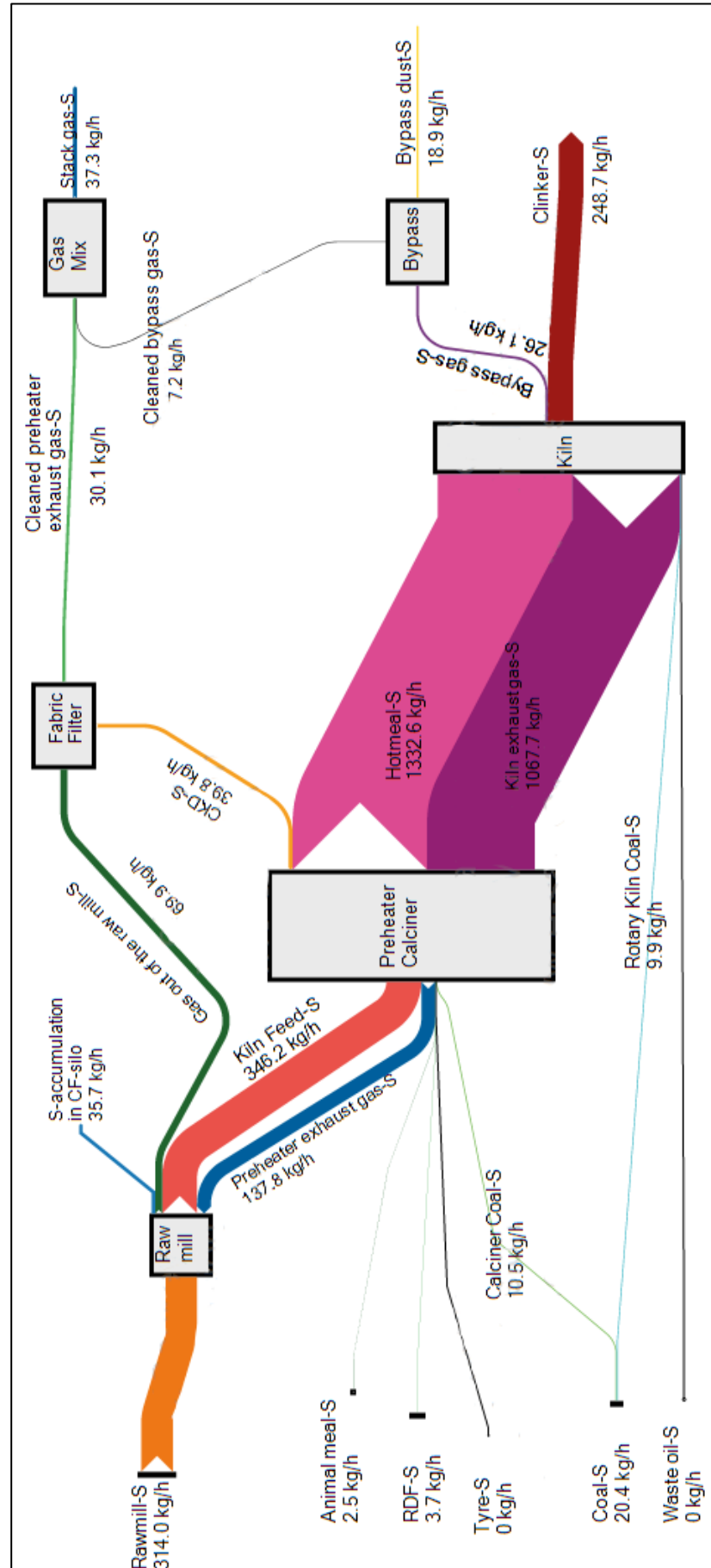Figure J.10: Sankey diagram representing sulphur flows in Test 10.

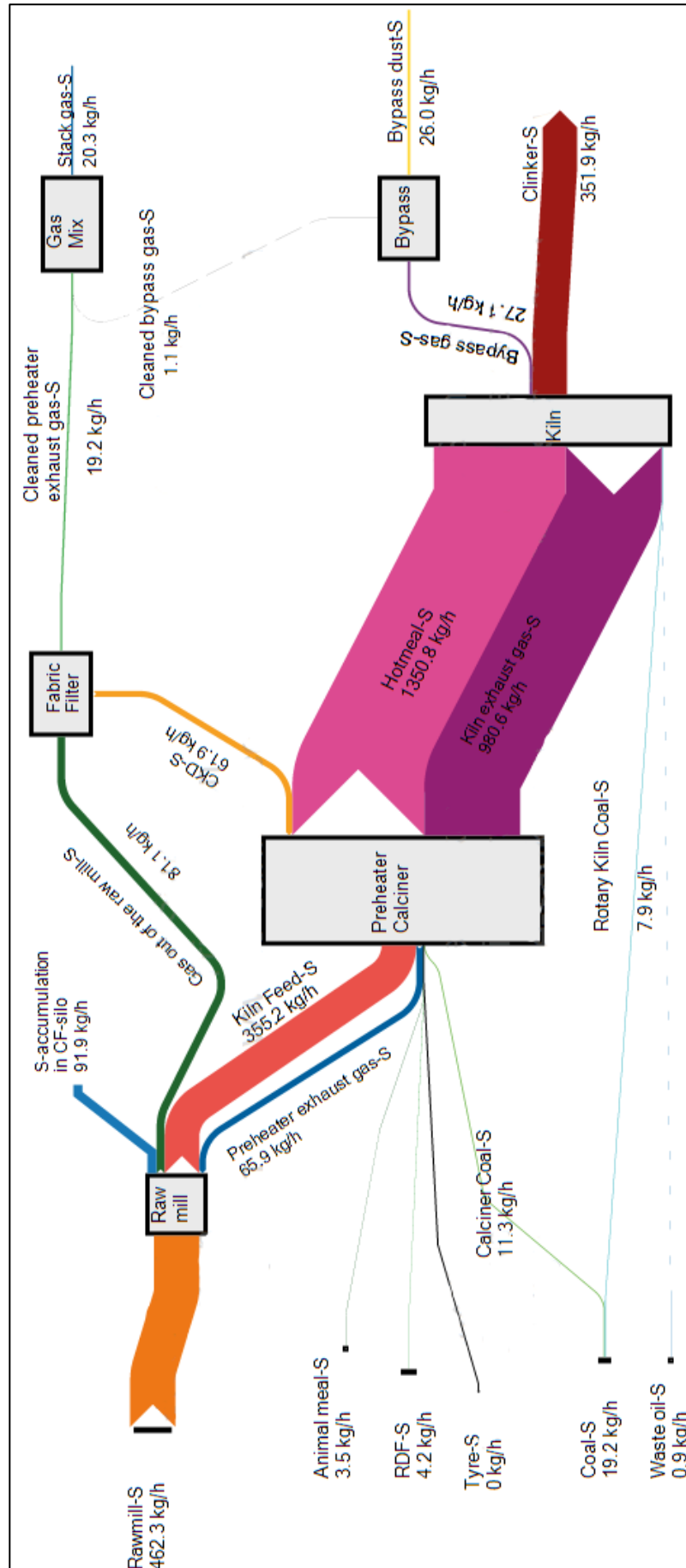Figure J.11: Sankey diagram representing sulphur flows in Test 11.

Figure J.12: Sankey diagram representing sulphur flows in Test 12.